

**PHYSIOLOGICAL SIGNIFICANCE OF
AUTOPHAGY IN PROTEIN TURNOVER**

JUN ONODERA

DOCTOR OF PHILOSOPHY

Department of Molecular Biomechanics
School of Life Science
The Graduate University for Advanced Studies

2004 (School Year)

ACKNOWLEDGEMENTS

I wish to express deepest appreciation to Professor Yoshinori Ohsumi for giving a chance of this study in his laboratory, his constant supervision, extensive advice, insightful discussion and encouragement throughout this study. I am grateful to Dr. Misuzu Baba for her excellent electron microscopic analyses. I would like to thank Misses Shigemi Takami (Center for Analytical Instruments, National Institute for Basic Biology) and Hideko Yomo (Suntory Limited) for their assistance in amino acids analysis. I also express my thanks to present and past members in Professor Yoshinori Ohsumi's laboratory for their continuous supports and good company along my stay in National Institute for Basic Biology, Okazaki.

June 30, 2004

Jun Onodera

小野寺純



**The Graduate University
for Advanced Studies**



**National Institute
for Basic Biology**

TABLE OF CONTENTS

SUMMARY	1
INTRODUCTION	4
<i>Protein Degradation</i>	4
<i>Autophagy in the Yeast</i>	5
<i>The Cytoplasm to Vacuole Targeting Pathway</i>	8
<i>One of Problem to Be Solved in Autophagy</i>	11
MATERIALS AND METHODS	15
<i>Yeast Strain and Media</i>	15
<i>Plasmid Construction</i>	15
<i>Two-dimensional PAGE</i>	17
<i>Peptide Mass Finger-printing</i>	18
<i>Antibodies</i>	18
<i>Immuno-blot of Whole-cell Lysates</i>	19
<i>Pulse-chase Experiments and Immuno-precipitation</i>	19
<i>Light Microscopy</i>	20
<i>Immuno-electron Microscopy</i>	20
<i>Subcellular Fractionation</i>	20
<i>Proteinase K Protection Assay</i>	21
<i>Determination of Cell Viability</i>	21
<i>Assay of Ald6p Enzymatic Activity</i>	21
<i>Northern Blot</i>	22
<i>Amino Acid Analysis of Whole Cell</i>	22
<i>Assay of in vivo Protein Synthesis</i>	22

RESULTS	26
I. Studies on Degradation of Ald6p, a Preferential Substrate of Autophagy	26
<i>Screen for Proteins Reduced under Nitrogen Starvation</i>	26
<i>Ald6p, Cytosolic Acetaldehyde Dehydrogenase</i>	27
<i>Proteins Required for the Reduction of Ald6p</i>	28
<i>Reduced Ald6p Levels Implied a Rapid Degradation</i>	29
<i>Ald6p Was Degraded in the Vacuole with Autophagic Body</i>	30
<i>Ald6p Was Preferentially Transported to the Vacuole via the Autophagosome</i>	31
<i>Phenotype of ALD6 Disruptant Cells</i>	32
<i>Ald6p Enzymatic Activity May Be Disadvantageous during Nitrogen Starvation</i>	33
II. Amino Acids Supply from Autophagy Is Essential for Protein Synthesis	59
<i>Several Proteins Increased under Nitrogen Starvation</i>	59
<i>Autophagy Contributes to the Maintenance of Amino Acids Pool</i>	60
<i>Transient Accumulation of Cysteine during Nitrogen Starvation</i>	61
<i>Protein Synthesis Require Amino Acids Pool</i>	62
DISCUSSION	75
<i>Rate of Ald6p Degradation</i>	75
<i>Molecular Mechanism of Preferential Ald6p Segregation</i>	75
<i>Physiological Significance of Autophagic Ald6p Degradation</i>	76
<i>Metabolic Dynamics in Early Phase of Starvation</i>	78
<i>Autophagy Is Essential for the Formation of Amino Acids Pool</i>	79
REFERENCES	83

LIST OF FIGURES AND TABLES

Table I. New nomenclature of autophagy-related genes.	10
Figure 1. Model of autophagy and the Cvt transport to the vacuole.	13
Figure 2. Immuno-staining image of alcohol dehydrogenase in the yeast cell.	14
Table II. Yeast strains used in this study.	24
Table III. Ald6p activity of overexpression and C306S mutant.	35
Figure 3. Two-dimensional PAGE of cell lysate in before and after nitrogen starvation.	36
Figure 4. Illustration of procedures of peptide mass finger-printing.	37
Figure 5. Three expression patterns of protein spots before/after nitrogen starvation.	38
Figure 6. Cytosolic acetaldehyde dehydrogenase involves in a production of cytosolic acetyl-CoA and NADPH.	39
Figure 7. Preparation of anti-Ald6p antibodies.	40
Figure 8. Time course of Ald6p reduction under nitrogen starvation.	41
Figure 9. Proteins required for the reduction of Ald6p.	42
Figure 10. Proteasome degradation does not require for the Reduction of Ald6p.	43
Figure 11. Pulse-chase analysis of Ald6p and ADH during nitrogen starvation.	44
Figure 12. Detection of Ald6p in the autophagic bodies.	45
Figure 13. Visualization of vacuolar transport of Ald6p-GFP.	46
Figure 14. Immunological detection of Ald6p.	47
Figure 15. Illustrated of collection of the autophagosome-enriched fraction.	48
Figure 16. Ald6p was preferentially sequestered in the autophagosome.	49
Figure 17. Proteinase K protection assay of API and Ald6p in each subcellular fraction.	51
Figure 18. Ald6p is not degraded under carbon starvation, or nitrogen and carbon starvation.	52
Figure 19. Cell viability and growth curve of $\Delta ald6$ cells.	53
Figure 20. Cell viability and growth curve of $\Delta ald4$ cells.	54

Figure 21. Ald6p does not decrease in their overexpression cells.	55
Figure 22. Cell viability phenotype of Ald6p overexpressing cells.	56
Figure 23. Site-direct mutagenesis of Ald6p to yield enzymatic activity deficient mutant.	57
Figure 24. Cell viability phenotype of <i>ald6</i> ^{C306S} cells.	58
Table IV. Cycloheximide inhibited TCA-insoluble [¹⁴ C]valine uptake.	64
Figure 25. Autophagy is required for the synthesis of starvation induced proteins.	65
Figure 26. Expression of nitrogen starvation induced gene, <i>ARG1</i> and <i>HSP26</i> .	67
Figure 27. Change in the total content of free amino acids during nitrogen starvation.	68
Figure 28. Change in the individual content of free amino acid during nitrogen starvation.	69
Figure 29. Change in cysteine content during nitrogen or sulfur starvation.	72
Figure 30. Protein synthesis during nitrogen starvation.	73
Figure 31. Protein synthesis in supplement of amino acids ahead of the assay.	74
Figure 32. Model of physiological roles of the preferential Ald6p degradation.	81
Figure 33. Model of contribution of autophagic degradation for the amino acids pool formation in yeast cells under nitrogen starvation.	82

ABBREVIATIONS

A ₆₀₀	absorbance at 600 nm
ADH	alcohol dehydrogenase
API	aminopeptidase I
ATP	adenosine triphosphate
CPY	carboxypeptidase I
DNA	deoxyribonucleic acid
DTT	dithiothreitol
EDTA	ethylenediamine tetraacetic acid
G6PDH	glucose-6-phosphate dehydrogenase
GFP	green fluorescent protein
GST	glutathione <i>S</i> -transferase
HA	hemagglutinin
MALDI-TOF	matrix associated laser deionization - time of flight
NAD ⁺	oxidized form of reduced form of nicotinamide adenine dinucleotide
NADH	reduced form of nicotinamide adenine dinucleotide
NADP ⁺	oxidized form of nicotinamide adenine dinucleotide phosphate
NADPH	reduced form of nicotinamide adenine dinucleotide phosphate
ORF	open reading frame
PAGE	polyacrylamide gel electrophoresis
PBS	phosphate-buffered saline
PCR	polymerase chain reaction
PGK	phosphoglycerate kinase
PMSF	phenylmethanesulfonyl fluoride
RNA	ribonucleic acid
SD	synthetic dextrose
SDS	sodium dodecyl sulfate
TBS	Tris-buffered saline

SUMMARY

Cellular activities require the maintenance of a balance between the synthesis and degradation of proteins. Macroautophagy (hereafter referred to as autophagy) is an intracellular bulk degradation system, which is well conserved in eukaryotes; autophagy transports cytoplasmic components to the lysosome/vacuole for degradation. This degradation is a cellular response to starvation and also plays a role in the recycling of cytoplasmic components, which may be important for cellular remodeling, development and differentiation. A total of 16 genes, which are essential for autophagy, and which are named *APG* and *AUT* (current nomenclature is *ATG*), have been identified by genetic screens in the yeast, *Saccharomyces cerevisiae*. Much progress has been made in the functional analysis of these genes.

Autophagy is initiated by the sequestration of cytoplasmic components in a double-membrane structure termed the autophagosome. Immuno-electron microscopy has shown that ribosomes and typical cytosolic marker enzymes are present in the autophagosome and autophagic bodies at the same densities as in the cytosol. It is indicated that autophagy is a nonselective degradation. If degradation of long-lived proteins is exclusively mediated by autophagy, all proteins might be expected to have similar lifetimes. However, long-lived proteins have a variety of lifetimes; therefore, the autophagic pathway might have some selectivity.

To investigate the possibility of selective autophagic degradation, I attempted to compare the amounts of each intracellular protein under growth and starvation conditions in the yeast, *S. cerevisiae*. I performed a systematic analysis using two-dimensional PAGE and MALDI-TOF mass spectrometry to detect the autophagy dependent degradation of intracellular proteins. During this analysis, I detected that the Mg^{2+} - and NADPH-dependent cytosolic acetaldehyde dehydrogenase (Ald6p) decreased under nitrogen starvation. This enzyme catalyzes the conversion of acetaldehyde to acetate in the cytosol (acetaldehyde + $NADP^+$ → acetate + NADPH). As assessed by immuno-blot, Ald6p was reduced by greater than 82% after 24 h of nitrogen starvation. This reduction was dependent on Atg/Apg proteins and vacuolar

proteases, but was not dependent on the proteasome degradation, the Cvt pathway or the Vid protein.

I hypothesized that the decrease in Ald6p levels was the result of degradation during nitrogen starvation. To examine this possibility, the kinetics of Ald6p degradation was measured by pulse-chase experiments, which suggest that Ald6p is degraded much more rapidly than typical cytosolic proteins. Ald6p was visualized by Ald6p-GFP fusion protein and immuno-electron microscopy analyses. In $\Delta pep4$ vacuolar proteinase deficient cells, Ald6p or Ald6p-GFP was localized in autophagic bodies in the vacuole under nitrogen starvation. These results indicate that Ald6p is degraded in the vacuole under nitrogen starvation. Furthermore, using subcellular fractionation and pulse-chase experiments, I also demonstrated that Ald6p was preferentially transported to the vacuole via autophagosome.

To address the physiological significance of this preferential degradation, I analyzed cells of Ald6p over-producer and its disruptant. $\Delta atg7 \Delta ald6$ double mutant cells were able to maintain higher rates of viability than $\Delta atg7$ cells under nitrogen starvation, and *ALD6* overexpressing cells were not able to maintain high rates of viability. Furthermore, the Ald6p^{C306S} mutant, which lacks enzymatic activity, had viability rates similar to $\Delta ald6$ cells. Ald6p enzymatic activity may be disadvantageous for survival under nitrogen starvation; therefore, yeast cells may preferentially eliminate Ald6p via autophagy.

These results show that Ald6p is one example of a preferential substrate for autophagic degradation. Ald6p was the only major protein on the two-dimensional PAGE gel to decrease during starvation; however, it is still possible that other minor proteins behave like Ald6p. If further studies were able to find such proteins, it would help clarify the molecular mechanisms of selective autophagy and the physiological significance of the preferential degradation.

I also found several specific proteins are induced under nitrogen starvation on the above-mentioned screening using two-dimensional PAGE. These proteins included typical proteins of environment stress responses (Eno1p/Hsp48p and Hsp26p), enzyme of amino acid biosynthesis (Arg1p), quenching enzyme of reactive oxygen species

(Sod2p) and so on. These proteins did not increase in $\Delta atg7$ mutant cells; however, their mRNA levels were high as wild-type cells under nitrogen starvation. Thus, it is possible that these proteins synthesis are inhibited in the translational step.

It is generally thought that autophagic protein degradation supplies significant amounts of free amino acids under nitrogen starvation. From this perspective, I quantified the free amino acids in yeast cells. Wild-type cells could maintain the constant level of amino acids pool during nitrogen starvation, while $\Delta atg7$ cells depleted free amino acids after a few hours starvation. This result may indicate that $\Delta atg7$ cells cannot keep free amino acids enough to synthesize starvation-induced proteins. To ensure this consequence, I assessed *in vivo* protein synthesis using [^{14}C]valine; protein synthesis of $\Delta atg7$ cells was even lower level than that of wild-type cells after 6 h starvation. However, when nitrogen starved cells fed free amino acids beforehand, protein synthesis of $\Delta atg7$ cells was high level as well as that of wild-type cells. These results suggest that the pool size of free amino acids should limit the protein synthesis.

It is often presumed that the ubiquitin-proteasome degradation is the most important for protein turnover in all phase. In this study, I showed the direct evidence that autophagy is essential for protein turnover and formation of amino acids pool under nitrogen starvation condition.

INTRODUCTION

Protein Degradation

It is now well known that every cellular activity requires the maintenance of a balance between the synthesis and degradation of proteins. Every protein has its own lifetime of wide range, from a few minutes to more than ten days (Schimke and Doyle, 1970; Goldberg and Dice, 1974; Goldberg and John, 1976). We do not know yet the determinants of the lifetime of each protein and the exact meanings of protein turnover, but dynamic state of equilibrium itself must be crucial for maintenance of life. Recently it was realized that proteins are not degraded spontaneously but are degraded rather by active processes.

There are two major pathways of intracellular protein degradation. First, the ubiquitin-proteasome system in the cytosol is involved in degradation of short-lived, damaged or misfolded proteins (Hochstrasser, 1996; Hershko and Ciechanover, 1998). Target proteins to be degraded is first tagged with a small protein, ubiquitin and then digested by a huge proteinase complex, proteasome. Both ubiquitination and cleavage processes require ATP hydrolysis, and undergoes with strict recognition of target proteins by the sophisticated ubiquitin ligase system and proteasome. Short-lived proteins play crucial roles in important cellular events such as transcriptional regulation and cell cycle control.

Long-lived proteins are believed to be degraded within a specific compartment, lysosome/vacuole. So far, several delivery routes to this lytic compartment are proposed. Process of degradation of own intracellular components in lysosomes is generally called autophagy in contrast to heterophagy of extracellular materials (Mortimore and Poso, 1987). Macroautophagy is a major pathway in autophagy, and initiates by enwrapping a portion of cytoplasm by membrane sac called isolation membrane, to form a double membrane structure, autophagosome (Seglen and Bohley, 1992). Autophagosome then fuses with lysosome and turns to be autolysosome and its inner membrane and contents are digested for reuse. Microautophagy is a process in which the lysosome or vacuole directly engulfs a portion of cytoplasm. Hereafter in this thesis, macroautophagy will be

referred as simply autophagy.

Autophagy is characterized as nonselective and bulk degradation of cellular proteins. More than 99% of cellular proteins are long lived proteins, thus turnover of long-lived proteins is important to understand the control of cell growth, because their degradation mainly contributes to the pools of amino acids and other building blocks for biosynthesis. Bulk protein degradation is also play roles in the process of starvation response, cellular remodeling, development, differentiation and some aspects of organelle homeostasis (Tsukada and Ohsumi, 1993; Doelling *et al.*, 2002; Hanaoka *et al.*, 2002; Otto *et al.*, 2003; Otto *et al.*, 2004; Melendez *et al.*, 2003; Levine and Klionsky, 2004).

Already more than a half-century has passed since the lytic organelle; lysosome was discovered by de Duve using cell fractionation procedures (de Duve, 1959). Since then many electron micrographs showing autophagy have been reported in a variety of cells from different organs and cultured cells, and it is now generally accepted that autophagy is ubiquitous cellular activity of eukaryotic cells. However, mammalian lysosomes are so dynamic and complicated that a general picture of the autophagic process was difficult to draw. Moreover, there was no specific marker for monitoring autophagy or no good quantitative assay system for autophagy in mammalian cells. Therefore, any genes specifically involved in autophagy have not been identified so long time, and the molecular basis of autophagy has been remained to be uncovered. These years, genetical and molecular biological approaches using the yeast, *Saccharomyces cerevisiae* have begun to unravel a molecular dynamics of autophagy.

Autophagy in the Yeast

In early 1990s, Takeshige *et al.* found that the yeast, *S. cerevisiae*, cell induces autophagy under various nutrient starvation conditions by light microscopy. When vacuolar proteinase-deficient mutants grown in a rich medium were transferred to nitrogen-depleted medium, spherical structures appeared in the vacuole after 30–40 min, accumulated and almost filled the vacuole up to 10 h (Takeshige *et al.*, 1992). These structures, named autophagic bodies, were mostly single membrane-bound structures

containing a portion of cytoplasm (Takeshige *et al.*, 1992; Figure 1). Then double membrane structures, autophagosomes, were found in the cytosol of the starved cells. Autophagosome in yeast was about 300–900 nm in diameter and contained ribosomes and occasionally other various cellular structures including mitochondrion and rough endoplasmic reticulum (Takeshige *et al.*, 1992; Baba *et al.*, 1994; Figure 1).

Thus, autophagy in yeast is easily monitored by the accumulation of autophagic bodies under light microscopy. Based on loss of the accumulation of autophagic bodies, Tsukada and Ohsumi isolated a group of autophagy defective mutants, called *apg* (autophagy) mutants, in the yeast, *S. cerevisiae* (Tsukada and Ohsumi, 1994). The original *apg* mutant fell into 14 complementation groups, and all *APG* genes (*APG 1–10* and *APG 12–15*) were already cloned. In addition, the *APG16* and *APG17* genes were added to the original *APG* genes by two-hybrid screening with *APG12* and *APG1*, respectively (Mizushima *et al.*, 1999; Kamada *et al.*, 2000). The *APG16* gene was revealed to be identical to *APG15* (Okazaki *et al.*, 2004). Because all the *apg* mutants are defective in formation of autophagosomes, these gene products function before or at the step of membrane biogenesis of autophagosomes (M. Baba and Y. Ohsumi, unpublished results). Thumm *et al.* also isolated a series of autophagy-defective mutants, named *aut* (autophagocytosis) mutants. Fatty acid synthase is degraded in the vacuole under starvation depending on autophagy. The isolation of *aut* mutants was performed with based on retention of the synthase in the cytoplasm (Thumm *et al.*, 1994). Barth *et al.* screened about 5,000 deletion mutants of non-essential gene to clone further autophagy gene, and identified an autophagy gene *AUT10* (Barth *et al.*, 2001). The *APG/AUT* genes are novel except *APG6*, which turned out to be allelic to *VPS30* required for vacuolar protein sorting (Kametaka *et al.*, 1998).

The *APG/AUT* gene products have been characterized. Apg/Aut proteins has identified two ubiquitin-like conjugation systems utilizing approximately half of the Apg/Aut proteins (Ohsumi, 2001). These conjugation processes is essential for autophagy. Apg12p, an ubiquitin-like protein, is covalently attached to Apg5p to form an Apg12p-Apg5p conjugate controlled by the serial action of Apg7p and Apg10p (Mizushima *et al.*, 1998). Apg7p, a member of the ubiquitin E1-like activating enzymes,

from a thioester linkage with Apg12p (Tanida *et al.*, 1999; Kim *et al.*, 1999; Yuan *et al.*, 1999). Apg12p subsequently form a thioester intermediate with Apg10p, ubiquitin E2-like conjugating enzyme (Shintani *et al.*, 1999). Apg12p is then linked to lysine-149 of Apg5p through an isopeptide bond with C-terminal glycine. Apg16p then interact through its C-terminal coiled-coil region to form homo-oligomers following the direct interaction with the Apg12p-Apg5p conjugate (Mizushima *et al.*, 1999). Apg12p-Apg5p conjugate and Apg16p form an approximately 350-kDa complex in the cytosol (Kuma *et al.*, 2002).

Aut7p/Apg8p, a second ubiquitin-like protein involved in autophagy, is conjugated to phosphatidylethanolamine by the serial action of three Apg/Aut proteins, Aut2p/Apg4p, Apg7p and Aut1p/Apg3p (Kirisako *et al.*, 2000; Ichimura *et al.*, 2000). The C-terminal arginine-117 of Aut7 is removed through the action of Aut2p, a cysteine protease (Kirisako *et al.*, 2000), to expose glycine-116. Following activation by Apg7p (E1), the processed Aut7p is transferred to Aut1p (E2). Aut7p is then covalently linked to phosphatidylethanolamine. Aut2p further cleaves Aut7p-phosphatidylethanolamine, releasing Aut7p, an essential step in the normal progression of autophagy (Kirisako *et al.*, 2000). Aut7p is the first protein to localize to autophagosome and intermediate structures (Kirisako *et al.*, 1999; Huang *et al.*, 2000); this characteristic of Aut7p allows us to use Aut7p to monitor autophagosome formation.

Additional Apg/Aut proteins, not known to participate in ubiquitin-like systems, are also required for autophagy. Vps30p/Apg6p, in addition to a role in autophagy, function in vacuolar protein sorting (Kametaka *et al.*, 1998). Vps30p form a specific phosphoinositide-3-kinase complex required for autophagy, consisting of Vps30p, Apg14p, Vps34p and Vps15p. This data suggests that the dynamic membrane events mediated by the phosphoinositide-3-kinase complex are necessary for autophagy (Kihara *et al.*, 2001).

Tor-kinase negatively regulates the induction of autophagy; this kinase activity is inhibited by rapamycin (Noda and Ohsumi, 1998). As the inactivation of Tor activity causes a rapid dephosphorylation of Apg13p (Kamada *et al.*, 2000; Abeliovich *et al.*, 2000). Apg13p and Apg17p associate with Apg1p protein kinase form the Apg1p

protein kinase complex, an essential component of autophagy (Kamada *et al.*, 2000). Binding of dephosphorylated Apg13p to this complex enhances the kinase activity of Apg1p (Kamada *et al.*, 2000).

The Cytoplasm to Vacuole Targeting Pathway

The cytoplasm to vacuole targeting (Cvt) pathway is a selective transport for aminopeptidase I (API) and α -mannosidase, and occur constitutively in *S. cerevisiae*. The classical model for delivery of hydrolases to the vacuole is via a portion of the secretory pathway. Proteins transit from the endoplasmic reticulum through the Golgi complex, are sorted away from other proteins in the secretory pathway, diver to the endosome, and then to the vacuole. Analysis of API and α -mannosidase, which are vacuolar soluble hydrolases, indicate that they are not transported via the secretory pathway (Yoshihisa and Anraku, 1990; Klionsky *et al.*, 1992). It is constitutively synthesized as an inactive precursor form in the cytosol. It is targeted to the vacuole and then processed by vacuolar proteinase B at its N-terminal region to become mature (Segui-Real *et al.*, 1995).

After synthesis, precursor API rapidly oligomerizes in the cytosol into a dodecamer (Kim *et al.*, 1997). Then the complex (the Cvt complex) are specifically enwrapped by the Cvt vesicle, and delivered to the vacuole (Figure 1). The morphological studies of the Cvt pathway using electron microscopy showed that the Cvt complex is enclosed by autophagosome-like membrane, and the Cvt bodies inside the vacuole was detected in vacuolar proteinase deficient cells (Figure 1). The membrane topology between autophagosome and the Cvt vesicle is quite similar, although they are made in different sizes. The size of autophagosome is 300–900 nm, whereas that of the Cvt vesicle is 140–160 nm (Takeshige *et al.*, 1992; Baba *et al.*, 1997). Under starvation condition, since the Cvt complex is enriched in the autophagosome, the autophagy carries out the transport of precursor API.

Harding *et al.* initially isolated the complementation genes of *cvt* mutants (Harding *et al.*, 1995). Most of *APG/AUT* genes are also required for the Cvt pathway (Scott *et al.*, 1996; Table I). This substantial genetic overlap between autophagy and the

Cvt pathway suggests a mechanistic similarity between them.

Nomenclature of autophagy and its related genes has added confusion for that *APG*, *AUT* and *CVT* gene was overlapped intricately each other. Accordingly, following discussion at the first Gordon Research Conference on "Autophagy in Stress, Development, and Diseases", the different researcher working on these genes have recently decided to adopt a unified gene and protein nomenclature (Klionsky *et al.*, 2003). The new gene and protein names will be *ATG* and *Atg*, respectively, which stand for "autophagy-related" (Table I). Hereafter in this thesis autophagy-related genes (*APG*, *AUT* and *CVT*) and proteins (*Apg*, *Aut* and *Cvt*) will be referred as *ATG* and *Atg*, respectively.

Table I. New nomenclature of autophagy-related genes.

Current name	<i>APG</i>	<i>AUT</i>	<i>CVT</i>	
<i>ATG1</i>	1	3	10	
<i>ATG2</i>	2	8	–	
<i>ATG3</i>	3	1	–	
<i>ATG4</i>	4	2	–	
<i>ATG5</i>	5	–	–	
<i>VPS30/ATG6</i>	6	–	–	
<i>ATG7</i>	7	–	2	
<i>ATG8</i>	8	7	5	
<i>ATG9</i>	9	9	7	
<i>ATG10</i>	10	–	–	
<i>ATG11</i>	–	–	9	
<i>ATG12</i>	12	–	–	
<i>ATG13</i>	13	–	–	
<i>ATG14</i>	14	–	12	
<i>ATG15</i>	–	5	17	
<i>ATG16</i>	16	–	11	
<i>ATG17</i>	17	–	–	
<i>ATG18</i>	–	10	18	
<i>ATG19</i>	–	–	19	
<i>ATG20</i>	–	–	20	
<i>ATG21</i>	–	–	21	<i>MAI1</i>
<i>ATG22</i>	–	4	–	
<i>ATG23</i>	–	–	23	<i>MAI2</i>
<i>SNX4/ATG24</i>	–	–	13	
<i>ATG25</i>	–	–	–	<i>PDD1</i>
<i>ATG26</i>	–	–	–	<i>UGT51</i>
<i>ATG27</i>	–	–	24	<i>ETF1</i>

One of Problems to Be Solved in Autophagy

Much progress has been made in the functional analysis of Atg/Apg proteins. One of the interesting research subjects remained is the substrate selectivity in autophagy. It was suggested that Atg/Apg proteins function in the steps of autophagosome formation, so that we may continue paying attention to an autophagosome membrane and its associated proteins. Inside autophagosome, the cargo of autophagy is not analyzed in detail. Our laboratory previously indicated that autophagy transports cytoplasmic components to the vacuole non-selectively in morphological and biochemical experiments. Immuno-electron microscopy has shown that ribosomes and typical cytosolic marker enzymes, such as alcohol dehydrogenase (ADH) and phosphoglycerate kinase (PGK), are present in the autophagosome and autophagic bodies at the same densities as in the cytosol (Baba *et al.*, 1994; Figure 2). The measurement of the enzymatic activities of ADH, PGK, glucose-6-phosphate dehydrogenase (G6PDH) and glutamate dehydrogenase also supports this conclusion (Takeshige *et al.*, 1992; T. Noda and Y. Ohsumi., unpublished results).

If degradation of long-lived proteins is exclusively mediated by autophagy, all proteins might be expected to have similar lifetimes. However, long-lived proteins have a variety of lifetimes; therefore, the autophagic pathway might have some selectivity. It is known that precursor API and α -mannosidase (via the Cvt pathway), fructose-1, 6-bisphosphatase (via the vacuolar import and degradation, the Vid pathway; Chiang and Schekman, 1991; Hoffman and Chiang, 1996; Klionsky and Ohsumi, 1999) and the peroxisome (via macropexophagy; Tuttle and Dunn, 1995; Klionsky and Ohsumi, 1999) are selectively transported from the cytoplasm to the vacuole using autophagy-like vesicular machinery. Recently, Chiba *et al.* observed that autophagosome-like structure selectively sequestered to the part of chloroplast to the exclusion of thylakoid membranes termed Rubisco containing bodies in wheat leaf cells during natural senescence (Chiba *et al.*, 2003). Microautophagy (Muller *et al.*, 2000) may have the substrate selectivity potentially, in fact, peroxisome and cell nucleus were imported to the vacuole by microautophagy process (via microautophagy; Tuttel and Dunn, 1995; Sakai *et al.*, 1998; Klionsky and Ohsumi, 1999, via piecemeal microautophagy; Roberts

et al., 2003).

To investigate the possibility of selective autophagic degradation, I attempted to compare the amounts of each intracellular protein under growth and starvation conditions in the yeast, *S. cerevisiae*. I performed a systematic analysis using two-dimensional PAGE and MALDI-TOF mass spectrometry to detect the autophagy dependent degradation of intracellular proteins. If this study were able to clear the selective autophagy, it would help clarify another physiological roles of autophagy in the yeast cell.

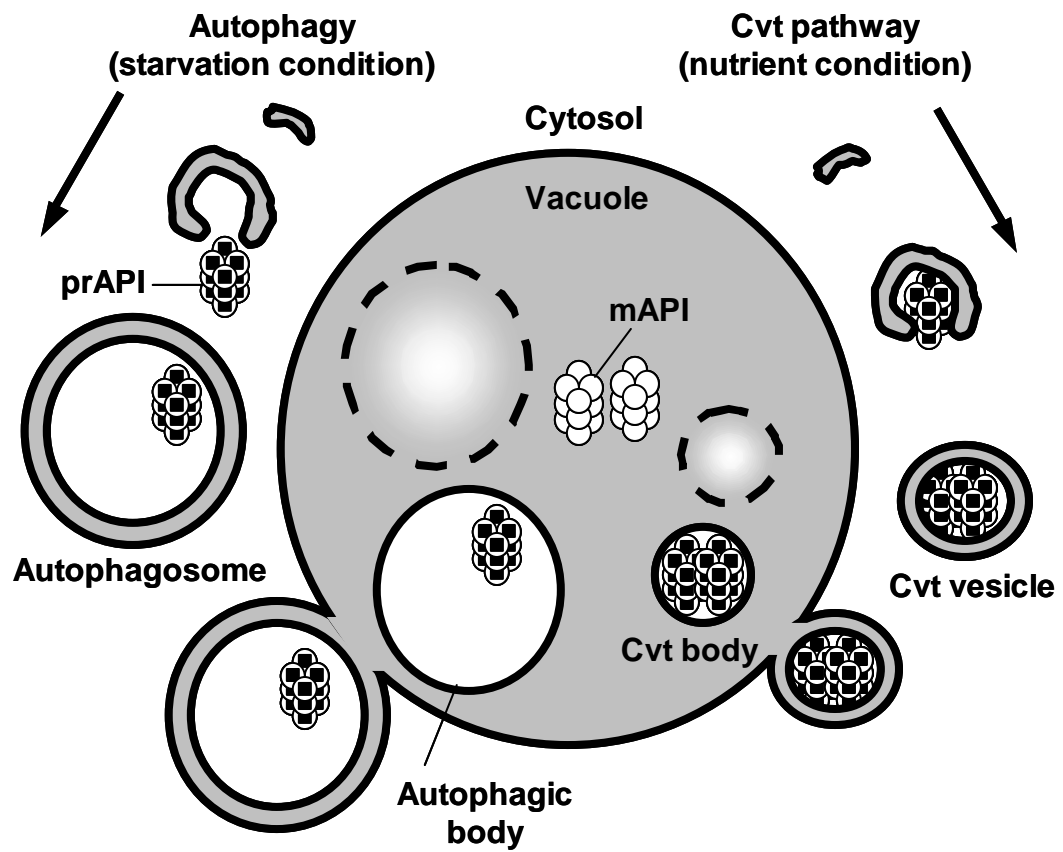


Figure 1. Model of autophagy and the Cvt transport to the vacuole.
 There are many shared mechanistic features for the two pathways.
 prAPI, precursor of aminopeptidase I; mAPI, mature form of
 aminopeptidase I.

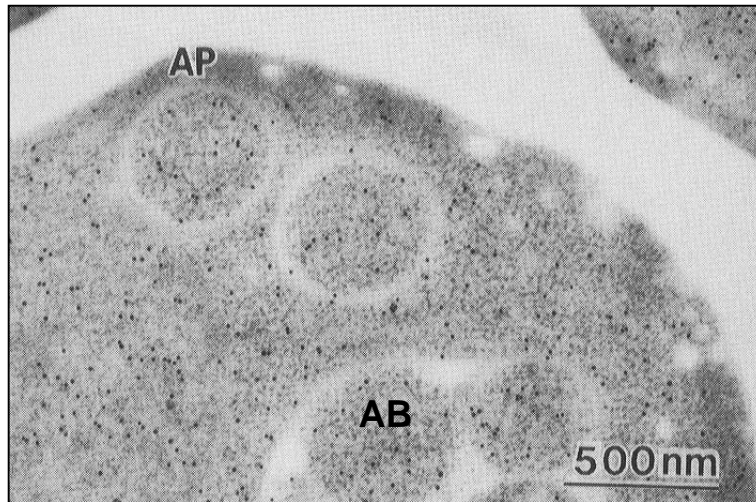


Figure 2. Immuno-staining image of alcohol dehydrogenase in the yeast cell.

Vacuolar proteinase deficient cell contains autophagic bodies in the vacuole and autophagosomes in cytosol (Baba *et al.*, 1994). AP, autophagosome; AB, autophagic body; Bar = 500 nm.

MATERIALS AND METHODS

Yeast Strain and Media

The yeast strains used in this study are listed in Table II. Standard techniques were used for yeast manipulation (Burke *et al.*, 2000). Yeast cells are grown in YPD medium (1% yeast extract, 2% polypeptone and 2% glucose), SD medium (0.17% yeast nitrogen base without amino acids and ammonium sulfate, 0.5% ammonium sulfate and 2% glucose), SD + CA medium (0.17% yeast nitrogen base without amino acids and ammonium sulfate, 0.5% casamino acid, 0.5% ammonium sulfate and 2% glucose) supplemented with 0.002% adenine sulfate, 0.002% uracil, and 0.002% tryptophan if necessary. For nitrogen starvation, SD(-N) medium (0.17% yeast nitrogen base without ammonium sulfate and amino acids, and 2% glucose), for carbon starvation, S(-C) medium (0.17% yeast nitrogen base without ammonium sulfate and amino acids, and 0.5% ammonium sulfate), for nitrogen and carbon starvation, S(-N, C) medium (0.17% yeast nitrogen base without ammonium sulfate and amino acids), and for sulfur starvation, SD(-S) medium (0.17% yeast nitrogen base without sulfur source, and 2% glucose) were used.

Plasmid Construction

DNA manipulations were performed using standard methods (Sambrook *et al.*, 1989). To create the glutathione *S*-transferase (GST)-Ald6p fusion construct (pJO1), the ORF of *ALD6/YPL061w* lacking the initiation codon (1.5 kb) was amplified by genomic PCR using the following primers:

5'-CGCGGATCCACTAAGCTACACTTTGACACTGC-3', and

5'-CCGCTCGAGCAACTTAATTCTGACAGCTTTTACTTC-3'.

This strategy incorporated novel BamHI and XhoI sites into the resulting DNA fragment, which was then cloned into the BamHI and XhoI sites of pGEX-4T-1 (Amersham Bioscience) to yield pJO1.

To create the Ald6p-green fluorescent protein (GFP) genome integration vector (pJO402), novel XbaI sites were added to the terminator sequence (0.5 kb) of *ALD6* by

genomic PCR amplification using the following primers:

5'-GCTCTAGATGTACCAACCTGCATTTCTTTC-3', and

5'-GCTCTAGACGAAGAAGGATGTTATTATATG-3'.

Novel XhoI and BamHI sites were added to the *ALD6* promoter region (0.3 kb) and the *ALD6* ORF lacking the stop codon (1.5 kb) by genomic PCR amplification using the following primers:

5'-CGCTCGAGCACCGACCATGTGGGCAAATTC-3', and

5'-CGCGGATCCCAACTTAATTCTGACAGCTTTTAC-3'.

BamHI sites were added to the ORF of modified GFP (S65T) lacking the initiation codon by PCR amplification using the following primers:

5'-CGCGGATCCCGTAAAGGAGAAGAACTTTTCACTGG-3', and

5'-CGGGATCCTTACTTGTATAGTTCATCCATG-3'.

The resulting DNA fragments were cloned into the pRS306 integration vector (Sikorski and Hieter, 1989) to yield pJO402.

To create the Ald6p overexpression construct (pJO203), XhoI and BamHI sites were added to a sequence containing the *ALD6* ORF (1.5 kb), the promoter region (0.3 kb), and the terminator sequence (0.5 kb) by genomic PCR amplification using the following primers:

5'-CCGCTCGAGCACCGACCATGTGGGCAAATTC-3', and

5'-CGCGGATCCCGAAGAAGGATGTTATTATATGATCTC-3'.

The resulting DNA fragment was cloned into the BamHI and XhoI sites of the pRS426 multicopy plasmid (Sikorski and Hieter, 1989) to yield pJO203.

A QuikChangeTM Site-Directed Mutagenesis Kit (Stratagene) was used to create the Ald6p^{C306S} mutant overexpression construct (pJO213). To generate pJO213, the pJO203 plasmid was amplified by PCR with the following primers:

5'-AGAACGCTGGTCAAATTTCTTCCTCTGGTT-3', and

5'-AACCAGAGGAAGAAATTTGACCAGCGTTCT-3'.

The site of mutagenesis in pJO213 was confirmed by automated DNA sequencing.

To create the expression vectors of Arg1p- or Hsp26p- 3 × hemagglutinin (HA) tagging protein, novel XbaI sites were added to the terminator sequence of *ALD6* (0.3

kb) by genomic PCR amplification using the following primers:

5'-GCTCTAGATGTACCAACCTGCATTTCTTTC-3', and

5'-GCTCTAGACGAAGAAGGATGTTATTATATG-3'.

And novel SpeI sites were added to the coding sequence of HA lacking the initiation codon (0.1 kb) by PCR amplification using the following primers:

5'-GACTAGTTACCCATACGATGTTCTGAC-3', and

5'- GACTAGTTTAAGCGTAATCTGGAACGTC-3'.

Novel XhoI and BamHI sites were added to the each promoter region and the ORF lacking the stop codon (*ARG1/YOL058w* 2.2 kb, and *HSP26/YBR072w* 1.6 kb) by genomic PCR amplification using each following primers:

ARG1: 5'-CCGCTCGAGAGGTTGCCACATACATGGCCAAG-3', and

5'-CGGGATCCCAAAGTCAACTCTTCACCTTTG-3';

HSP26: 5'-CCGCTCGAGCGTTGGACTTTTTTTAATATAAC-3', and

5'-CGGGATCCGTTACCCCACGATTCTTGAGAAG-3'.

The resulting DNA fragments were cloned into the pRS316 centromeric plasmid Sikorski and Hieter, 1989) to yield pJO128 (Arg1p^{HA}) and pJO129 (Hsp26p^{HA}).

Two-dimensional PAGE

Yeast cell lysates were prepared by breaking cells with glass beads in lysis buffer (50 mM Tris-HCl, pH 8.0, 1 mM EDTA, 1 mM PMSF and protease inhibitor cocktail, Roche Applied Science). The lysates were centrifuged at 100,000 × *g* for 1 h, and the supernatant was desalted with NAP-10TM (Amersham Bioscience) gel filtration column. Protein concentration was determined by BCA assay kit (Pierce), and 300 μg of each protein was applied to the gel. Isoelectrofocusing was performed with IPGphor and ImmobilineTM DryStrip pH 4–7, 13 cm (Amersham Bioscience) as described (O'Farrell, 1975; Görg *et al.*, 2000). Strips were re-hydrated together with the isoelectrofocusing buffer (8 M urea, 0.5% v/v IPG Buffer, Amersham Bioscience, and 65 mM DTT) contained sample proteins and isoelectrofocusing was performed for 10 h at 30 V, for 1 h at 200 V, for 1 h at 500 V, for 1 h at 1000 V and for 40000 Vh at 8000 V, at 50 μA/strip and 20°C. Strips were equilibrated by SDS equilibration buffer (50 mM

Tris-HCl, pH 8.8, 6 M urea, 30% v/v glycerol and 2% SDS) with 70 mM DTT for 15 min and then with 140 mM iodoacetamide and 0.004% bromphenol blue for 15 min. Equilibrated gel was subjected to SDS-PAGE (12.5% acrylamide concentration) and stained with Coomassie brilliant blue R-250.

Peptide Mass Finger-printing

Protein spots on two-dimensional PAGE gel were picked, washed with 100 mM ammonium bicarbonate, dehydrated with acetonitrile, and dried in an evaporator. Spots were digested in the gel with 0.5 mg/ml of trypsin (Promega) with 100 mM ammonium bicarbonate for 12 h at 30°C. Digested peptides were extracted from the gel with 10% formic acid and 50% acetonitrile, and desalted with the ZipTip™ C-18 (Millipore). The samples and α -cyano-4-hydroxy-cinnamic acid (Fluka) were mixed at a 1:1 ratio and analyzed by matrix associated laser deionization - time of flight (MALDI-TOF) mass spectrometry, REFLEX III (Bruker). Proteins were identified by searching the ProFound database (<http://129.85.19.192/>).

Antibodies

Ald6p specific antibodies were prepared as follows. The pJO1 plasmid was transformed into *Escherichia coli* (DH5 α), and transformants were grown in LB medium containing 50 μ g/ml ampicillin to $A_{600} = 0.6$. Recombinant protein expression was induced with 1 mM isopropyl- β -D-thiogalactopyranoside for an additional 6 h at 37°C. The recombinant protein was separated by SDS-polyacrylamide gel electrophoresis and simultaneously stained with Gel code (Pierce). The protein band was excised from the gel and eluted with an electric current. The eluted protein-dye complex was used to immunize rabbits. Anti-Ald4p/6p antibodies were purchased from Rockland. Anti-PGK antibody was purchased from Molecular Probes. Anti-ADH antibodies have been described previously (Baba *et al.*, 1994). Anti-API antibodies have been described previously (Hamasaki *et al.*, 2003). Anti-HA epitope antibody (16B12) has purchased from BabCo.

Immuno-blot of Whole-cell Lysates

Immuno-blot was performed as previously described (Kirisako *et al.*, 1999). Whole-cell lysates were prepared by disrupting cells with glass beads in lysis buffer (50 mM Tris-HCl, pH 8.0, 1 mM EDTA, 1 mM PMSF and the protease inhibitor cocktail, Roche Applied Science). Cell lysates were boiled with SDS-sample buffer for 5 min, and these proteins content was determined by BCA assay kit (Pierce). Total protein (10 µg) was subjected to SDS-PAGE (Laemmli, 1970), and transferred to polyvinylidene fluoride membrane (ImmobilonTM-P, Millipore) and detected with a combination of each antibody and peroxidase-conjugated goat anti-rabbit IgG antibody (Jackson) or peroxidase-conjugated goat anti-mouse IgG antibody (Jackson) by the ECL system (Amersham Bioscience).

Pulse-chase Experiments and Immuno-precipitation

Pulse-chase experiments were performed as previously described (Ishihara *et al.*, 2001). Yeast cells were cultured in YPD medium to $A_{600} = 1.0$ at 30°C and were then washed twice and suspended in SD(-N) medium. Cells were pulse labeled for 30 min by adding 1 MBq of [³⁵S]methionine (Perkin-Elmer) / A_{600} unit and chased by adding 0.004% methionine and 0.003% cysteine at 30°C. Each sample was collected at the incubate time

Immuno-precipitation was performed as follows. Cell lysates were prepared by breaking cells with the glass beads in TBS (50 mM Tris-HCl, pH 7.4 and 150 mM NaCl) and 1% SDS. Moreover, they were boiled 5 min, diluted by adding two fold volume TBS and 2% Triton X-100, and centrifuged at $15,000 \times g$ for 1 min to remove insoluble materials. Cell lysate, 0.1% v/v anti-Ald6p or anti-ADH antibodies, 1.25% v/v protein A-SepharoseTM beads (Amersham Bioscience) and the protease inhibitor cocktail (Roche Applied Science) were incubated at 4°C for 2 h. Sample were centrifuged for 1 min precipitated beads were washed once with IP buffer (TBS, 5 mM EDTA, 0.2% SDS and 1% and Triton X-100), once with urea buffer (IP buffer and 2 M Urea), high salt buffer (50 mM Tris-HCl, pH 7.4, 500 mM NaCl, 5 mM EDTA, 0.2% SDS and 1% Triton X-100), once with detergent free buffer (TBS and 5 mM EDTA).

Proteins were eluted in SDS-sample buffer with 5 min boil, and were analyzed by SDS-PAGE (Laemmli, 1970) and autoradiographed with BAS-2000 analyzer (Fuji Film).

Light Microscopy

Fluorescence microscopy was performed using a Delta Vision microscope (Applied Precision) as described (Suzuki *et al.*, 2001). To observe GFP-tagged proteins under a fluorescence microscope, I employed a FITC filter.

Immuno-electron Microscopy

Yeast cells were subjected to rapid freezing and freeze-substitution fixation, and observed as previously reported (Baba *et al.*, 1997). For immuno-electron microscopy, ultrathin sections were collected onto formvar-coated nickel grids and blocked in PBS containing 2% BSA at room temperature for 15 min. Incubations were carried out by floating grids on a 20 μ l drop of a 1:1,000 dilution of anti-Ald6p antiserum, at room temperature for 1.5 h. After washing, the grids were incubated for 1 h with 5 or 10 nm gold-conjugated goat anti-mouse IgG (Bio Cell Lab.). The grids were washed several times in PBS followed by several drops of distilled water and fixed with 1% glutaraldehyde for 3 min. The sections were stained with 4% uranyl acetate for 7 min and examined.

Subcellular Fractionation

Subcellular fractionation was performed as previously described (Ishihara *et al.*, 2001). Growing or nitrogen starved cells (50 A_{600} unit) were harvested, washed with 100 mM Tris-HCl, pH 9.0, 40 mM 2-mercaptoethanol, and were converted to spheroplasts in 1 ml of SD + CA or SD(-N) supplemented with 1.4 M sorbitol and 20 mM Tris-HCl, pH 7.5. After the addition of 0.5 mg of Zymolyase-100T (Seikagaku Corporation), the cell suspensions were incubated at 30°C for 30 min. The spheroplasts were harvested, washed with 1 M sorbitol, and re-suspended at 50 A_{600} unit/ml in a lysis buffer (1 M sorbitol, 0.5% FicollTM 400 and 1 mM MgCl₂). The lysates were passed

through a polycarbonate filter with 3 μm pores (Nucleopore, Whatman). Cleared lysate (Total) was generated by two consecutive centrifugations at $500 \times g$ for 5 min. The lysates were spun at $13,000 \times g$ for 15 min to separate the pellet (P13), and the supernatant was centrifuged again at $100,000 \times g$ for 1 h to generate a pellet (P100) and supernatant (S100). P13 and P100 were re-suspended in lysis buffer equal to the original volume.

Proteinase K Protection Assay

Proteinase K protection assay was performed as previously described (Ishihara *et al.*, 2001). To examine proteinase K-sensitivity, each Subcellular fraction without protease inhibitors was treated with 2 mg/ml proteinase K (Roche) on ice for 30 min with or without 1% Triton X-100. The samples were precipitated with 10% trichloroacetic acid, washed once with cold acetone, re-suspended in SDS-sample buffer, and analyzed by SDS-PAGE (Laemmli, 1970) and immuno-blot.

Determination of Cell Viability

Determination of yeast cell viability was performed as previously described (Tsukada and Ohsumi, 1994). Cell viability was measured by phloxine B (final concentration 2 $\mu\text{g}/\text{ml}$; Sigma) stain, and fluorescence microscopy with a blue filter. Brightly fluorescent cells were counted as dead cells.

Assay of Ald6p Enzymatic Activity

The activity of NADP^+ - and Mg^{2+} -dependent acetaldehyde dehydrogenase (Ald6p) was determined by monitoring the NADPH production of NADP^+ using fluorophotometer (Hitachi F-3010), as described (Dickinson, 1996) with some modifications. The assay mixture containing 50 mM Tris-HCl, pH 8.0, 1 mM acetaldehyde, 0.5 mM NADP^+ , 15 mM MgCl_2 , 1 mM pyrazole and a preparation of enzyme.

Northern Blot

Total RNA isolation was performed RNeasy Mini Kit (QIAGEN) according to the appended protocol. Total RNA (5 µg) separated on 1% agarose containing 2.2 M formaldehyde by electrophoresis, and transferred to BIODYNE A membrane (Pall). DIG-labeled probes (0.5 kb) for *ARG1*, *HSP26* and *ACT1/YFL039c* mRNA were prepared from each ORF fragment using PCR DIG Probe Synthesis Kit (Roche Applied Science) according to the appended protocol, and PCR amplification using each following primers:

ARG1: 5'-TCTAAGGGAAAAGTTTGTTT-3', and

5'-TGGTTTGGGCGACGGGAATA-3';

HSP26: 5'-TCATTTAACAGTCCATTTTT-3', and

5'-TGTCTGCATCCACACCTGGG-3';

ACT1: 5'-CGGTAGAGATTTGACTGACT-3', and

5'-TTGTTGGAAGGTAGTCAAAG-3'.

The mRNA-transferred membrane was incubated with each probe at 50°C overnight, and signals were detected by Anti-Digoxigenin-AP (Roche Applied Science), CDP-*Star* (Roche Applied Science) and LAS-1000 system (Fuji Film).

Amino Acid Analysis of Whole Cell

Determinate quantity of free amino acids in whole cell was performed as previously described (Ohsumi *et al.*, 1988; Kitamoto *et al.*, 1988). Yeast cells of 10 A₆₀₀ unit were harvested and washed twice with distilled water. The cells were suspended in 500 µl of distilled water and boiled for 15 min. The suspension was centrifuged for 3 min at 5,000 rpm, and the supernatant was collected as extraction of whole-cell amino acid. This extract was analyzed with an amino acid analyzer (Hitachi L-8500A).

Assay of in vivo Protein Synthesis

Yeast cells of 1 A₆₀₀ unit were washed in SD(-N) medium twice, and were suspended in SD(-N) medium containing [¹⁴C]valine (Moravec MC277) at a final concentration of 74 kBq/ml and 10 µM. The cultures were labeled for 0, 2 and 4 min at

30°C and were then added 10 volumes cold distilled water or 11% w/v TCA solution. In TCA suspension, it kept at 90°C, 10 min for peptidyl-tRNA degradation, following it kept at 4°C, 30 min for protein precipitation. Both distilled water and 10% TCA suspensions were then filtered with 0.45 µm pore membranes (MFTM-membrane, Millipore). These membranes were dried up and were determined radioactivity in a liquid scintillation counter (Packard TRI-CARB 2700TR).

Table II. Yeast strains used in this study.

Strain	Genotype	Source
SEY6210	<i>MATα his3Δ200 leu2-3,112 lys2-801 trp1Δ901 ura3-52 suc2Δ9 GAL</i>	Robinson <i>et al.</i> , 1988
KVY118	SEY6210; Δ atg7:: <i>HIS3</i>	Kirisako <i>et al.</i> , 2000
JOY67	SEY6210; Δ atg7:: <i>kanMX4</i>	This study
JOY676	SEY6210; Δ atg7:: <i>HIS3</i> Δ ald6:: <i>kanMX4</i>	This study
JOY674	SEY6210; Δ atg7:: <i>HIS3</i> Δ ald4:: <i>kanMX4</i>	This study
JOY617	SEY6210; Δ atg17:: <i>HIS3</i>	This study
TVY1	SEY6210; Δ pep4:: <i>LEU2</i>	Gerhardt <i>et al.</i> , 1998
JOY6p4	SEY6210; Δ pep4:: <i>kanMX4</i>	This study
JOY6005	SEY6210; Δ pep4:: <i>LEU2</i> Δ ald6:: <i>ALD6-GFP</i>	This study
JOY6006	SEY6210; Δ pep4:: <i>LEU2</i> Δ atg7:: <i>HIS3</i> Δ ald6:: <i>ALD6-GFP</i>	This study
JOY66	SEY6210; Δ ald6:: <i>kanMX4</i>	This study
JOY64	SEY6210; Δ ald4:: <i>kanMX4</i>	This study
JOY69	SEY6210; Δ atg11:: <i>URA3</i>	This study
JOY622	SEY6210; Δ vid22:: <i>kanMX4</i>	This study
KVY4	SEY6210; Δ ypt7:: <i>LEU2</i>	Kihara <i>et al.</i> , 2001
YAK1	SEY6210; Δ ypt7:: <i>HIS3</i> Δ atg1:: <i>LEU2</i>	This study
X2180-1B	<i>MATα SUC2 mal mel gal2 CUP1</i>	Y. G. S. C.
JOY27	X2180-1B; Δ atg7:: <i>kanMX4</i>	This study
MT13-3A	<i>MATα SUC2 mal mel gal2 CUP1 atg1-1</i>	Tsukada and Ohsumi, 1994
MT2-4-1	<i>MATα SUC2 mal mel gal2 CUP1 atg2-4-1</i>	Tsukada and Ohsumi, 1994
WCG4a	<i>MATα leu2-3,112 ura3 his3-11,15</i>	Heinemeyer <i>et al.</i> , 1993
WCG4-11a	<i>MATα leu2-3,112 ura3 his3-11,15 pre1-1</i>	Heinemeyer <i>et al.</i> , 1993
BY4741	<i>MATα his3Δ1 leu2Δ0 met15Δ0 ura3Δ0</i>	Brachmann <i>et al.</i> , 1998
Y00753	BY4741; Δ ald2:: <i>kanMX4</i>	Brachmann <i>et al.</i> , 1998

Y00752	BY4741; $\Delta ald3::kanMX4$	Brachmann <i>et al.</i> , 1998
Y01671	BY4741; $\Delta ald4::kanMX4$	Brachmann <i>et al.</i> , 1998
Y00213	BY4741; $\Delta ald5::kanMX4$	Brachmann <i>et al.</i> , 1998
<u>Y02767</u>	<u>BY4741; $\Delta ald6::kanMX4$</u>	<u>Brachmann <i>et al.</i>, 1998</u>

Y. G. S. C., Yeast Genetic Stock Center.

RESULTS

I. Studies on Degradation of Ald6p, a Preferential Substrate of Autophagy

Screen for Proteins Reduced under Nitrogen Starvation

To investigate the possibility of selective autophagic degradation, I attempted to compare the amounts of each intracellular protein under nutrient growth and nitrogen starvation conditions in the yeast, *S. cerevisiae*. I investigated the expression profiles of soluble proteins using two-dimensional PAGE. Using this method, I expected to be able to identify cellular proteins whose levels decreased during nitrogen starvation. Yeast cells were grown at 30°C in YPD medium, were harvested at middle logarithmic phase ($A_{600} = 1.0$), and were washed twice with starvation medium. The cells were then transferred to SD(-N) medium and incubated for 24 h. I chose a long-term stress period of 24 h in order to observe obvious differences in protein expression; importantly, most of the cells were still viable at this time point (Tsukada and Ohsumi, 1994).

In my two-dimensional PAGE experiments, the soluble fraction of cell lysate separated approximately 800–1,000 spots on a Coomassie brilliant blue R-250 stained the gel. Nitrogen starved wild-type cells (SEY6210) showed the protein spots more than nutrient growing cells (Figure 3). However, nitrogen starved autophagy defective $\Delta atg7/apg7$ cells (KVY118) showed the same number of protein spots as growing cells (data not shown). Trabalzini *et al.* recently detected many protein fragments on the two-dimensional PAGE gel in the yeast cells of late stationary phase. These fragments did not appear in the presence of 1 mM PMSF, inhibitor of vacuolar proteinase B (Trabalzini *et al.*, 2003). Thus, the part of increased spots may come from fragmentation of abundant proteins.

The intense protein spots by tryptic digestion and MALDI-TOF mass spectrometry analyses (see Materials and Methods; Figure 4) allowed the identification of several proteins. In both wild-type (SEY6210) and autophagy defective $\Delta atg7$ (KVY118) yeast cells, most proteins showed little change after starvation (Figure 5

lanes 1–4).

In figure 5 lanes 5–8, several proteins showed increased levels after nitrogen starvation, including typical proteins of environment stress responses (Eno1p/Hsp48p, enolase I; Hsp26p, heat shock protein of 26-kDa), enzyme of amino acid biosynthesis (Arg1p, argininosuccinate synthetase) and quenching enzyme of reactive oxygen species (Sod2p, mitochondrial manganese superoxide dismutase). However, these specific proteins did not increase by nitrogen starvation in autophagy-defective cells (Figure 5 lanes 5–8), suggesting that starvation-induced up-regulation of these proteins requires the supply of amino acids produced by autophagy. I will describe particulars about this phenomenon in "Result – II. Amino Acids Supply from Autophagy Is Essential for Protein Synthesis".

In contrast, only few as proteins exhibited the apparent decrease during starvation in wild-type cells (Figure 5 lanes 9 and 10). Among them, cytosolic acetaldehyde dehydrogenase (Ald6p) showed the most distinctive difference between the wild-type and $\Delta atg7$ mutants. Therefore, I focused on this protein for further analysis.

Ald6p, Cytosolic Acetaldehyde Dehydrogenase

Ald6p is Mg^{2+} - and NADPH-dependent cytosolic acetaldehyde dehydrogenase, which catalyzes the conversion of acetaldehyde to acetate in the cytosol (EC 1.2.1.3; acetaldehyde + $NADP^+$ \rightarrow acetate + NADPH; Meaden *et al.*, 1997). The *S. cerevisiae* genome encodes five or more different members of the aldehyde dehydrogenase family. Ald4p is the major K^+ - and NAD^+ -dependent mitochondrial acetaldehyde dehydrogenase (Tessier *et al.*, 1998) and Ald5p is a minor K^+ -dependent mitochondrial acetaldehyde dehydrogenase, which is induced when cells are grown in ethanol containing medium (Kurita and Nishida, 1999). Ald2p and Ald3p are closely related cytosolic enzymes that are required for *in vivo* pantothenic acid biosynthesis via conversion of 3-aminopropanol to β -alanine (White *et al.*, 2003). Ald4p, Ald5p and Ald6p function in the conversion of acetaldehyde to acetate, which is a key intermediate during fermentation of sugars and growth on ethanol, and are consequently important

for acetyl-CoA production (Saint-Prix *et al.*, 2004). In contrast, Ald2p and Ald3p may not contribute to the oxidation of acetaldehyde *in vivo* (Saint-Prix *et al.*, 2004). Therefore, Ald6p is the only cytosolic acetaldehyde dehydrogenase in the yeast cell.

During fermentative growth in yeast, pyruvate is decarboxylated into acetaldehyde by pyruvate decarboxylase, which is, in its turn, reduced into ethanol in the cytosol by ADH (Murray *et al.*, 2003; Figure 6). During respiratory metabolism in yeast, pyruvate can enter the mitochondria by a specific carrier and is decarboxylated and oxidized into acetyl-CoA by pyruvate dehydrogenase, a multi-enzyme complex located in the matrix (Murray *et al.*, 2003). In addition, a pyruvate dehydrogenase bypass located in the cytosol converts pyruvate into acetyl-CoA by the action of the following enzymes: pyruvate decarboxylase, Ald6p, Ald4p and acetyl-CoA synthetases (Gounaris *et al.*, 1971; van den Berg and Steensma, 1995; Dicinson, 1996; van den Berg *et al.*, 1996; Meaden *et al.*, 1997; Boubekour *et al.*, 1999; Figure 6). Acetyl-CoA synthesized in the cytosol is either directly used for the fatty acid biosynthetic pathway or enters the mitochondria via the carnitine acetyltransferase system (Kispal *et al.*, 1991; Kispal *et al.*, 1993; Murray *et al.*, 2003; Figure 6). Acetyl-CoA can only move from the cytosol into mitochondria (Kispal *et al.*, 1991). Ald6p contributes to the productions both cytosolic acetyl-CoA and NADPH in the yeast cell.

Proteins Required for the Reduction of Ald6p

I could purchase anti-yeast aldehyde dehydrogenase polyclonal antibodies as a commercial product (Rockland). However, these commercial antibodies cross-reacted both Ald4p and Ald6p (Figure 7A). I also prepared Ald6p specific antibodies (see Material and Methods). Prepared antiserum detected Ald6p nicely much more than Ald4p at immuno-blot (Figure 7B). In this study, I used two types antibodies both anti-Ald4p/6p and Anti-Ald6p as appropriate.

Using immuno-blot analyses, I attempted to determine which proteins are required for the reduction of Ald6p. In wild-type cells (SEY6210), the amount of Ald6p decreased in a near-linear manner, and was ultimately reduced to 18% of the original level after 24 h starvation (Figure 8). In contrast, Ald6p levels decreased only slightly in

$\Delta atg7$ mutant cells (KVY118). I next investigated whether the amount of Ald6p was reduced in various yeast strains that are defective in various steps of autophagy. $\Delta atg7$ (KVY118), $\Delta atg17/apg17$ (JOY617) and all $\Delta atg/apg$ mutant cells tested showed a similar defect in the loss of Ald6p (parts shown in Figure 9 lanes 1, 2, 4, 5, 7 and 8). The decrease of Ald6p also required Ypt7p, a protein that is essential for the fusion of autophagosomes to vacuoles (Kirisako *et al.*, 1999), and Pep4p, vacuolar proteinase A (Figure 9 lanes 1, 2 and 9–12). In the presence of 1 mM PMSF, the decrease of Ald6p was inhibited under nitrogen starvation (Figure 9 lanes 1–6).

The selective transport of vacuolar enzymes (via the Cvt pathway), such as API and α -mannosidase, is known to utilize all of the Apg/Atg proteins except Atg17p (Kamada *et al.*, 2000). Atg11p/Cvt9p and Atg19p/Cvt19p function only in the Cvt vesicle formation, and do not play a role in autophagosome formation (Kim *et al.*, 2001; Scott *et al.*, 2001). In $\Delta atg11$ (JOY69) and $\Delta atg19$ mutant cells, Ald6p was reduced in a similar manner to wild-type cells under nitrogen starvation (Figure 9 lanes 1, 2, 13 and 14; data for $\Delta atg19$ not shown). As expected, another system of vacuolar transport, the Vid pathway (Hoffman and Chiang, 1996; Klionsky and Ohsumi, 1999; Brown *et al.*, 2002) was not involved in this phenomenon (Figure 9 lanes 1, 2, 15, 16).

One mutant allele of the proteasome subunit PRE1 is *pre1-1*, which is frequently used for the following reasons: the *pre1-1* mutation causes a defect in the degradation of short-lived proteins, ubiquitinated proteins (Heinemeyer *et al.*, 1991; Heinemeyer *et al.*, 1993) and N-end rule substrates (Richer-Ruoff *et al.*, 1992; Seufert and Jentsch, 1992) at 30°C. In *pre1-1* mutant cells (WCG4-11a), Ald6p was decreased similarly to wild-type cells (WCG4a) under nitrogen starvation, indicating that Ald6p is not a substrate for proteasome-mediated degradation (Figure 10). Taken together, these mutant studies indicate that the reduction of Ald6p requires all of the Atg/Apg proteins and the processes of vacuolar proteolysis. However, Atg/Cvt proteins, Vid proteins, and proteasomal degradation are not involved in this phenomenon.

Reduced Ald6p Levels Implied a Rapid Degradation

I hypothesized that the decrease in Ald6p levels was the result of rapid

degradation during nitrogen starvation. To examine this possibility, the kinetics of Ald6p degradation was measured by pulse-chase experiments. I sought an optimal ratio of yeast cells lysate per antibodies using non-radioactive immuno-precipitation and immuno-blot to accomplish quantitative pulse-chase experiments. Since Ald6p and ADH exist abundantly in yeast cells, "the ratio of 0.1% antibodies in 1 A₆₀₀ unit cell lysate" did not saturate the binding capacity of antibodies (data not shown). The binding capacity of both anti-Ald6p and anti-ADH antibodies was saturated by "the ratio of 0.1% antibodies in 0.05 A₆₀₀ unit cell lysate" (Figure 11A). These conditions were adopted for radioactive pulse-chase experiment.

Wild-type (SEY6210) and $\Delta atg7$ (KVY118) cells were pulse-labeled for 30 min with [³⁵S]methionine and chased with cold methionine and cysteine for 0, 3, 6 and 9 h. In wild-type cells, the Ald6p was rapidly degraded and was barely detectable after 6 h of chase (Figure 11B). In contrast, the degradation rate of Ald6p was clearly slower in $\Delta atg7$ mutant cells. In addition, ADH, a known non-selective marker of autophagy (Baba *et al.*, 1994), did not show rapid degradation like Ald6p (Figure 11B). The reduction of Ald6p levels implied a rapid degradation dependent on Atg7p during nitrogen starvation. These results suggest that Ald6p is transported to the vacuole and degraded much more rapidly than typical cytosolic proteins.

Ald6p Was Degraded in the Vacuole with Autophagic Body

The process of Ald6p vacuolar transport was detected by subcellular fractionation using $\Delta pep4$ cells that accumulate autophagic bodies in the vacuole under nitrogen starvation. Cytosolic Ald6p was mostly recovered in the S100 fraction, and mitochondrial Ald4p was in the P13 fraction in the growing cell (Figure 12 lanes 1–4). In nitrogen-starved $\Delta pep4$ cells (TVY1), API was fractionated as a precursor form in the P13 fraction, which is dependent on Atg7p (Figure 12 lanes 9–24). This suggests that a precursor form of API is in the autophagic bodies. In nitrogen-starved $\Delta pep4$ cells, Ald6p behaved similarly (Figure 12 lanes 9–24), and was fractionated into the P13 fraction (Figure 12 lane 14). Ald6p was also expected to be in the autophagic bodies.

The process of Ald6p vacuolar transport was also visualized by expressing

physiological levels of an Ald6p-GFP fusion protein from the authentic *ALD6* promoter. Upon starvation, the vacuoles gradually became fluorescent. In addition, in $\Delta pep4$ cells (JOY6005), many bright dots, which were presumably autophagic bodies, were observed moving around in the vacuole (Figure 13). In $\Delta pep4 \Delta atg7$ double mutant cells (JOY6006), no fluorescence was observed in the vacuoles, but rather, the cytosol was evenly stained (Figure 13). Furthermore, I performed immuno-electron microscopy using anti-Ald6p and anti-ADH sera. In cells after 24 h starvation, gold particles for Ald6p were concentrated in autophagic bodies (Figure 14). Quantitative measurement revealed that the vacuole contained a 5.0 ± 0.6 ($n = 8$) fold greater signal than the cytosol. Because Ald6p was transported to the vacuole in autophagic bodies during nitrogen starvation, I hypothesized that transport of Ald6p from the cytosol to the vacuole occurred via the autophagosome.

Ald6p Was Preferentially Transported to the Vacuole via the Autophagosome

Our laboratory previously reported that $\Delta ypt7$ cells accumulate autophagosomes in the cytosol under nitrogen starvation (Kirisako *et al.*, 1999). Using precursor API as a selective cargo marker of autophagosomes, Ishihara *et al.* showed the low speed pellet (P13) fraction enriches the autophagosomes (Ishihara *et al.*, 2001; Figure 15). So next, I studied the behavior of Ald6p in $\Delta ypt7$ cells (KVY4). Under growing conditions precursor API was exclusively resided in the high speed supernatant (S100), but under nitrogen starvation conditions a significant portion was recovered in the P13 fraction as reported (Ishihara *et al.*, 2001, Figure 16A). Similarly, Ald6p was recovered in the P13 fraction only under nitrogen starvation condition (Figure 16A). This fraction completely diminished in $\Delta ypt7 \Delta atg1/apg1$ mutant (YAK1, Figure 16B lanes 5–8), indicating that certain amount of Ald6p is in the autophagosomes. As shown in Figure 17, Ald6p and precursor API in P13 fraction were resistant to proteinase K treatment, but were digested in the presence of 1% Triton X-100. This also supported that Ald6p is sequestered into autophagosomes.

I also quantified the amount of Ald6p in the P13 fraction. Precursor API forms one or a few large complexes named the Cvt complex in the cytosol, and are taken up

by an autophagosome at once (Suzuki *et al.*, 2002). PGK is shown to be distributed evenly in the autophagosome, autophagic bodies and cytosol (Baba *et al.*, 1994). As shown in Figure 16C, Ald6p translocated to the P13 fraction much more efficiently than PGK (Recovery in P13 fraction; Ald6p = $38.2 \pm 2.1\%$ n = 5; PGK = $14.9 \pm 1.5\%$ n = 5, Figure 16C), but less than Precursor API ($67.2 \pm 5.9\%$ n = 5). Taken together, I concluded that Ald6p is preferentially sequestered into autophagosome, possibly in a different manner with the substrates for the Cvt pathway.

Phenotype of ALD6 Disruptant Cells

All *atg/apg* mutants showed quite similar growth phenotypes; they grew normally just like wild-type cells. They failed to induce bulk protein degradation under various nutrient-depletion conditions. As expected homozygous diploid with any *atg/apg* cells could not perform sporulation (Tsukada and Ohsumi, 1993). This cell differentiation triggered by nitrogen depletion must require bulk protein degradation via autophagy for intracellular remodeling. Another characteristic feature of autophagy-defective mutants is loss of viability during nitrogen starvation. These mutants start to die after 2 days of starvation and almost completely lose viability after 5 days (Tsukada and Ohsumi, 1993). Under carbon starvation, they can maintain their viability even prolonged starvation. Unbalance of nitrogen and carbon sources may cause this phenotype. I interested whether Ald6p was also degraded under carbon starvation; however, the amount of Ald6p was not decreased under carbon or nitrogen/carbon starvation condition (Figure 18). From this result, I expected that the absence of Ald6p might be important for the survival under nitrogen starvation.

Using $\Delta ald6$ mutant cells, I examined the physiological relevance of the preferential degradation of Ald6p during starvation. The growth of $Atg^+ \Delta ald6$ (JOY66) and $\Delta atg7 \Delta ald6$ (JOY676) cells were slower than wild-type (SEY6210) and $\Delta atg7$ (KVY118) cells in YPD medium (Figure 19A; Meaden *et al.*, 1996). $\Delta atg7 \Delta ald6$ mutant (JOY676) cells also started to die after 2 days of nitrogen starvation; but its viability decreased more slowly than that of $\Delta atg7$ mutant cells (KVY118; Figure 19B). The viability of $Atg^+ \Delta ald6$ cells (JOY66) also improved slightly than that of wild-type

cells (Atg⁺ *ALD6*; SEY6210) under nitrogen starvation. However, disruption of a mitochondrial acetaldehyde dehydrogenase (Ald4p), Atg⁺ Δ *ald4* (JOY64) and Δ *atg7* Δ *ald4* (JOY674) cells had no effect on the viabilities of wild-type (SEY6210) and Δ *atg7* (KVY118) cells, respectively (Figure 20B).

Furthermore, I also examined on the Ald6p overexpressing cells harboring multicopy plasmid. The overproducers expressed about three folds as much as wild-type in the enzymatic activity (Table III). Overexpressed Ald6p was not degraded fully by autophagy for 24 h nitrogen starvation (Figure 21). It is possible that the autophagic degradation for Ald6p may reach saturation, however, it is a suitable condition for the propose of the physiological relevance of Ald6p under nitrogen starvation. Wild-type cells (Atg⁺) expressing Ald6p via multicopy plasmid (JOY66 harboring on pJO203 multicopy plasmid) showed a defect in the maintenance of viability during nitrogen starvation (Figure 22). These results indicate that abundant Ald6p causes the decrease of viability, and absence of Ald6p improves viability under nitrogen starvation.

Ald6p Enzymatic Activity May Be Disadvantageous during Nitrogen Starvation

I next asked whether Ald6p enzymatic activity or the protein molecule itself is harmful to the cell under nitrogen starvation. To address it I constructed an inactive Ald6p mutant. Farres *et al.* isolated recombinant Aldh2^{C321S} from *Rattus norvegicus* liver mitochondrial class-II aldehyde dehydrogenase (Aldh2). This highly conserved cysteine-321 is an active site residue whose thiol group binds to the aldehyde group of the substrate (Farres *et al.*, 1995; Figure 25A). Ald6p cysteine-306, which corresponds to *R. norvegicus* Aldh2 cysteine-321, was changed to a serine residue by site-directed mutagenesis (Figure 25B). Ald6p^{C306S} completely lost NADP⁺ and Mg²⁺-dependent acetaldehyde dehydrogenase activity (Table III), however, this mutant protein showed the stable expression (data not shown).

Overexpression of Ald6p^{C306S} in Atg⁺ and Δ *atg7* cells (JOY66 harboring pJO213 plasmid, and JOY676 harboring pJO213 plasmid) had no effect on viabilities of Atg⁺ Δ *ald6* (JOY66) and Δ *atg7* Δ *ald6* (JOY676), respectively (Figure 24). These results indicate that the acetaldehyde dehydrogenase activity of cytosolic Ald6p may have a

disadvantageous effect on the survival of yeast cells during nitrogen starvation.

Table III. Ald6p activity of overexpression and C306S mutant.

Wild-type (SEY6210), $\Delta atg7$ (KVY118), $\Delta ald6$ (JOY66) and $\Delta atg7 \Delta ald6$ (JOY676) cells growing in YPD medium ($A_{600} = 1.0$) were used. Blank, harboring pRS426 multicopy plasmid; *ALD6*, harboring pRS426::*ALD6* (pJO203) multicopy plasmid; *ald6*^{C306S}, harboring pRS426::*ald6*^{C306S} (pJO213) multicopy plasmid; Ald6p specific activity, NADP⁺ and Mg²⁺-dependent acetaldehyde dehydrogenase specific activity ($\mu\text{mol NADPH}\cdot\text{min}^{-1}\cdot\text{mg protein}^{-1}$).

<u>Genotype</u>	<u>Plasmid</u>	<u>Ald6p specific activity</u>
Wild-type	Blank	45.3 ± 1.9
$\Delta atg7$	Blank	43.1 ± 1.1
$\Delta ald6$	Blank	Not detected
$\Delta atg7 \Delta ald6$	Blank	Not detected
$\Delta ald6$	<i>ALD6</i>	128.3 ± 2.9
$\Delta atg7 \Delta ald6$	<i>ALD6</i>	128.1 ± 3.0
$\Delta ald6$	<i>ald6</i> ^{C306S}	Not detected
$\Delta ald6 \Delta atg7$	<i>ald6</i> ^{C306S}	Not detected

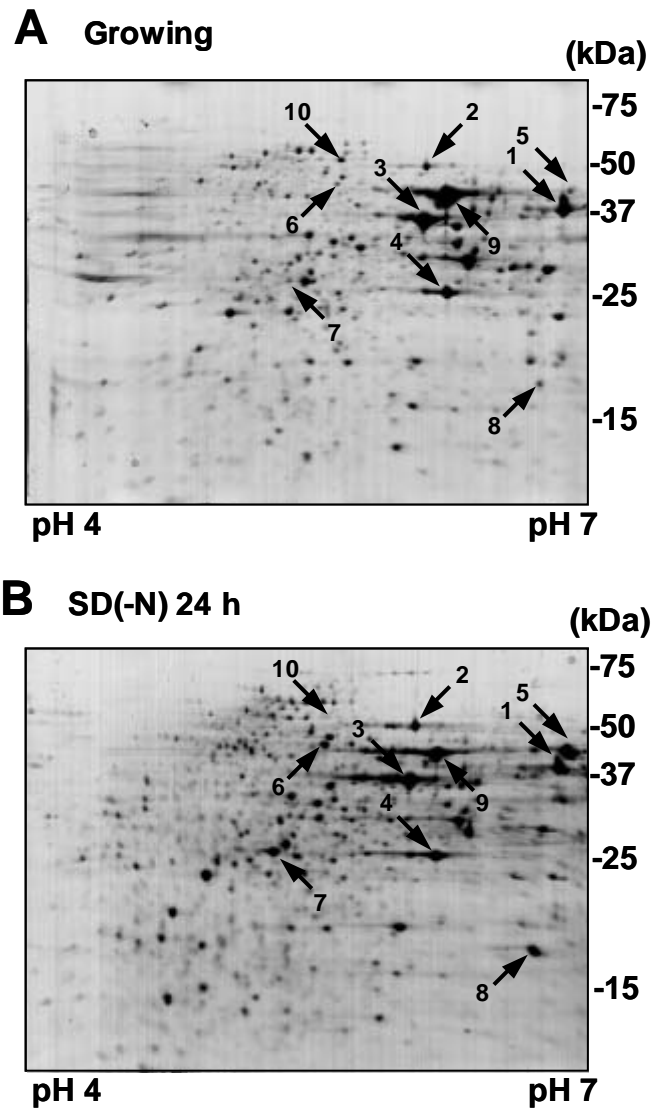


Figure 3. Two-dimensional PAGE of cell lysate before and after nitrogen starvation.

Soluble fraction of wild-type (SEY6210) cell lysate (300 μ g protein) was subjected. Proteins on the gel were stained by Coomassie brilliant blue R-250. Growing, growing in YPD medium ($A_{600} = 1.0$); SD(-N) 24 h, nitrogen-starved in SD(-N) medium for 24 h.

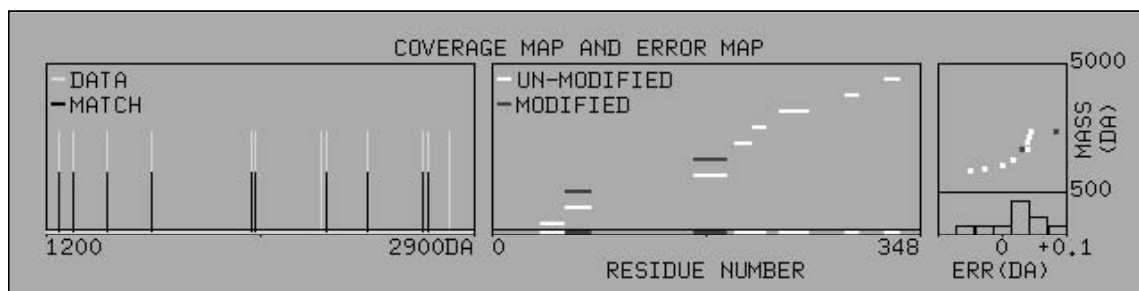
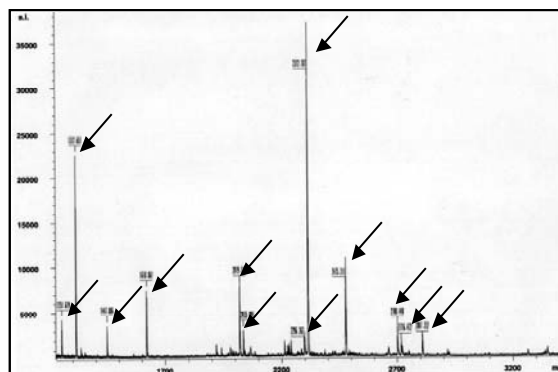
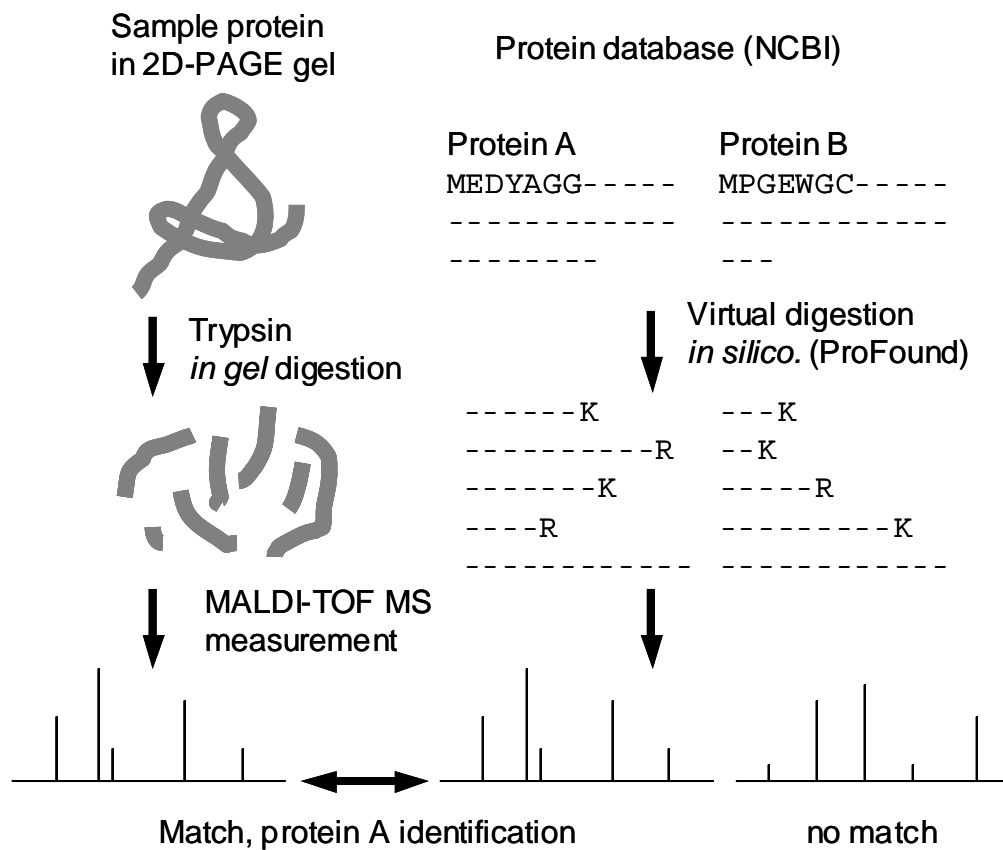


Figure 4. Illustration of procedures of peptide mass finger-printing.

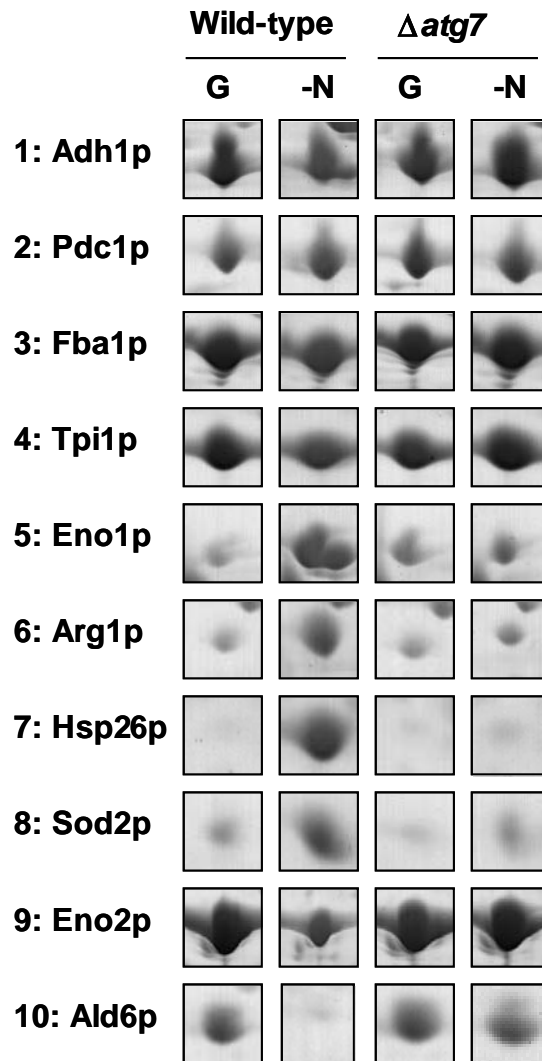


Figure 5. Three expression patterns of protein spots before/after nitrogen starvation.

These spots were identified by peptide mass-finger printing. These spot numbers correspond to arrowheads of figure 4. Wild-type (SEY6210) and $\Delta atg7$ (KVY118) cells were used. G, growing in YPD medium ($A_{600} = 1.0$); -N, nitrogen-starved in SD(-N) medium for 24 h; Adh1p, alcohol dehydrogenase I; Pdc1p, pyruvate dehydrogenase isozyme I; Fba1p, fructose-bisphosphate aldolase II; Tpi1p, triosephosphate isomerase; Eno1p, enolase I; Arg1p, argininosuccinate synthetase; Hsp26p, heat shock protein of 26-kDa; Sod2p, mitochondrial manganese superoxide dismutase; Eno2p, enolase II; Ald6p, cytosolic acetaldehyde dehydrogenase.

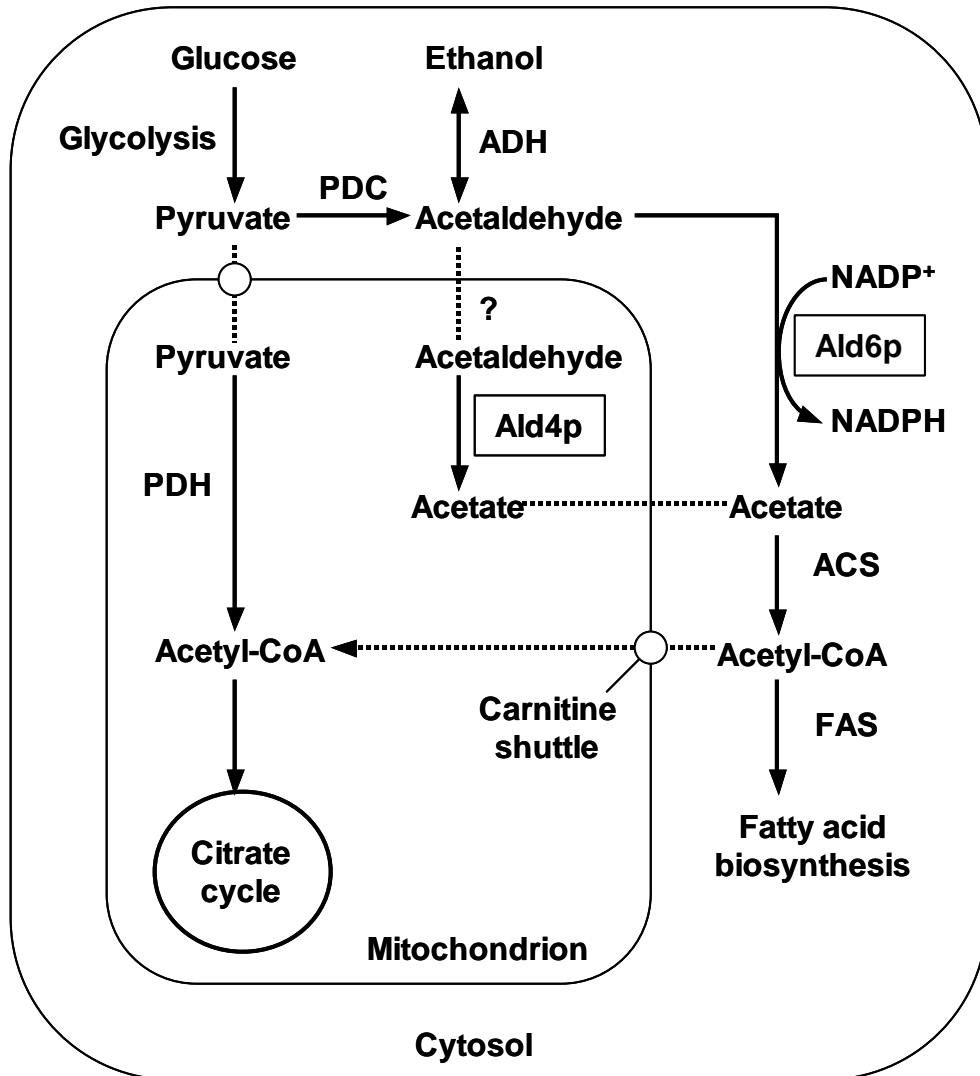


Figure 6. Cytosolic acetaldehyde dehydrogenase involves in a production of cytosolic acetyl-CoA and NADPH.

Cytosolic acetyl-CoA is utilized as the substrate of fatty acid biosynthesis or citrate cycle. ACS, acetyl-CoA synthase; ADH, alcohol dehydrogenase; Ald4p, mitochondrial acetaldehyde dehydrogenase; Ald6p, cytosolic acetaldehyde dehydrogenase; FAS, fatty acid synthase; PDC, pyruvate decarboxylase; PDH, pyruvate dehydrogenase complex.

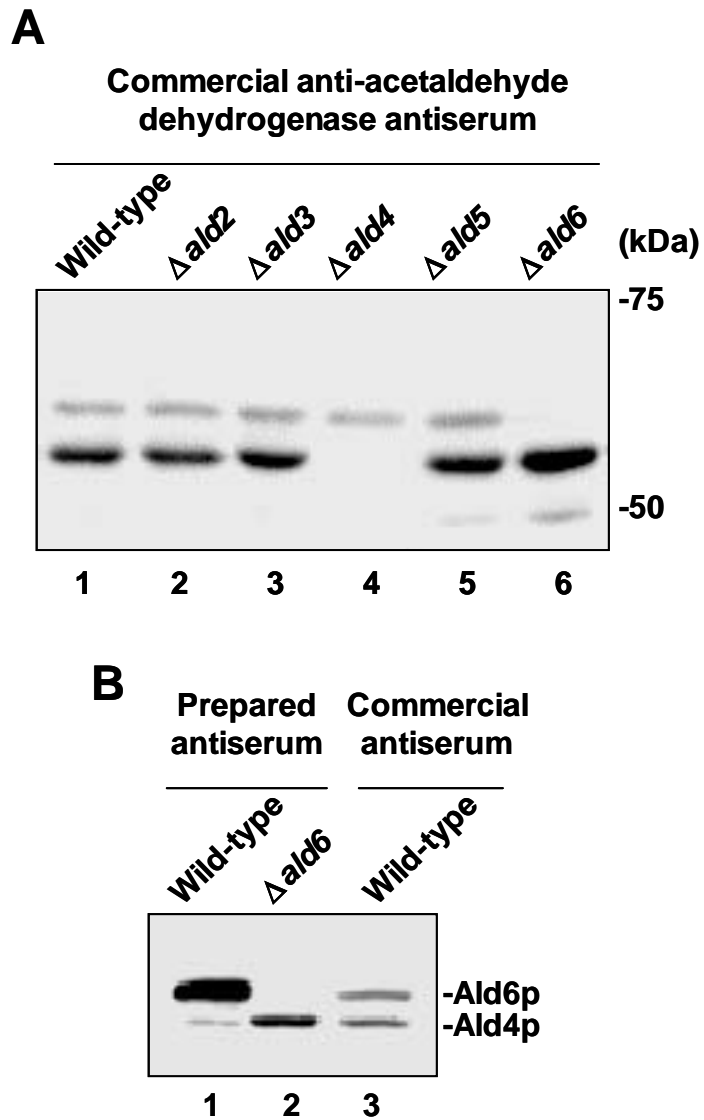


Figure 7. Preparation of anti-Ald6p antibodies.

Each cell lysate (10 μ g protein) was analyzed by immuno-blot. (A) Commercial anti-acetaldehyde dehydrogenase polyclonal antibodies (Rockland) detected both Ald4p and Ald6p. Wild-type (BY4741), $\Delta ald2$ (Y00753), $\Delta ald3$ (Y00752), $\Delta ald4$ (Y01671), $\Delta ald5$ (Y00213) and $\Delta ald6$ (Y02767) cells were used. (B) I also prepared anti-Ald6p polyclonal antibodies (see Materials and Methods), which detected Ald6p adequately. Wild-type (SEY6210) and $\Delta ald6$ (JOY66) cells were used.

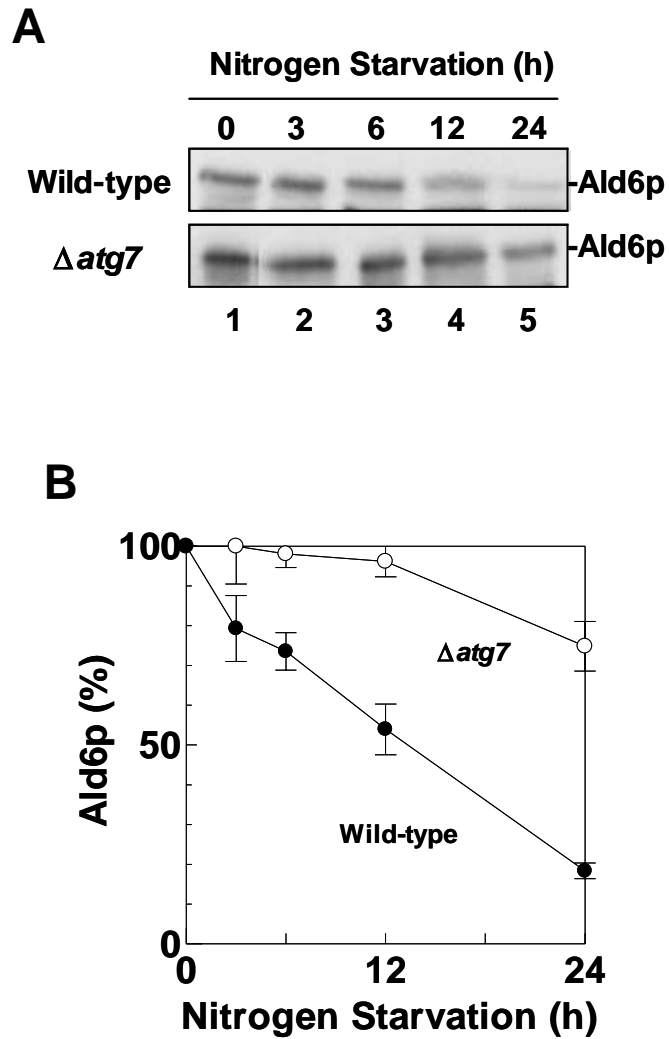


Figure 8. Time course of Ald6p reduction under nitrogen starvation.

(A, B) Each cell lysate (10 μ g protein) was analyzed by immuno-blot with antisera to Ald4p/6p. These band intensities were determined using LAS-1000 system (Fuji Film). These data were the average of three independent experiments. Wild-type (SEY6210) and $\Delta atg7$ (KVY118) cells were used.

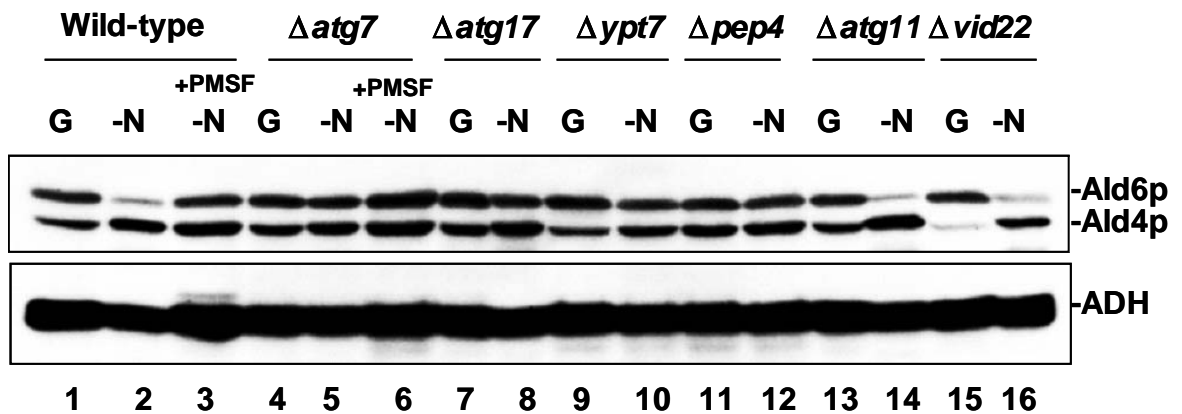


Figure 9. Proteins required for the reduction of Ald6p.

Each cell lysate (10 μ g protein) was analyzed by immuno-blot with antisera to Ald4p/6p and ADH. Wild-type (SEY6210), $\Delta atg7$ (KVY118), $\Delta atg17$ (JOY617), $\Delta ypt7$ (KVY4), $\Delta pep4$ (TVY1), $\Delta atg11$ (JOY69) and $\Delta vid22$ (JOY622) cells were used. G, growing in YPD medium ($A_{600} = 1.0$); -N, nitrogen-starved in SD(-N) medium for 24 h; +PMSF, adding 1 mM PMSF; ADH, alcohol dehydrogenase; Ald4p, mitochondrial aldehyde dehydrogenase; Ald6p, cytosolic acetaldehyde dehydrogenase.

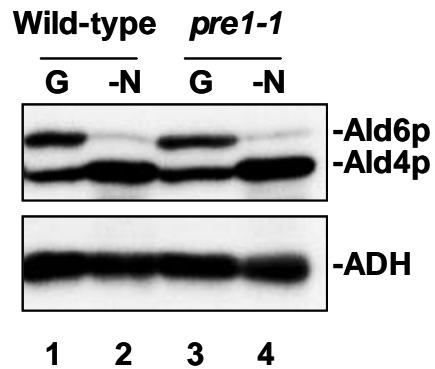


Figure 10. Proteasome degradation does not require for the Reduction of Ald6p.

Each cell lysate (10 μ g protein) was analyzed by immuno-blot with antisera to Ald4p/6p and ADH. Wild-type (WCG4a) and *pre1-1* (WCG4-11a) cells were used. G, growing in YPD medium ($A_{600} = 1.0$); -N, nitrogen-starved in SD(-N) medium for 24 h; ADH, alcohol dehydrogenase; Ald4p, mitochondrial aldehyde dehydrogenase; Ald6p, cytosolic acetaldehyde dehydrogenase.

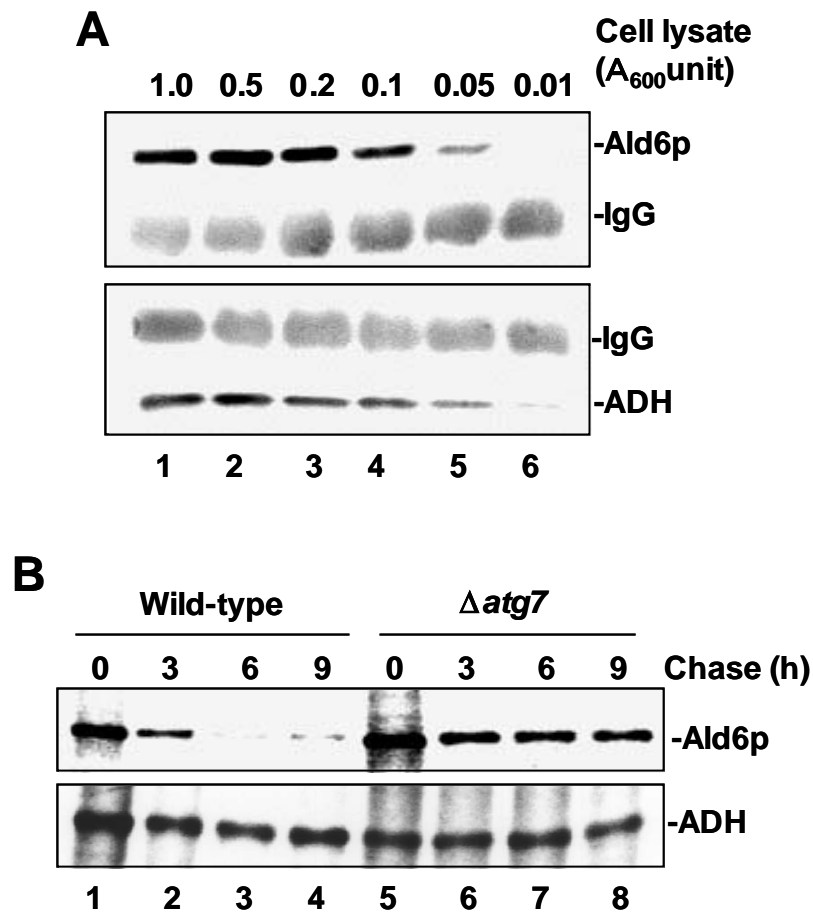


Figure 11. Pulse-chase analysis of Ald6p and ADH during nitrogen starvation.

(A) Immuno-precipitation and immuno-blot using anti-Ald6p and anti-ADH antisera. Wild-type cells (SEY6210) growing in YPD medium ($A_{600} = 1.0$) were used. Immuno-precipitation experiments were performed by 0.1% each antibodies and indicated yeast cell lysate. IgG, immuno-globulin G heavy chain. (B) Wild-type (SEY6210) and $\Delta atg7$ (KVY118) cells were grown to $A_{600} = 1.0$, pre-incubated in SD(-N) medium for 1 h, pulse labeled with [35 S]methionine for 30 min, and chased in SD(-N) medium for 0, 3, 6 and 9 h. Lysates were prepared and subjected to immuno-precipitation with anti-Ald6p or anti-ADH serum. Proteins were eluted and analyzed by SDS-PAGE followed by autoradiography.

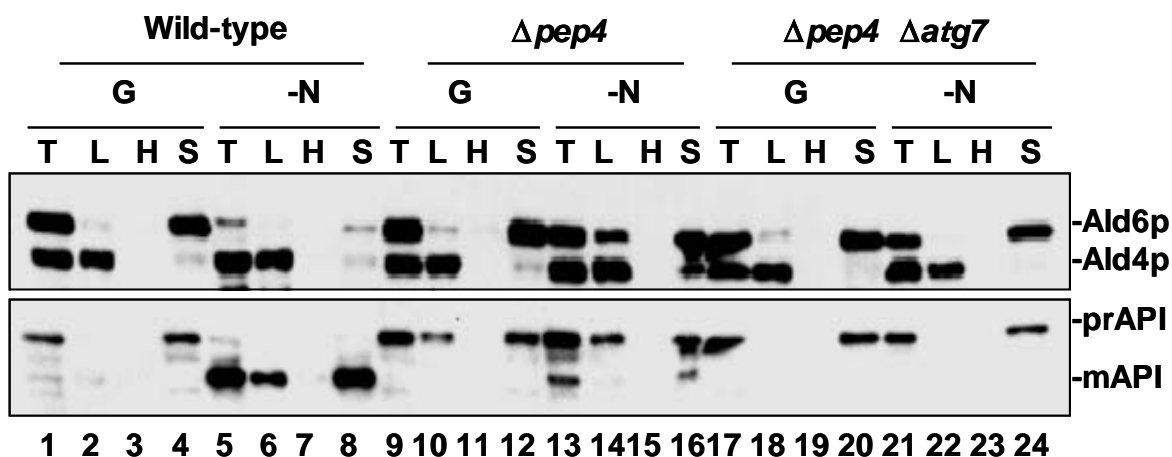


Figure 12. Detection of Ald6p in the autophagic bodies.

Subcellular fractionation of Ald6p in wild-type (SEY6210), $\Delta pep4$ (TVY1) and $\Delta pep4 \Delta atg7$ (JOY647) cells. Spheroplast lysates were spun at $500 \times g$ for 5 min to remove unbroken-cells (T, Total lysate). Total lysates were spun at $13,000 \times g$ for 15 min to separate the pellet (L, P13) fraction. The supernatant was centrifuged at $100,000 \times g$ for 1 h to generate a pellet (H, P100) fraction and supernatant (S, S100) fraction. Each fraction (0.1 A_{600} unit) was analyzed by immuno-blot with antisera to Ald4p/6p or API. G, growing in YPD medium ($A_{600} = 1.0$); -N, nitrogen-starved in SD(-N) medium for 24 h; prAPI, precursor of aminopeptidase I; mAPI, mature form of aminopeptidase I.

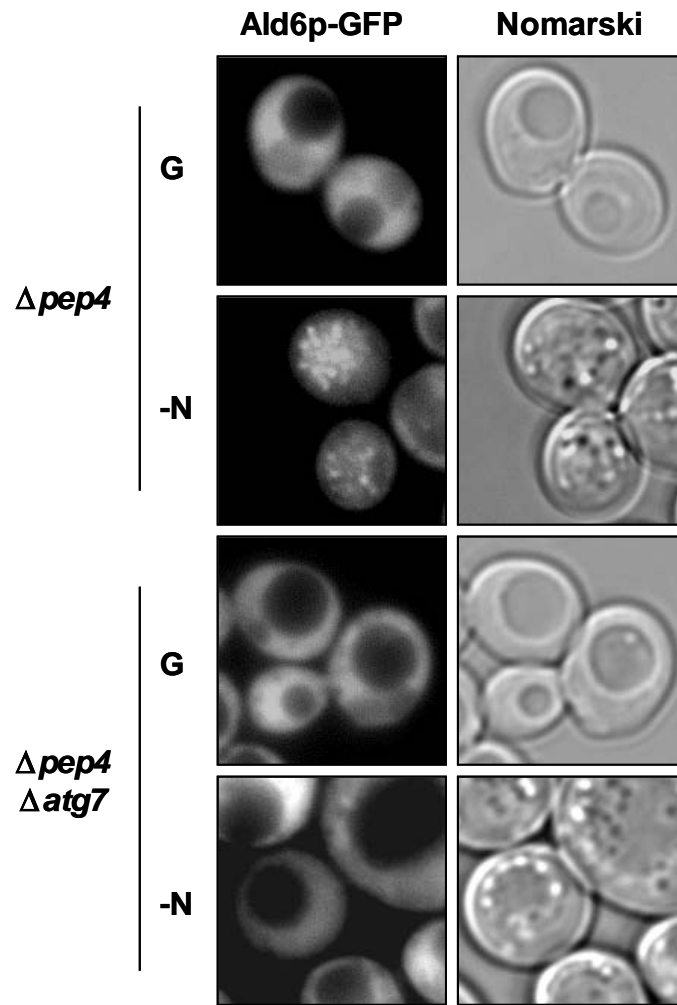


Figure 13. Visualization of vacuolar transport of Ald6p-GFP. Localization of Ald6p-GFP in growing cells and nitrogen-starved cells. *Δpep4 Δald6::ALD6-GFP* cells (JOY6005) and *Δpep4 Δatg7 Δald6::ALD6-GFP* cells (JOY6006) were used. G, growing in YPD medium ($A_{600} = 1.0$); -N, nitrogen-starved in SD(-N) medium for 24 h; bar = 5 μm .

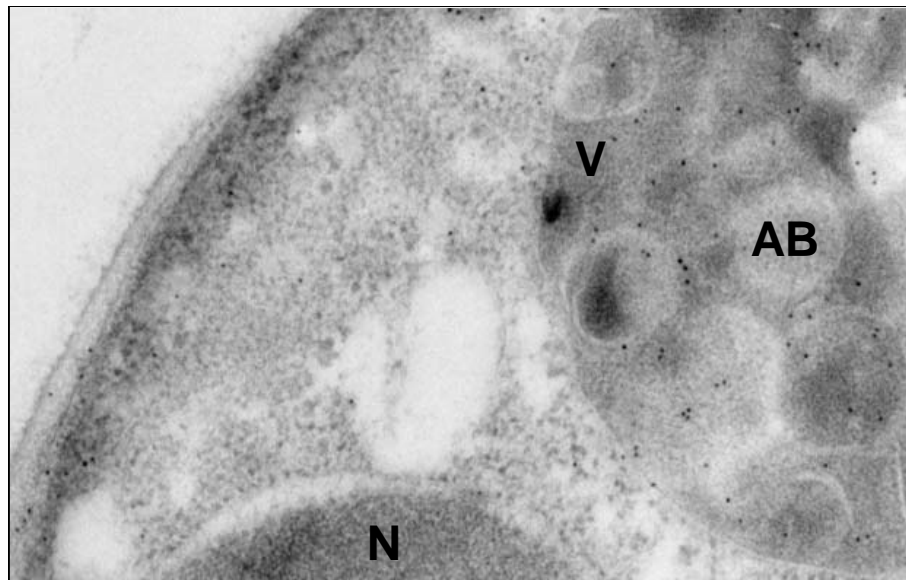


Figure 14. Immunological detection of Ald6p.

Thin sections were immuno-labeled with anti-Ald6p antiserum followed by colloidal gold-conjugated protein. *Δpep4* cells (TVY1) starved in SD(-N) medium for 24 h. AB, autophagic body; N, nucleus. Bar = 1 μ m.

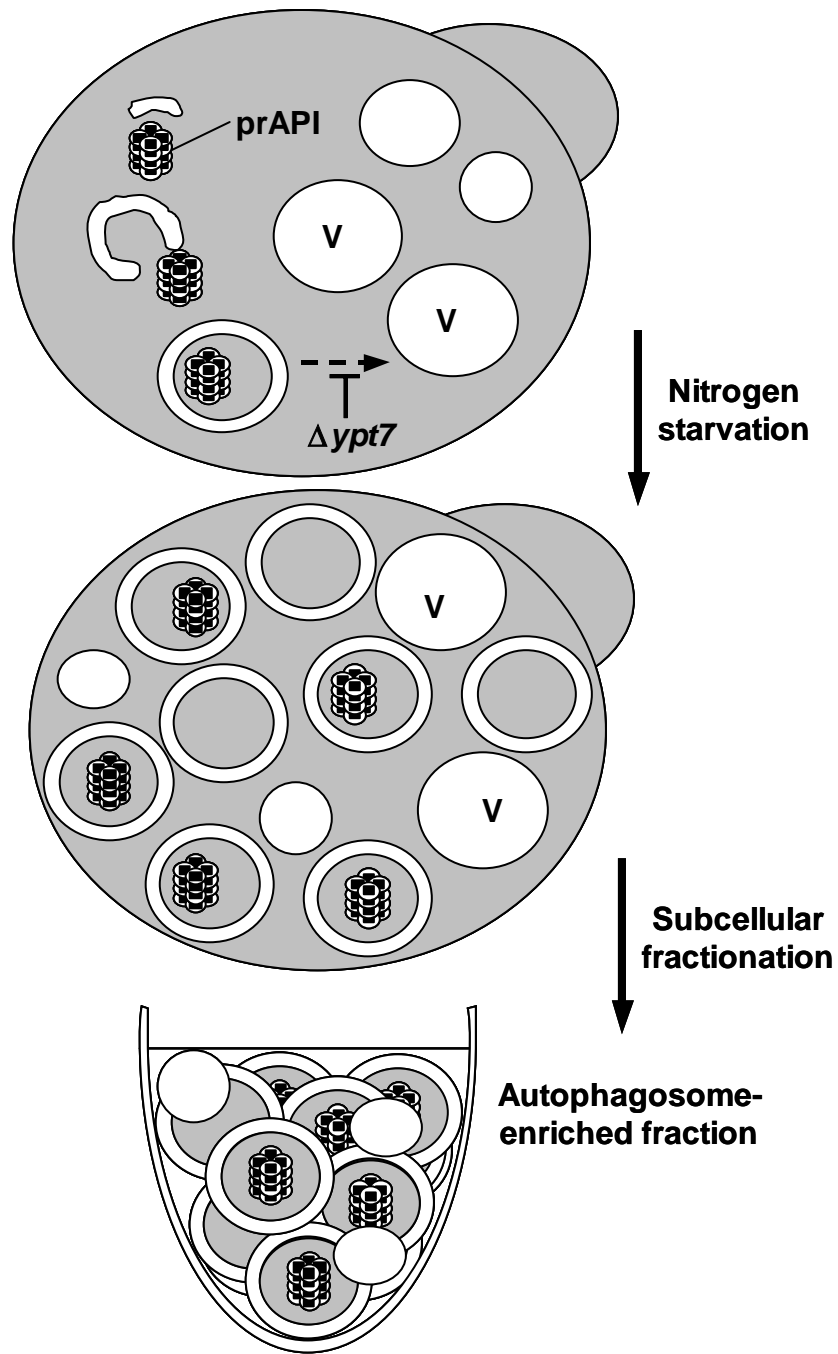
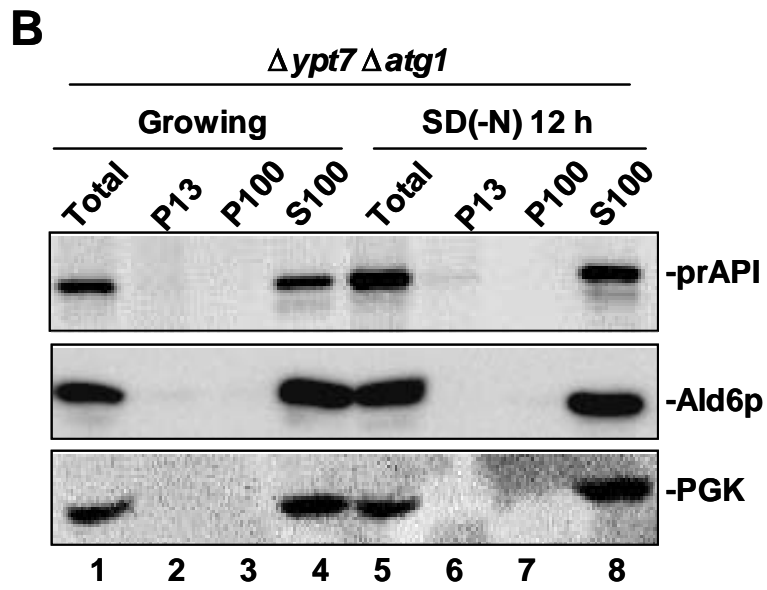
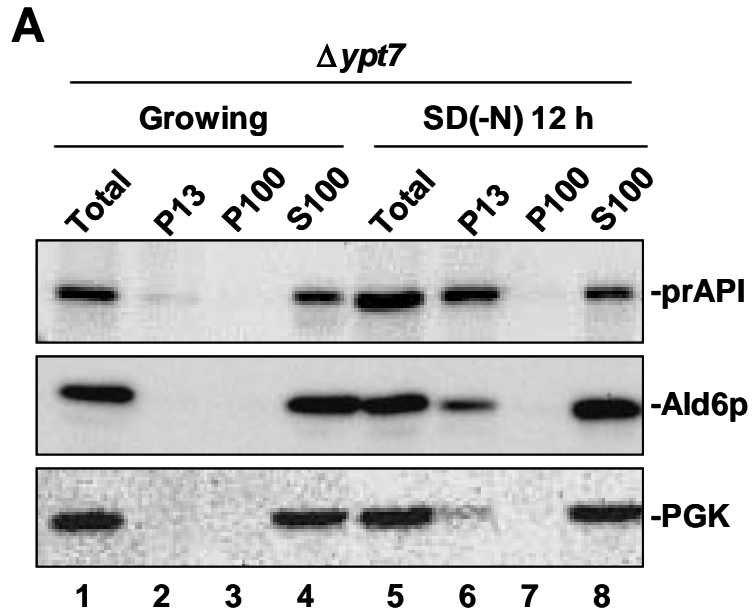
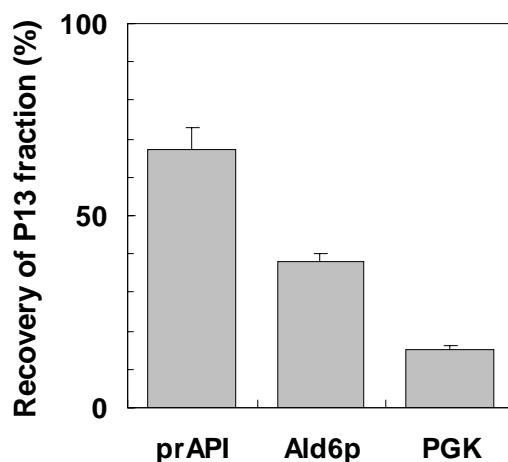


Figure 15. Illustration of collection of the autophagosome-enriched fraction.

prAPI, precursor of aminopeptidase I; V, fragmented vacuole



C**Figure 16. Preferential segregation of Ald6p into the autophagosome.**

(A, B) Subcellular fractionation of Ald6p in $\Delta ypt7$ (KVY4; A) and $\Delta ypt7 \Delta atg1/apg1$ (YAK1; B) cells. Spheroplast lysates were spun at $500 \times g$ for 5 min to remove unbroken-cells (Total, total lysate). Total lysates were spun at $13,000 \times g$ for 15 min to separate the pellet (P13) fraction. The supernatant was centrifuged at $100,000 \times g$ for 1 h to generate a pellet (P100) fraction and supernatant (S100) fraction. Each fraction (0.1 OD_{600} unit) was analyzed by immuno-blot with antibodies to API, Ald6p or PGK. Growing, growing in YPD medium ($A_{600} = 1.0$); SD(-N) 12 h, nitrogen-starved in SD(-N) medium for 12 h; prAPI, precursor of aminopeptidase I; PGK, phosphoglycerate kinase. (C) Quantification of precursor API, Ald6p and PGK in autophagosome-enrich fraction. The recovery of each protein in P13 fraction was calculated. Band intensities were determined using LAS-1000 system (Fuji Film). These data were the average of five independent experiments.

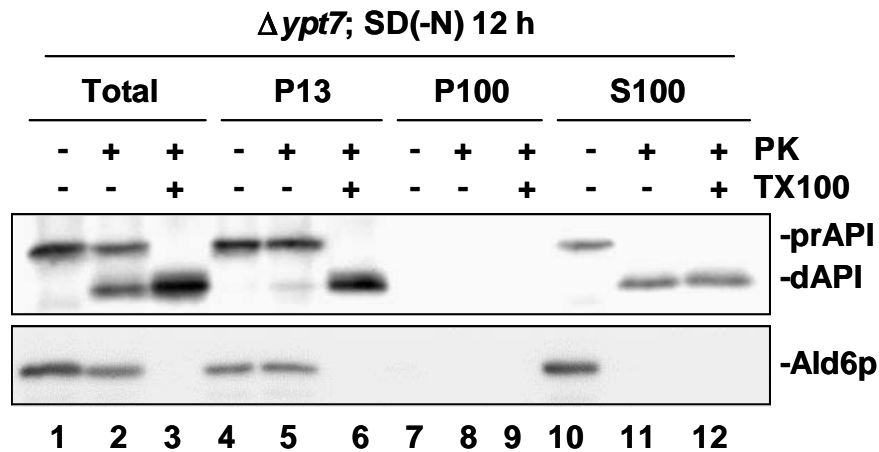


Figure 17. Proteinase K protection assay of precursor API and Ald6p in each subcellular fraction.

Spheroplast lysates were spun at $500 \times g$ for 5 min to remove unbroken-cells (Total). Total lysates were spun at $13,000 \times g$ for 15 min to separate the pellet (P13) fraction. The supernatant was centrifuged at $100,000 \times g$ for 1 h to generate a pellet (P100) fraction and supernatant (S100) fraction. Each subcellular fraction was subjected to proteinase K protection assay. Each fraction ($0.2 A_{600}$ unit) was treated with 2 mg/ml proteinase K with or without 1% Triton X-100 on ice for 30 min and then analyzed by immuno-blot with antibodies to API and Ald6p. prAPI, precursor of aminopeptidase I; dAPI, the proteinase K digestion product of precursor of aminopeptidase I; PK, proteinase K; TX100, Triton X-100.

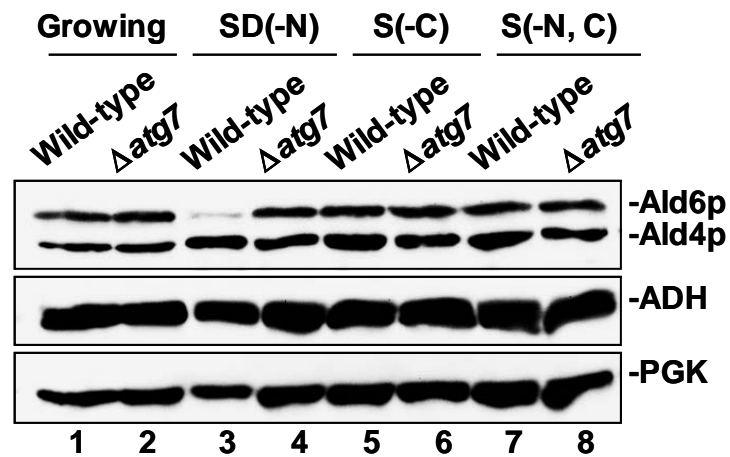


Figure 18. Ald6p is not degraded under carbon starvation, or nitrogen and carbon starvation.

Each cell lysate (10 μ g protein) was analyzed by immuno-blot with antisera to Ald4p/6p, ADH and PGK. Wild-type (SEY6210) and $\Delta atg7$ (KVY118) cells were used. G, growing in YPD medium ($A_{600} = 1.0$); -N, nitrogen-starved in SD(-N) medium for 24 h; -C, carbon-starved in S(-C) medium for 24 h; -NC, nitrogen/carbon-starved in S(-N, C) medium for 24 h; ADH, alcohol dehydrogenase; PGK, phosphoglycerate kinase.

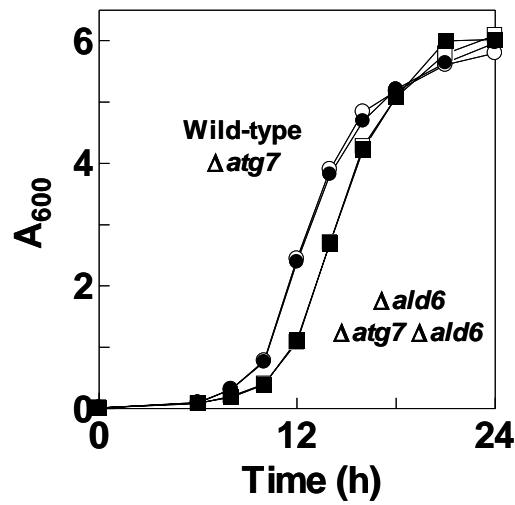
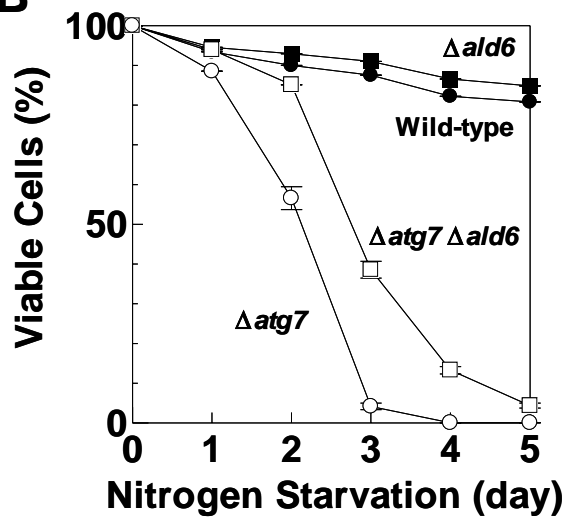
A**B**

Figure 19. Cell viability and growth curve of $\Delta ald6$ cells.

Wild-type (SEY6210, closed circle), $\Delta atg7$ (KVY118, open circle), $\Delta ald6$ (JOY66, closed square) and $\Delta atg7 \Delta ald6$ (JOY676, open square) cells were used. (A) Loss of viability during nitrogen starvation. Cells were grown in YPD medium to $A_{600} = 1.0$, washed twice with SD(-N) medium, and suspended in SD(-N) medium. Data are the average of three independent experiments. (B) Growth of cells in YPD medium. Overnight cultures of each cells were diluted to $A_{600} = 0.01$ with YPD medium and incubated at 30°C. Growth was monitored by measuring of A_{600} .

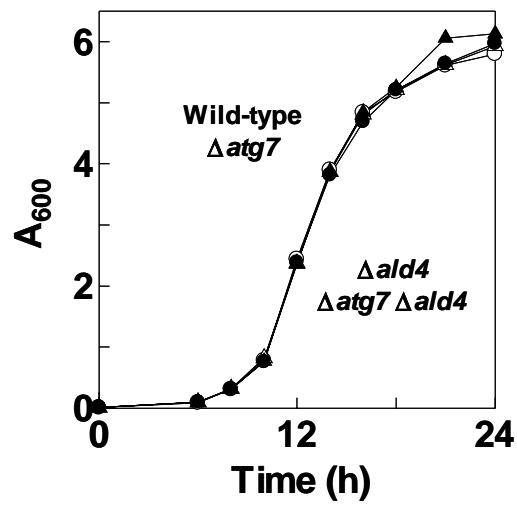
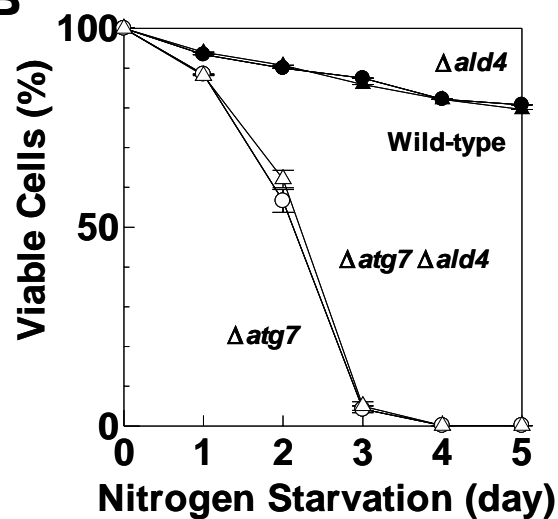
A**B**

Figure 20. Cell viability and growth curve of $\Delta ald4$ cells.

Wild-type (SEY6210, closed circle), $\Delta atg7$ (KVY118, open circle), $\Delta ald4$ (JOY64, closed triangle) and $\Delta atg7 \Delta ald4$ (JOY674, open triangle) cells were used. (A) Loss of viability during nitrogen starvation. Cells were grown in YPD medium to $A_{600} = 1.0$, washed twice with SD(-N) medium, and suspended in SD(-N) medium. Data are the average of three independent experiments. (B) Growth of cells in YPD medium. Overnight cultures of each cells were diluted to $A_{600} = 0.01$ with YPD medium and incubated at 30°C. Growth was monitored by measuring of A_{600} .

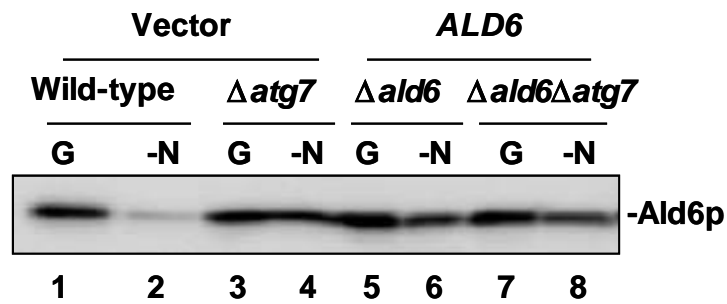


Figure 21. Ald6p does not decrease in their overexpression cells. Each cell lysate (10 μ g protein) was analyzed by immuno-blot with antiserum to Ald6p. Wild-type (SEY6210), $\Delta atg7$ (KVY118), $\Delta ald6$ (JOY66) and $\Delta atg7 \Delta ald6$ (JOY676) cells were used. Vector, harboring pRS426 multicopy plasmid; *ALD6*, harboring pRS426::*ALD6* (pJO203) multicopy plasmid; G, growing in YPD medium ($A_{600} = 1.0$); -N, nitrogen-starved in SD(-N) medium for 24 h.

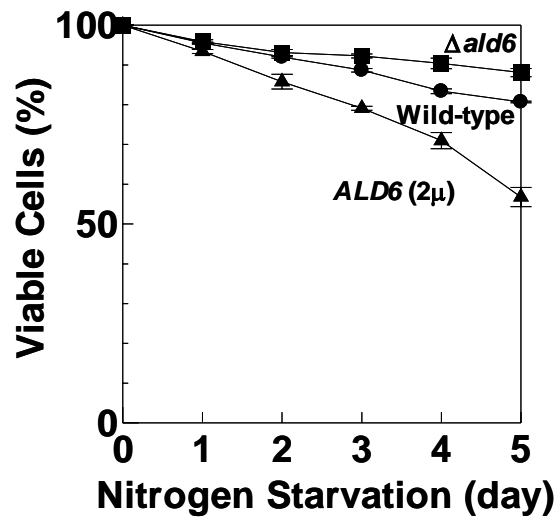


Figure 22. Cell viability phenotype of Ald6p overexpressing cells.

Loss of viability during nitrogen starvation. Cells were grown in YPD medium to $A_{600} = 1.0$, washed twice with SD(-N) medium, and suspended in SD(-N) medium. Data are the average of three independent experiments. 2μ , over expression via multicopy plasmid. Wild-type cells (SEY6210) harboring the pRS426 multicopy plasmid (open-square), $\Delta ald6$ cells (JOY66) harboring the pRS426 multicopy plasmid (closed-square), $\Delta ald6$ cells (JOY66) harboring the pRS426::*ALD6* (pJO203) multicopy plasmid (closed-triangle) were used.

A

```

Ald6p : VFDDA-NIKKTLPNLVNGIFKNAGQICSSGSRIYVOEGIYDEL : 322
Ald4p : VFADA-ELKKAVQNIILGIYYNSGEVCCAGSRVYVEESIYDKF : 340
Aldh2 : IMSDA-DMDWAVEQAHFALFFNQGQCCAGSRTEVQEDVYDEF : 337
AldH  : VFADCPDLQCAASATAAGIFYNQGQVCIAGTRLLLEESIADF : 318

```



B

Wild-type

```

CAA ATT TGT TCC TCT
Gln Ile Cys Ser Ser
304 305 306 307 308

```

***ald6*^{C306S}**

```

CAA ATT TCT TCC TCT
Gln Ile Ser Ser Ser
304 305 306 307 308

```

Site-direct mutagenesis

Figure 23. Site-direct mutagenesis of Ald6p to yield enzymatic activity deficient mutant.

(A) Cysteine-306 is one of active center residues (show arrowhead), which is highly conserved in aldehyde dehydrogenase family. Ald6p, *Saccharomyces cerevisiae* cytosolic acetaldehyde dehydrogenase; Ald4p, *S. cerevisiae* mitochondrial acetaldehyde dehydrogenase; Aldh2, *Rattus norvegicus* mitochondrial class-II aldehyde dehydrogenase. AldH, *Escherichia coli* aldehyde dehydrogenase. (B) Illustration of site-direct mutagenesis to yield *ald6*^{C306S} mutant (see Materials and Methods).

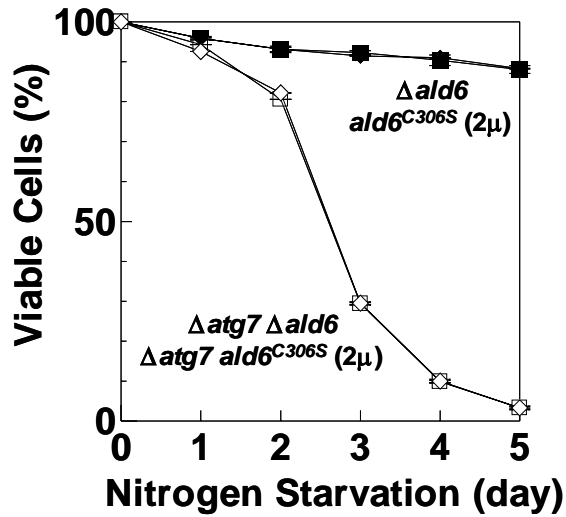


Figure 24. Cell viability phenotype of $ald6^{C306S}$ cells.

Loss of viability during nitrogen starvation. Cells were grown in YPD medium to $A_{600} = 1.0$, washed twice in SD(-N) medium, and suspended in SD(-N) medium. Data are the average of three independent experiments. 2μ , over expression via multicopy plasmid. $\Delta ald6$ cells (JOY66) harboring pRS426 plasmid (closed-square), $\Delta ald6$ cells (JOY66) harboring pRS426:: $ald6^{C306S}$ plasmid (closed-diamond), $\Delta atg7 \Delta ald6$ cells (JOY676) harboring pRS426 plasmid (open-square), and $\Delta atg7 \Delta ald6$ cells (JOY676) cells harboring pRS426:: $ald6^{C306S}$ plasmid (open-diamond) were used.

II. Amino Acids Supply from Autophagy Is Essential for Protein Synthesis

Some Proteins Increased under Nitrogen Starvation

I have shown the profiles of soluble proteins before and after long-term nitrogen starvation using two-dimensional PAGE (Figure 3). Especially, two protein-shifting patterns attracted my interest (Figure 5). Some starvation-induced proteins (Hsp26p, Arg1p, Sod2p and Eno1p/Hsp48p) were expressed during nitrogen starvation. Interestingly, these proteins did not increase in $\Delta atg7$ mutant cells (Figure 5 lanes 5–8).

Using HA-epitope tagging and immuno-blot analyses, I tried to quantify the amounts of these specific proteins in wild-type (SEY6210) and $\Delta atg7$ (JOY67) cells under nitrogen starvation. In wild-type cells, the amounts of Arg1p^{HA} and Hsp26p^{HA} increased in near linearly manner and were ultimately boosted to about 10 folds (Arg1p^{HA}) to 40 folds (Hsp26p^{HA}) of the original level after 24 h of nitrogen starvation (Figure 25A lanes 1–5, 25B and 25C). In contrast, $\Delta atg7$ cells showed a defect in the increase of these proteins (Figure 25 lanes 6–10, 25B and 25C). This protein induction was also observed on two vacuolar proteinases, API and carboxypeptidase Y (CPY) (Figure 25A, 25D and 25E). API and CPY were also known to induce markedly under nitrogen starvation condition (Scott *et al.*, 1996; Nakamura *et al.*, 1997). These protein expressions of wild-type are about 4–6 folds higher than those of $\Delta atg7$ after 6 h of nitrogen starvation (Figure 25B–25E).

Next, I performed northern blot analysis. Total mRNA was prepared from wild-type (SEY6210) and $\Delta atg7$ (JOY67) cells nutrient growing in YPD medium, and the cells shifted to SD(-N) medium for various periods of time. As shown in Figure 26, the amount of *ARG1* and *HSP26* mRNAs increased drastically in response to starvation, and reached at a maximum level within 3 h after shift to starvation in both wild-type and $\Delta atg7$ cells. After 12 h starvation in both cells, it was still many folds higher than that of the growing cells (Figure 26 lanes 1, 4, 5 and 8). These immuno- and northern-blot results may indicate that the protein synthesis of Arg1p, Hsp26p and other are

inhibited in the translational step under nitrogen starvation in autophagy defective mutant cells.

Autophagy Contributes to the Maintenance of Amino Acids Pool

Autophagy degrades significant amounts of cellular macromolecules, at present, we do not know precise fate of digested products, amino acids, nucleotides, monosaccharide and phospholipids. Autophagy-defective mutants (*atg/apg*) cannot maintain viability under long span nitrogen or sulfur starvation (Tsukada and Ohsumi, 1994; data not shown). So that the most important digested product is expected to be amino acids derived from the protein degradation in the vacuole, which may be the key metabolite for the survival under starvation environment. We generally think that the cytoplasmic proteins that are transported to the vacuole via autophagy are degraded into amino acids level. So, I hypothesized that the non-increase of levels of Arg1p and Hsp26p was the result of free amino acids depletion during nitrogen starvation in autophagy deficient cells.

Recently, Y. Ohsumi and K. Nakahara detected that *leu2 trp1* cells (SEY6210) released high concentration *iso*-propylmaleic acid (molecular weight: 158) and anthranillic acid (molecular weight: 137) in nitrogen starvation medium (Y. Ohsumi and K. Nakahara, unpublished results). These two low molecular weight compounds are each intermediates of leucine and tryptophan biosynthesis pathway, respectively. The lacking of enzymes, Leu2p (3-isopropylmalate dehydrogenase) and Trp1p (phosphoribosylanthranilate isomerase), caused accumulations of two intermediates in medium. $\Delta atg/apg$, $\Delta ypt7$ or $\Delta pep4$ mutant cells release small amount of these metabolites less than wild-type under nitrogen starvation (Y. Ohsumi and K. Nakahara, unpublished results), so that the metabolic flows of amino acid biosynthesis would reflect on the protein degradation by autophagy. To examine this possibility more directly, I analyzed the changes in the amino acids contents under nitrogen starvation by ninhydrin colorimetric method.

For further physiological analysis, I used the prototrophic yeast strains (X2180-1B) that had no requirement for amino acids. In $\Delta atg7$ cells (JOY27), the total

contents of free amino acids (19 amino acids; glycine, alanine, serine, threonine, valine, leucine, isoleucine, tyrosine, phenylalanine, cysteine, methionine, asparagine, glutamine, aspartate, glutamate, lysine, arginine, histidine and proline) were reduced markedly, and were ultimately reduced to 9.4 nmol / A₆₀₀ unit cells after 24 h of starvation (Figure 27). Other autophagy defective mutants, *atg1-1* (MT13-3A) and *atg2-4-1* (MT2-4-1) mutant cells, also could not maintain free amino acids pool under nitrogen starvation as Δ *atg7* cells (data not shown). In contrast, total free amino acids level of wild-type cells (X2180-1B) also decreased markedly during initial 2 h starvation, however, it was ebbed back and kept on the level of above 40 nmol / A₆₀₀ unit for 12 h starvation (Figure 27). In SD medium (0.17% yeast nitrogen base without amino acids and ammonium sulfate, 0.5% ammonium sulfate and 2% glucose), total free amino acids levels of yeast cells (X2180-1B or JOY27) were about 40 nmol / A₆₀₀ unit cells under growing condition (dashed line in Figure 27). This result may indicate that wild-type cells maintain free amino acids pool enough to survive under nitrogen starvation, but autophagy deficient cells may reduce protein synthesis due to an insufficient supply of amino acids derived from autophagic protein degradation.

Transient Accumulation of Cysteine during Nitrogen Starvation

Individual changes of 19 amino acids during nitrogen starvation are shown in Figure 28. The contents of most amino acids were decreased rapidly during initial 3 h nitrogen starvation; however, they were recovered after 6 h starvation (Figure 28). The content of glycine is recovered a little early than other amino acid (Figure 28G). The behavior of cysteine under nitrogen starvation is so unique. Cysteine was the minor amino acid in logarithmic growing phase (Figure 28C). As soon as transferring to nitrogen starvation medium, cysteine became the major amino acids in wild-type cells (X2180-1B). The level of cysteine reached 74.8% in the total free amino acids at 3 h nitrogen starvation (Figures 27 and 28C). Δ *atg7* cells (JOY27) also accumulated cysteine likewise; the relative content of one reached only 34.8% in 3 h starvation (Figure 28C). Cysteine content decreased rapidly after 6 h starvation, alternatively, other amino acids increase in wild-type cells. It seems like to happen the dynamic metabolic

change of amino acids under nitrogen starvation; yeast cells should convert available amino acids to cysteine by wherever possible, and cysteine may redistribute other amino acids after 3 h starvation.

In early nitrogen starvation phase, where does sulfur atom of cysteine come from? This answer cannot be explained for the simple conversion from methionine to cysteine (Figures 28C and 28M). Sulfur starvation condition is known to induce autophagy ever more intensely than nitrogen starvation condition (Noda *et al.*, 1995). However, cysteine contents did not increased in early sulfur starvation phase (Figure 29). This result shows the possibility that yeast cells actively assimilate sulfur from the culture medium in the early phase of nitrogen starvation. SD(-N) medium contains magnesium sulfate (0.5 g/l), manganese sulfate (0.4 mg/l) and zinc sulfate (0.4 mg/l) enough to be sulfur source. This dynamic change of cysteine might be an important process for the survival during starvation environment.

Protein Synthesis Require Amino Acids Pool

Next, I examined the *in vivo* protein synthesis under nitrogen starvation. If this activity of autophagy deficient cells was much lower than that of wild-type cells, it is possible that the pool size of free amino acids limited the protein synthesis during starvation. I have estimated the protein synthesis using [¹⁴C]valine by the procedure described under "Materials and Methods". Total uptake of [¹⁴C]valine was estimated by the radioactivity of whole cell, and protein assimilation of [¹⁴C]valine was estimated by the radioactivity of 10% w/v TCA insoluble fraction. When cycloheximide (25 µg/ml) was added as the inhibitor of protein synthesis, total uptake of [¹⁴C]valine was not inhibited sensitively, but protein assimilation of [¹⁴C]valine was inhibited by cycloheximide completely (Table IV).

I approximatey calculated a degree of protein synthesis from these factors of total uptake of [¹⁴C]valine for initial 1 min (Figure 30A), protein assimilation of [¹⁴C]valine for initial 1 min (Figure 30B) and contents of non-radioactive valine in the yeast cells (Figure 28V). "Protein assimilation of [¹⁴C]valine for initial 1 min" divides by "the ratio of [¹⁴C]valine in total ([¹⁴C] and non-radioactive) valine pool after initial 1

min" shows the protein assimilation of total valine for initial 1 min. It would reflect on the degree of protein synthesis in primary approximation. The results of this calculation were shown in Figure 30C, protein synthesis of both wild-type (X2180-1B) and $\Delta atg7$ (JOY27) cells was come down at one point of 3 h starvation. Over 6 h starvation, this activity of wild-type cells was restored (Figure 30C black bar), however, $\Delta atg7$ cells remained in low activity (Figure 30C gray bar). The result of 24 h starvation show that protein synthesis activity of wild-type cells was higher than it of $\Delta atg7$ cells about 6 folds (Figure 30C).

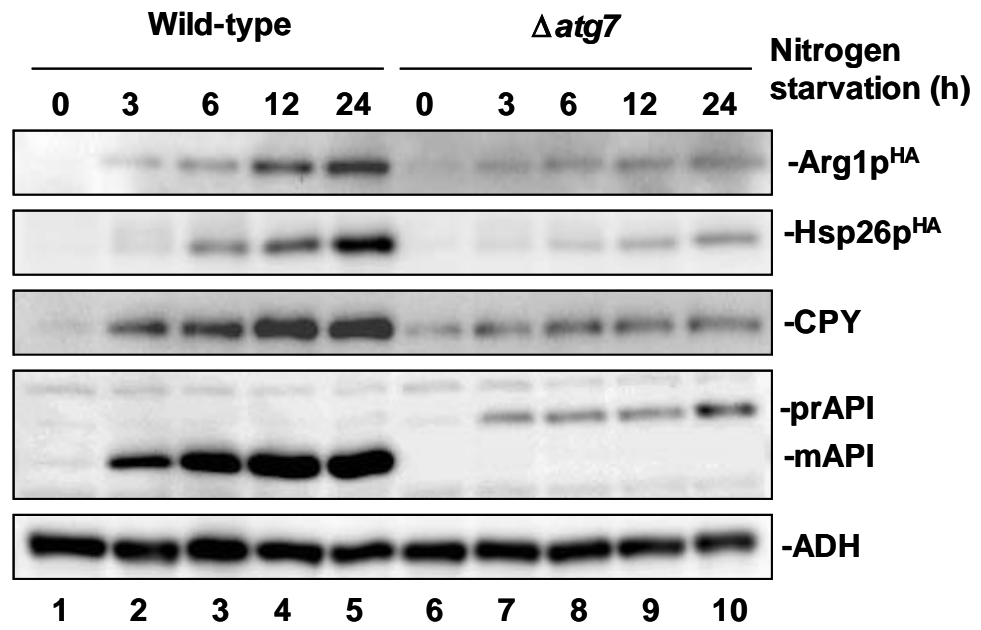
It was necessary to show more certain evidence whether the pool size of free amino acids limited the protein synthesis activity. To address it I modified the assay method of protein synthesis activity. Nitrogen-starved cells were pre-incubated in SD + CA medium containing free amino acids for 5 min at 30°C, and were washed twice with SD(-N) medium, and then cells were subjected to the assay of protein synthesis using [¹⁴C]valine. By the processing of amino acids supply, $\Delta atg7$ cells (JOY27) showed the drastic increase of valine pool (Figure 31A grey and white bars), which should reflect on the high activity of [¹⁴C]valine uptake (Figure 30A). Amino acids re-supplied $\Delta atg7$ cells also show the high activity of protein synthesis as well as wild-type cells (X2180-1B) (Figure 31B mesh and white bars). These results indicated that the pool size of free amino acids should limit the protein synthesis.

Table IV. Cycloheximide inhibited TCA-insoluble [¹⁴C]valine uptake.

Wild-type cells (X2180-1B) were cultured in YPD medium until $A_{600} = 1.0$ and washed in SD(-N) medium. -CHX, cycloheximide free assay (control); +CHX, adding 2.5 $\mu\text{g/ml}$ cycloheximide assay; Total [¹⁴C]valine uptake specific activity ($\text{nmol}^{-1} \cdot \text{min}^{-1} \cdot A_{600}$ unit); TCA-insoluble [¹⁴C]valine uptake specific activity ($\text{nmol}^{-1} \cdot \text{min}^{-1} \cdot A_{600}$ unit).

<u>Assay</u>	<u>-CHX</u>	<u>+CHX</u>
Total [¹⁴ C]valine uptake specific activity	0.448	0.314
<u>TCA-insoluble [¹⁴C]valine uptake specific activity</u>	<u>0.0496</u>	<u>Not detected</u>

A



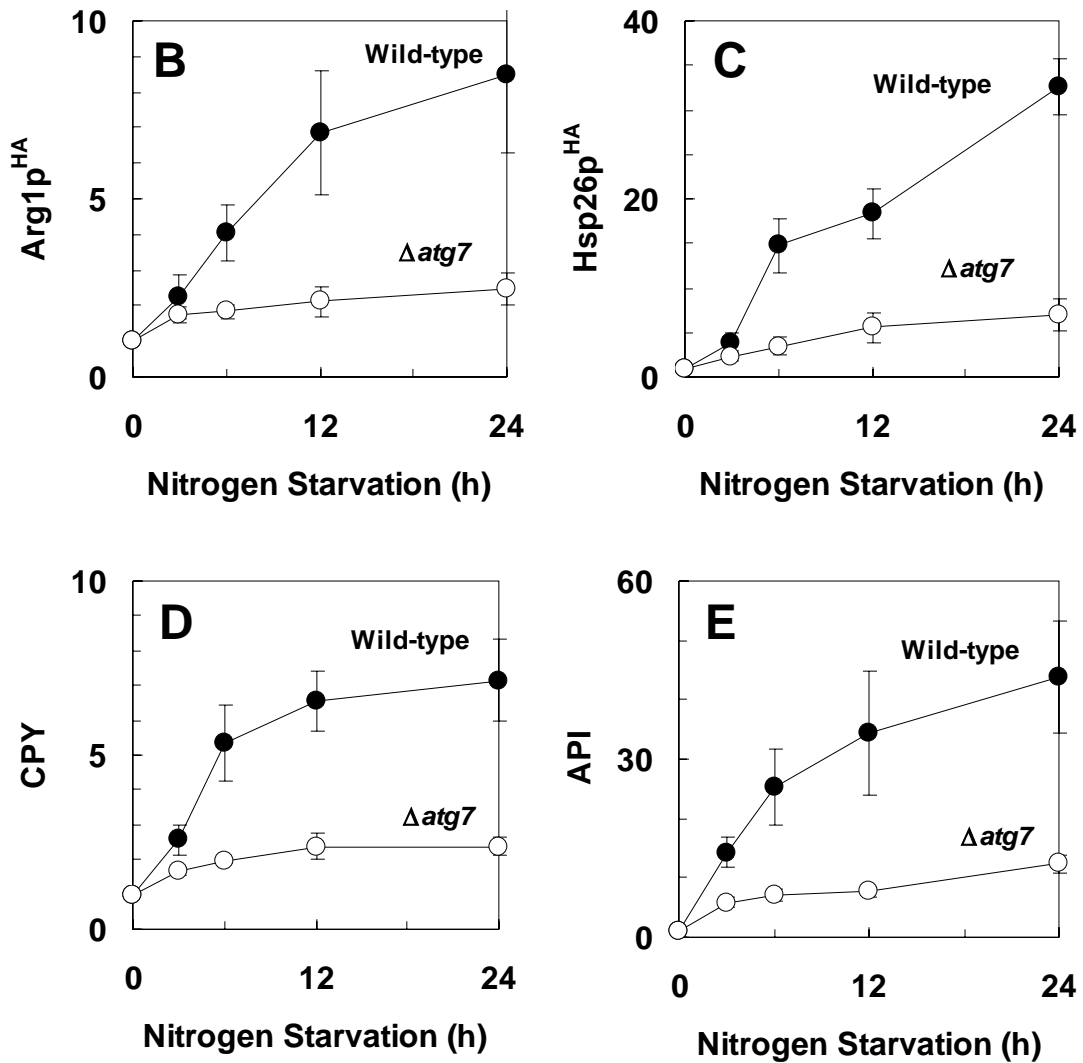


Figure 25. Autophagy is required for the synthesis of starvation induced proteins.

(A) Each cell lysate (10 μ g protein) was analyzed by immuno-blot with antibody to HA, antisera to CPY, API and ADH. Wild-type cells (SEY6210) and $\Delta atg7$ (JOY67) cells were cultured in YPD medium until $A_{600} = 1.0$ (0 h) and shifted to SD(-N) medium for 3, 6, 12 and 24 h at 30 °C. (B–E) The quantification of immuno-blot image each wild-type (closed circle) and $\Delta atg7$ (open circle) cells. These band intensities were determined using LAS-1000 system (Fuji Film). These data were the average of three independent experiments. CPY, matured form of carboxy peptidase Y.

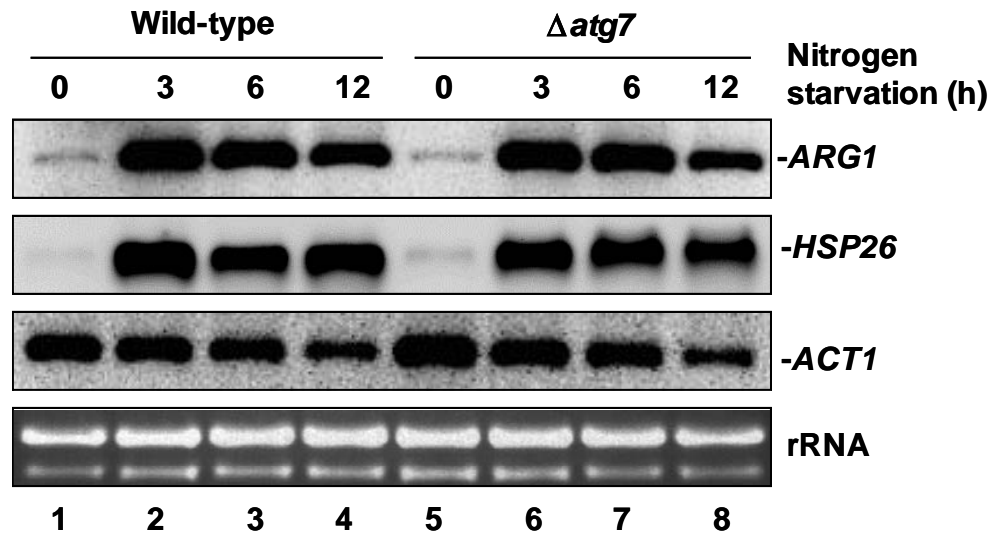


Figure 26. Expression of nitrogen starvation induced gene, *ARG1* and *HSP26*.

Wild-type (SEY6210) and $\Delta atg7$ (JOY67) cells were cultured in YPD medium until $A_{600} = 1.0$ (0 h) and shifted to SD(-N) medium for 3, 6 and 12 h at 30 °C, and total RNA was prepared from each culture as described under "Materials and Methods". *ARG1*, *HSP26* and *ACT1* mRNA were detected by northern blot with each specific probe. *ACT1* blotting and ethidium bromide staining of rRNA were shown as a loading control of RNA. Each lane has 5 μ g of total RNA.

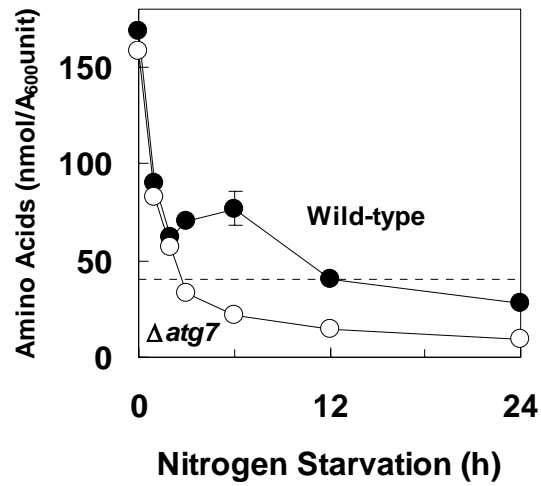
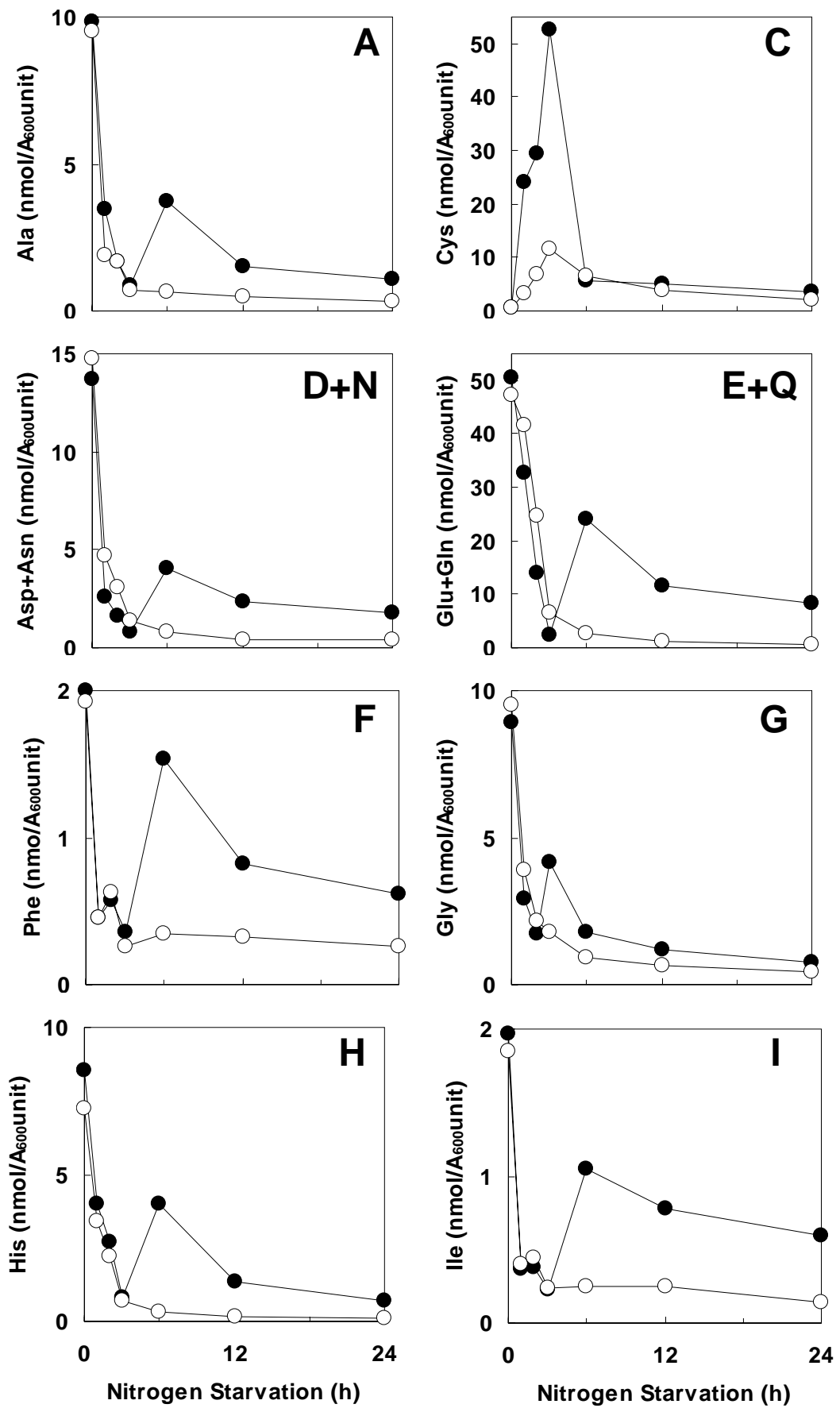
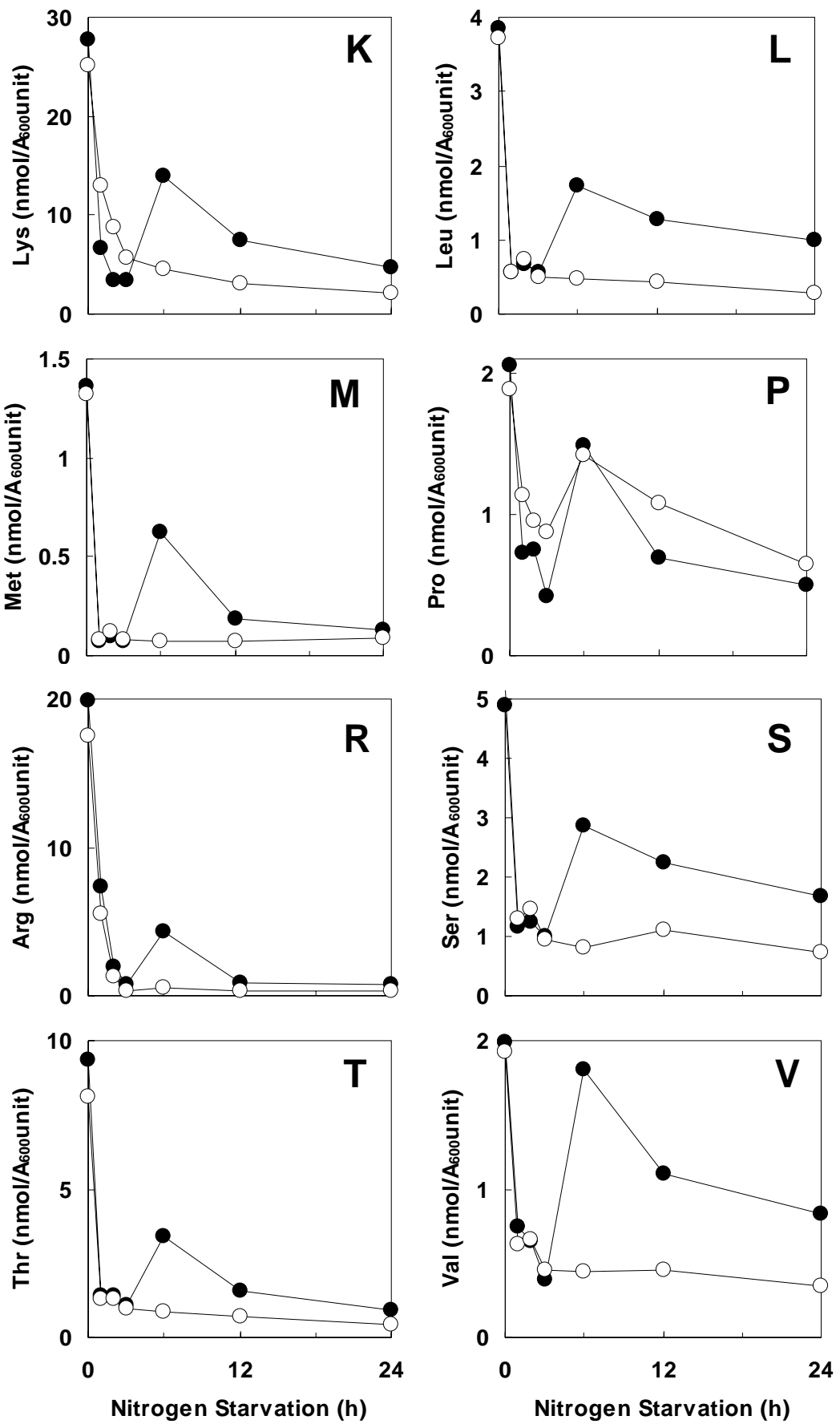


Figure 27. Change in the total content of free amino acids during nitrogen starvation.

Wild-type (X2180-1B; closed circle) and $\Delta atg7$ (JOY27; open circle) cells were cultured in YPD medium until $A_{600} = 1.0$ (0 h) and shifted to SD(-N) medium for 1, 2, 3, 6, 12 and 24 h at 30 °C. These data were shown the contents per 1 A_{600} unit, and were the averages of three independent experiments.





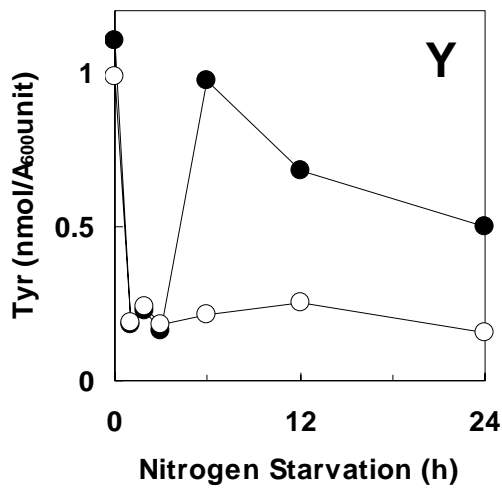


Figure 28. Change in the individual content of free amino acid during nitrogen starvation.

Wild-type (X2180-1B; closed circle) and $\Delta atg7$ (JOY27; open circle) cells were cultured in YPD medium until $A_{600} = 1.0$ (0 h) and shifted to SD(-N) medium for 1, 2, 3, 6, 12 and 24 h at 30 °C. These data were shown the contents per 1 A_{600} unit, and were the averages of three independent experiments. (A) Alanine (C) Cysteine (D + N) Aspartate and asparagine (E + Q) Glutamate and glutamine (F) Phenylalanine (G) Glycine (H) Histidine (I) Isoleucine (K) Lysine (L) Leucine (M) Methionine (P) Proline (R) Arginine (S) Serine (T) Threonine (V) Valine (Y) Tyrosine.

A

Starvation (h)	Cysteine (nmol/A ₆₀₀ unit)	
	SD(-N)	SD(-S)
0	0.68	0.68
3	52.5	0.25
6	5.54	8.13
12	4.98	6.4

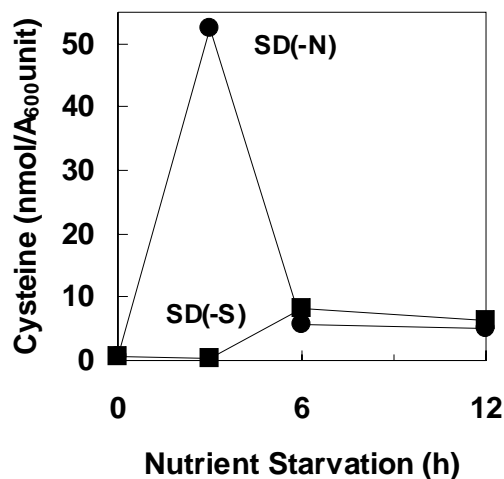
B

Figure 29. Change in cysteine content during nitrogen or sulfur starvation.

(A and B) Wild-type cells (X2180-1B) were cultured in YPD medium until $A_{600} = 1.0$ (0 h) and shifted to SD(-N) (closed circle) or SD(-S) (closed square) medium for 3, 6 and 12 h at 30 °C. These data were shown the contents per A_{600} unit.

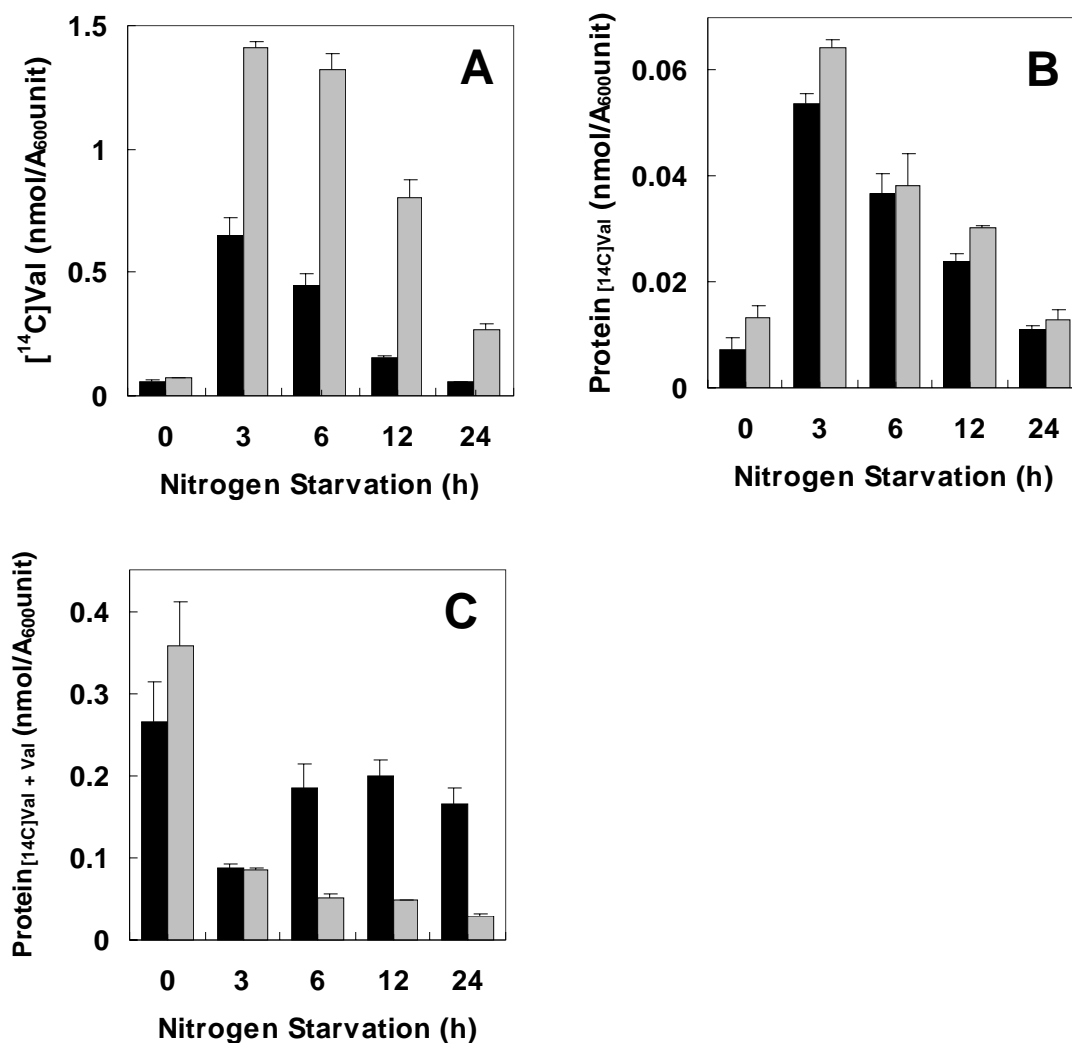


Figure 30. Protein synthesis during nitrogen starvation.

Wild-type (X2180-1B; black bar) and $\Delta atg7$ (JOY27; grey bar) cells were cultured in YPD medium until $A_{600} = 1.0$ (0 h) and shifted to SD(-N) medium for 0, 3, 6, 12 and 24 h at 30°C. These data were shown the contents per A_{600} unit, and were the averages of three independent experiments. (A) [^{14}C]Val, uptake of [^{14}C]valine into the cells for initial 1 min. (B) Protein_{[^{14}C]Val}, proteins assimilation of [^{14}C]valine for initial 1 min (C) Protein_{[^{14}C]Val + Val}, protein assimilation of total (^{14}C -radioactive and non-radioactive) valine for initial 1 min.

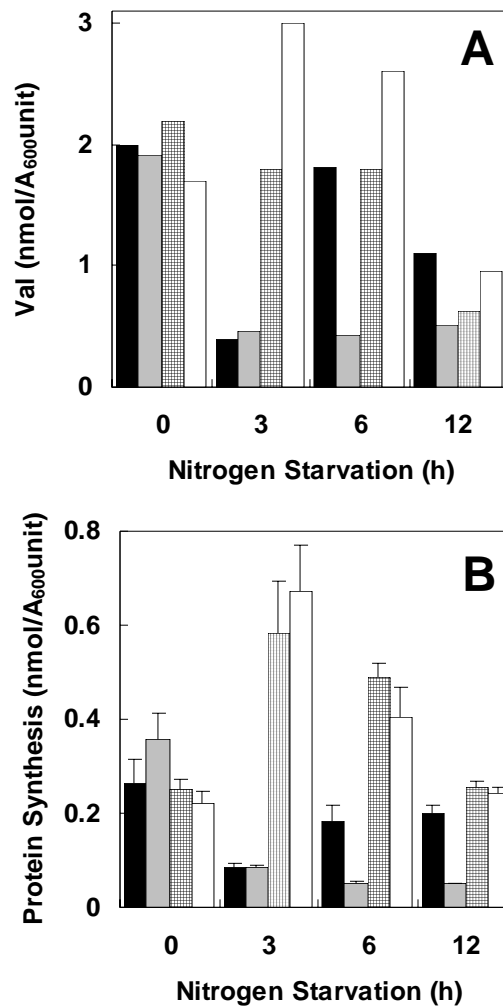


Figure 31. Protein synthesis activity in supplement of amino acids ahead of the assay.

Wild-type (X2180-1B; meshed bar) and $\Delta atg7$ (JOY27; white bar) cells were cultured in YPD medium until $A_{600} = 1.0$ (0 h) and shifted to SD(-N) medium for 3, 6 and 12 h at 30°C. Each cells were pre-incubated in SD + CA medium for 5 min at 30°C, washed in SD(-N) twice, and then yeast cells were subjected to the assay of protein synthesis using [¹⁴C]valine. Black and grey bars are same data as black and grey bar of Figure 28V or 30C. (A) Val, non-radioactive valine contents measured by amino acids analyzer. (B) Protein_{[¹⁴C]Val + val}, protein assimilation of total (¹⁴C-radioactive and non-radioactive) valine for initial 1 min. These data were shown the contents per A_{600} unit, and were the averages of three independent experiments.

DISCUSSION

Rate of Ald6p Degradation

I surveyed the change of soluble proteins before and after nitrogen starvation using two-dimensional PAGE. Ald6p showed a clear reduction, which was dependent on Atg/Apg proteins, under nitrogen starvation for 24 h as compare with other proteins (Figures 5, 6, 9 and 10). Previous morphological studies have indicated that autophagy degrades about 2% of the cytosol/h in yeast (Takeshige *et al.*, 1992; Baba *et al.*, 1994). Scott *et al.* showed by [³⁵S]methionine pulse-chase experiments that the rate of vacuolar delivery of cytosolic Pho8Δ60p by autophagy was 4%/h during the initial 6 h of nitrogen starvation (Scott *et al.*, 1996). Autophagy proceeds linearly during the first 6 h of starvation, and then gradually slows down (Scott *et al.*, 1996). We know that both diploid and haploid cells induce autophagy in sporulation medium, 2% potassium acetate (Tskada and Ohsumi, 1993). In a previous report, Betz and Weiser showed that protein degradation in haploid cells occurred at a slower rate than in diploid cells in a sporulation medium (Betz and Weiser, 1976). Diploid cells degraded 2.5% of the cellular protein / h in a sporulation medium (Betz and Weiser, 1976). Taken together, these results indicate that most proteins should not decrease below 62% of their original levels due to autophagy, even after 24 h starvation (2% degradation of the cytosol / h). In wild-type cells, the amount of Ald6p was reduced to 18% of the initial level after 24 h nitrogen starvation (Figure 8). This large decrease in Ald6p level reflects preferential autophagic degradation.

Molecular Mechanism of Preferential Ald6p Segregation

The result shown in Figure 16 indicates that the specificity of Ald6p degradation may be achieved by a step of sequestration to the autophagosome. Suzuki *et al.* indicated that the vacuolar targeting of the precursor API (via the Cvt pathway) required localization with the pre-autophagosomal structure in perivacuolar region (Suzuki *et al.*, 2002). This punctuate structure was defined by the co-localization of several Atg/Apg proteins, and plays a central role in autophagosome formation (Suzuki

et al., 2001; Noda *et al.*, 2002; Suzuki *et al.*, 2002). In both $\Delta atg11/cvt9$ and $\Delta atg19/cvt19$ mutant cells, the precursor API localized to the cytosol away from the pre-autophagosomal structure, and was not targeted to the vacuole (Suzuki *et al.*, 2002; Shintani *et al.*, 2002). It was expected that Atg11p and Atg19p would be membrane receptors for the precursor API (Kim *et al.*, 2001; Scott *et al.*, 2001). However, Ald6p degradation was not dependent on Atg11p (Figure 10 lanes 1, 2, 13 and 14) and Atg19p (data not shown). During nitrogen starvation, the half-life ($t_{1/2}$) of Ald6p was 100 min (Figure 12B) and the half-time of maturation of precursor API was 30–45 min (Klionsky *et al.*, 1992; Scott *et al.*, 1996; Klionsky and Ohsumi, 1999), and the recovery of autophagosome-enriched fraction of Ald6p was lower than the recovery of precursor API (Figure 16). These results indicate that Ald6p is not likely to be a cargo of the Cvt pathway. One factor contributing to protein targeting is the existence of a membrane receptor; it is possible that the selective sequestration of Ald6p is mediated by a yet unknown molecule(s) on the autophagosome. Further studies of the molecular mechanisms underlying targeted autophagy are now in progress to investigate these possibilities.

Physiological Significance of Ald6p Degradation

To address the physiological significance of this preferential degradation, I analyzed the viability of $\Delta ald6$ or *ALD6* overexpressing cells (Figures 19 and 22). I have demonstrated that Ald6p enzymatic activity might be disadvantageous for the survival of yeast cells during nitrogen starvation (Figure 24). Brejning and Jespersen have previously reported that Ald6p level increased during lag phase, the first hours after inoculation of the culture (Brejning and Jespersen, 2002). Meaden *et al.* reported that the growth of $\Delta ald6$ mutant cells is slower than wild-type cells in both YPD and synthetic medium (Meaden *et al.*, 1996; Figure 21). It is known that acetaldehyde dehydrogenase is closely related to lipid biosynthesis through the intermediary of acetyl-CoA synthase and fatty acid synthase in the cytosol (Figure 6). As lipid biosynthesis is a critical process, the expression of Ald6p would be necessary during growth under nutrient conditions.

Why is cytosolic Ald6p acetaldehyde dehydrogenase activity harmful under nitrogen starvation conditions? A possible explanation might be: Ald6p may disturb NADPH flux during nitrogen starvation. It is well known that glucose-6-phosphate dehydrogenase (G6PDH; Zwf1p; glucose-6-phosphate + NADP⁺ → 6-phosphogluconolactone + NADPH) is the greatest contributor to the reduction of NADP⁺ in the yeast cell. Inactivation of the *ZWF1* gene does not affect the cell growth in rich media supplemented with a variety of carbon sources, although it increases their sensitivity to oxidizing agents (Nogae and Johnston, 1990) and leads to methionine auxotrophy (Thomas *et al.*, 1991; Thomas and Surdin-Kerjan, 1997). It was suggested that the growth deficiencies are caused by an increased utilization of NADPH required for reductive assimilation of inorganic sulfur or for restoration of cellular pools of reduced glutathione and thioredoxin, which rapidly deplete under oxidative stress growth conditions (Slekar *et al.*, 1996). Grabowska and Chelstowska have recently demonstrated that $\Delta ald6 \Delta zwf1$ double mutant cells are not viable under normal growth conditions or under anaerobic growth conditions even in the presence of glutathione (Grabowska and Chelstowska, 2003). It is suggested that Ald6p plays an important role in maintaining a high rate of NADPH/NADP⁺ cycling in the yeast cell. However, upon nitrogen starvation, both fatty acid and deoxyribonucleoside biosynthesis, which consume large amounts of NADPH, shut down immediately with cell division and DNA replication (Gasch *et al.*, 2000; Murray *et al.*, 2003). During starvation, fatty acid was degraded to acetyl-CoA by β -oxidation in peroxisome (Palkova *et al.*, 2002; Figure 25).

I speculate that the reduction of NADP⁺ by Ald6p might be excessive in nitrogen-starved cells. An excessive amount of NADPH might inhibit the enzymatic activity of G6PDH, which catalyzes the initial reaction of the pentose phosphate pathway. This pathway contributes to the synthesis of ribose-5-phosphate, which is an essential material for the generation of some amino acids and ribonucleotides (Murray *et al.*, 2003). Ald4p, the mitochondrial acetaldehyde dehydrogenase, utilizes mainly NAD⁺ as a co-enzyme (Tessier *et al.*, 1998), and is induced during nitrogen or sulfur starvation instead of Ald6p (Gasch *et al.*, 2000; Fauchon *et al.*, 2002; Figure 9). NADH production of citrate cycle is inactivated under starvation condition, so that I expect

Ald4p is partially contributed to NADH regeneration in mitochondria (Figure 5; Boubekour *et al.*, 1999; Gusch *et al.*, 2000; Palkova *et al.*, 2002). In our experiments, $\Delta atg7 \Delta ald4$ mutant cells were not able to maintain higher rates of viability as compared with $\Delta atg7 \Delta ald6$ cells (Figure 20). It is likely that the down regulation of Ald6p by preferential autophagic degradation may optimize NADPH/NADP⁺ levels in the cytosol (Figure 32). Thus, Ald6p may have a bilateral character: it is beneficial in growth under nutrient conditions, but disadvantageous to survival under nitrogen starvation.

Ald6p is one example of a preferential substrate for autophagic degradation. Ald6p was the only major protein on the two-dimensional PAGE gel to decrease during starvation; however, it is still possible that other minor proteins behave like Ald6p (Ghaemmaghami *et al.*, 2003). If I were able to find such proteins, it would help to clarify the molecular mechanisms of selective autophagy and more broad physiological significance of the preferential degradation.

Metabolic Dynamics in Early Phase of Starvation

Both wild-type and $\Delta atg7$ cells drastically reduced the pools of most of free amino acids during initial 3 h starvation (Figures 27 and 28). However, biochemical and morphological previous reports showed that autophagy was induced from the early phase of nitrogen starvation (Takeshige *et al.*, 1992; Noda *et al.*, 1995; Scott *et al.*, 1996). The metabolic flows of leucine and tryptophan biosynthetic pathways immediately increased shift to nitrogen starvation medium (Y. Ohsumi and K. Nakahara, unpublished results). Even in wild-type cells, I suppose that the demand of amino acids greatly exceeds the supply rate in the early phase of nitrogen depletion. Many specific genes show the transient and high-level expressions for initial 0.5–3 h of nitrogen starvation (Gusch *et al.*, 2000). After 6 h starvation, the accumulation of translatable mRNAs decline, but then free amino acid may gradually increase in wild-type cells. However, an imbalance of demand and supply of amino acids is not able to explain the low-level protein synthesis at the time point of 3 h starvation (Figure 28C). This time point should be an abnormal state, because the rate of cysteine in all free amino acids is

very high (Figures 27 and 28C). High rate existence of cysteine is inextricably linked to fail other amino acids, and I assume that the low-level protein synthesis caused to a depletion of free amino acids except cysteine (Figure 28). This evidence shown in Figure 31, amino acids supplemental experiment indicate that 3 h starved cells potentially have high protein synthesis ability.

Why do the yeast cells need to accumulate the cysteine? The result of Figure 29 suggests that yeast cells actively assimilate sulfur to synthesize cysteine from sulfate in early phase of nitrogen starvation. This is supported that the expressions of sulfur assimilation genes (*SUL1/2*, *MET3*, *MET14*, *MET16*, *MET10* and *MET17*) also show so high-levels for 0.5–4 h nitrogen starvation (Gusch *et al.*, 2000). The sulfur assimilation (sulfide synthesis) from the sulfate via sulfite requires many intracellular reducing powers such as NADPH and thioredoxin (Thomas and Surdin-Kerjan, 1997). In above discussion, I have argued about the possibility that the preferential Ald6p degradation down-regulated NADPH level under nitrogen starvation. However, the kinetics of this degradation show a near linear manner thought the long time, so that many Ald6p is in early phase of nitrogen depletion (Figure 8). The assimilation of sulfur with the consumption of many NADPH may be important for the dissipation of excess reducing power under early phase of nitrogen starvation. Autophagy deficient cells have the neither of Ald6p degradation nor cysteine synthesis (Figures 8 and 28C), so that this mutant cells may be damaged to cellular components by excess reduction powers.

Autophagy Is Essential for the Formation of Amino Acids Pool

In order to synthesize proteins wholesomely and smoothly, it is important to maintain intracellular amino acids pool in just proportion. Intracellular amino acids pool is defined the total of protein pool, free amino acids pool, and the dynamic conversion between both pools. If yeast cells face nitrogen starvation environment, they would have to manage their amino acids pool rigorously. Not only free amino acids are got from the extracellular nutrient, but also the supply by the degradation of intracellular protein occupies large proportion. Proteasome large exists on about 1% of all cytosolic proteins (Tanaka *et al.*, 1986; Tanaka *et al.*, 1988), so that ubiquitin-proteasome system

was regarded the most major process of protein degradation. However, in this study, I have demonstrated that autophagy maintained the intracellular contents of free amino acids during nitrogen starvation (Figures 27 and 28); furthermore, I have also shown that protein synthesis was relative to the contents of free amino acids (Figures 30 and 31). These results show that the autophagic protein degradation and amino acids supply are essential for protein synthesis under nitrogen depletion condition. In other word, the contribution of proteasome degradation should be not sufficient for the formation of amino acids pool (Figure 33).

Several starvation-induced proteins, Arg1p, Hsp26p, API, CPY and so on, were expressed during nitrogen starvation, however, these proteins did not increase in $\Delta atg7$ cells (Figures 5 and 25). These defects would be obvious proofs of the bankruptcy of intracellular amino acids pool in autophagy deficient cells. This critical deficiency of proteins required for the survival might be one of the reasons of the loss of viability under nitrogen starvation.

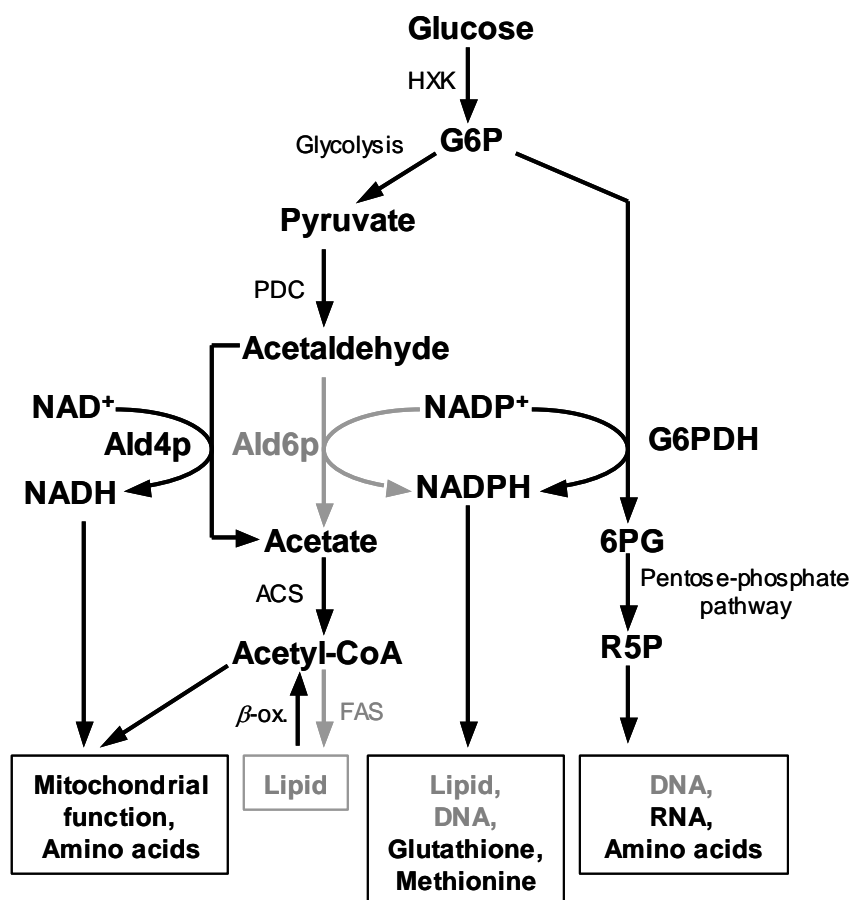
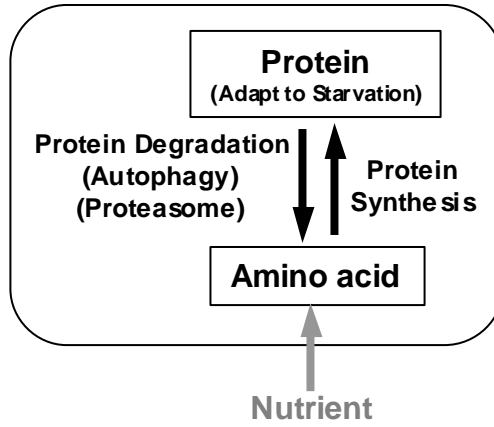


Figure 32. Model of physiological significance of the preferential Ald6p degradation.

Gray text shows the pathways that were down regulated under nitrogen starvation. Ald6p, cytosolic acetaldehyde dehydrogenase; Ald4p, mitochondrial aldehyde dehydrogenase; G6P, glucose-6-phosphate; G6PDH, glucose-6-phosphate dehydrogenase; 6PG, 6-phosphogluconate; R5P, ribose-5-phosphate; HXK, hexokinase; PDC, pyruvate decarboxylase; ACS, acetyl-CoA synthase; FAS, fatty acid synthase; β -ox., β -oxidation of fatty acid in peroxisome.

Wild-type cells



Autophagy deficient cells

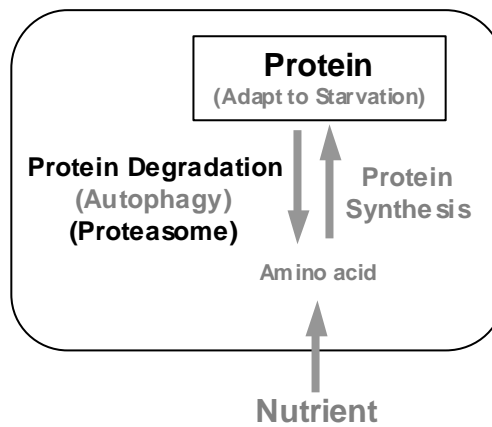


Figure 33. Model of contribution of autophagic degradation for the amino acids pool formation in yeast cells under nitrogen starvation.

REFERENCES

- Abeliovich, H., Dunn, W.A. Jr, Kim, J. and Klionsky, D.J. (2000) Dissection of autophagosome biogenesis into distinct nucleation and expansion steps. *J. Cell Biol.* 151:1025-1034.
- Baba, M., Takeshige, K., Baba, N. and Ohsumi, Y. (1994) Ultrastructural analysis of the autophagic process in yeast: detection of autophagosomes and their characterization. *J. Cell Biol.* 124:903-913.
- Baba, M., Osumi, M., Scott, S.V., Klionsky, D.J. and Ohsumi, Y. (1997) Two distinct pathways for targeting proteins from the cytoplasm to the vacuole/lysosome. *J. Cell Biol.* 139:1687-1695.
- Barth, H., Meiling-Wesse, K., Epple, U.D. and Thumm, M. (2001) Autophagy and the cytoplasm to vacuole targeting pathway both require Aut10p. *FEBS Lett.* 508:23-28
- Betz, H. and Weiser, U. (1976) Protein degradation during yeast sporulation. Enzyme and cytochrome patterns. *Eur. J. Biochem.* 70:385-395.
- Boubekeur, S., Bunoust, O., Camougrand, N., Castroviejo, M., Rigoulet, M. and Guerin, B. (1999) A mitochondrial pyruvate dehydrogenase bypass in the yeast *Saccharomyces cerevisiae*. *J. Biol. Chem.* 274:21044-21048.
- Brachmann, C.B., Davies, A., Cost, G.J., Caputo, E., Li, J., Hieter, P. and Boeke, J.D. (1998) Designer deletion strains derived from *Saccharomyces cerevisiae* S288C: a useful set of strains and plasmids for PCR-mediated gene disruption and other applications. *Yeast* 14:115-132.
- Brejning, J. and Jespersen, L. (2002) Protein expression during lag phase and growth initiation in *Saccharomyces cerevisiae*. *Int. J. Food Microbiol.* 75:27-38.
- Brown, C.R., McCann, J.A., Hung, G.G., Elco, C.P. and Chiang, H.L. (2002) Vid22p, a novel plasma membrane protein, is required for the fructose-1,6-bisphosphatase degradation pathway. *J. Cell Sci.* 115:655-666.
- Bruke, D., Dawson, D. and Stearn, T. (2000) *Method in Yeast Genetics: A Cold Spring Harbor Laboratory Course Manual*, 2000 Ed., Cold Spring Harbor Laboratory, Cold Spring Harbor, NY.

- Chiang, H.L. and Schekman, R. (1991) Regulated import and degradation of a cytosolic protein in the yeast vacuole. *Nature* 350:313-318.
- Chiba, A., Ishida, H., Nishizawa, N.K., Makino, A. and Mae, T. (2003) Exclusion of ribulose-1,5-bisphosphate carboxylase/oxygenase from chloroplasts by specific bodies in naturally senescing leaves of wheat. *Plant Cell Physiol.* 44:914-921.
- de Duve, C. (1959) Lysosomes, a new group of cytoplasmic particles, in *Subcellular Particles*; Hayashi, T (ed): Ronald, New York. 128-159
- Dickinson, F.M. (1996) The purification and some properties of the Mg²⁺-activated cytosolic aldehyde dehydrogenase of *Saccharomyces cerevisiae*. *Biochem. J.* 315 (Pt 2):393-399.
- Doelling, J.H., Walker, J.M., Friedman, E.M., Thompson, A.R. and Vierstra, R.D. (2002) The APG8/12-activating enzyme APG7 is required for proper nutrient recycling and senescence in *Arabidopsis thaliana*. *J. Biol. Chem.* 277:33105-33114.
- Farres, J., Wang, T.T., Cunningham, S.J. and Weiner, H. (1995) Investigation of the active site cysteine residue of rat liver mitochondrial aldehyde dehydrogenase by site-directed mutagenesis. *Biochemistry* 34:2592-2598.
- Fauchon, M., Lagniel, G., Aude, J.C., Lombardia, L., Soularue, P., Petat, C., Marguerie, G., Sentenac, A., Werner, M. and Labarre, J. (2002) Sulfur sparing in the yeast proteome in response to sulfur demand. *Mol. Cell* 9:713-723
- Gasch, A.P., Spellman, P.T., Kao, C.M., Carmel-Harel, O., Eisen, M.B., Storz, G., Botstein, D. and Brown, P.O. (2000) Genomic expression programs in the response of yeast cells to environmental changes. *Mol. Biol. Cell* 11:4241-4257.
- Gerhardt, B., Kordas, T.J., Thompson, C.M., Patel, P. and Vida, T. (1998) The vesicle transport protein Vps33p is an ATP-binding protein that localizes to the cytosol in an energy-dependent manner. *J. Biol. Chem.* 273:15818-15829.
- Ghaemmaghami, S., Huh, W.K., Bower, K., Howson, R.W., Belle, A., Dephoure, N., O'Shea, E.K. and Weissman, J.S. (2003) Global analysis of protein expression in yeast. *Nature* 425:737-741.
- Goldberg, A.L. and Dice, J.F. (1974) Intracellular protein degradation in mammalian and bacterial cells. *Annu. Rev. Biochem.* 43:835-869.

- Goldberg, A.L. and St John, A.C. (1976) Intracellular protein degradation in mammalian and bacterial cells: Part 2. *Annu. Rev. Biochem.* 45:747-803.
- Görg, A., Obermaier, C., Boguth, G., Harder, A., Scheibe, B., Wildgruber, R. and Weiss, W. (2000) The current state of two-dimensional electrophoresis with immobilized pH gradients. *Electrophoresis* 21:1037-1053.
- Gounaris, A.D., Turkenkopf, I., Buckwald, S. and Young, A. (1971) Pyruvate decarboxylase. I. Protein dissociation into subunits under conditions in which thiamine pyrophosphate is released. *J. Biol. Chem.* 246:1302-1309.
- Grabowska, D. and Chelstowska, A. (2003) The *ALD6* gene product is indispensable for providing NADPH in yeast cells lacking glucose-6-phosphate dehydrogenase activity. *J. Biol. Chem.* 278:13984-13988.
- Hamasaki, M., Noda, T. and Ohsumi, Y. (2003) The early secretory pathway contributes to autophagy in yeast. *Cell Struct. Funct.* 28:49-54.
- Hanaoka, H., Noda, T., Shirano, Y., Kato, T., Hayashi, H., Shibata, D., Tabata, S. and Ohsumi, Y. (2002) Leaf senescence and starvation-induced chlorosis are accelerated by the disruption of an Arabidopsis autophagy gene. *Plant Physiol.* 129:1181-1193.
- Harding, T.M., Morano, K.A., Scott, S.V. and Klionsky, D.J. (1995) Isolation and characterization of yeast mutants in the cytoplasm to vacuole protein targeting pathway. *J. Cell Biol.* 131:591-602.
- Heinemeyer, W., Kleinschmidt, J.A., Saidowsky, J., Escher, C. and Wolf, D.H. (1991) Proteinase yscE, the yeast proteasome/multicatalytic-multifunctional proteinase: mutants unravel its function in stress induced proteolysis and uncover its necessity for cell survival. *EMBO J.* 10:555-562.
- Heinemeyer, W., Gruhler, A., Mohrle, V., Mahe, Y. and Wolf, D.H. (1993) *PRE2*, highly homologous to the human major histocompatibility complex-linked *RING10* gene, codes for a yeast proteasome subunit necessary for chymotryptic activity and degradation of ubiquitinated proteins. *J. Biol. Chem.* 268:5115-5120.
- Hershko, A. and Ciechanover, A. (1998) The ubiquitin system. *Annu. Rev. Biochem.* 67:425-479.
- Hochstrasser, M. (1996) Protein degradation or regulation: Ub the judge. *Cell*

84:813-815.

- Hoffman, M. and Chiang, H.L. (1996) Isolation of degradation-deficient mutants defective in the targeting of fructose-1,6-bisphosphatase into the vacuole for degradation in *Saccharomyces cerevisiae*. *Genetics* 143:1555-1566.
- Huang, W.P., Scott, S.V., Kim, J. and Klionsky, D.J. (2000) The itinerary of a vesicle component, Aut7p/Cvt5p, terminates in the yeast vacuole via the autophagy/Cvt pathways. *J. Biol. Chem.* 275:5845-5851.
- Ichimura, Y., Kirisako, T., Takao, T., Satomi, Y., Shimonishi, Y., Ishihara, N., Mizushima, N., Tanida, I., Kominami, E., Ohsumi, M., Noda, T. and Ohsumi, Y. (2000) A ubiquitin-like system mediates protein lipidation. *Nature* 408:488-492.
- Ishihara, N., Hamasaki, M., Yokota, S., Suzuki, K., Kamada, Y., Kihara, A., Yoshimori, T., Noda, T. and Ohsumi, Y. (2001) Autophagosome requires specific early Sec proteins for its formation and NSF/SNARE for vacuolar fusion. *Mol. Biol. Cell* 12:3690-3702.
- Kamada, Y., Funakoshi, T., Shintani, T., Nagano, K., Ohsumi, M. and Ohsumi, Y. (2000) Tor-mediated induction of autophagy via an Apg1 protein kinase complex. *J. Cell Biol.* 150:1507-1513.
- Kametaka, S., Okano, T., Ohsumi, M. and Ohsumi, Y. (1998) Apg14p and Apg6/Vps30p form a protein complex essential for autophagy in the yeast, *Saccharomyces cerevisiae*. *J. Biol. Chem.* 273:22284-22291.
- Kihara, A., Noda, T., Ishihara, N. and Ohsumi, Y. (2001) Two distinct Vps34 phosphatidylinositol 3-kinase complexes function in autophagy and carboxypeptidase Y sorting in *Saccharomyces cerevisiae*. *J. Cell Biol.* 152:519-530.
- Kim, J., Scott, S.V., Oda, M.N. and Klionsky, D.J. (1997) Transport of a large oligomeric protein by the cytoplasm to vacuole protein targeting pathway. *J. Cell Biol.* 137:609-618.
- Kim, J., Dalton, V.M., Eggerton, K.P., Scott, S.V. and Klionsky, D.J. (1999) Apg7p/Cvt2p is required for the cytoplasm-to-vacuole targeting, macroautophagy, and peroxisome degradation pathways. *Mol. Biol. Cell* 10:1337-1351.
- Kim, J., Kamada, Y., Stromhaug, P.E., Guan, J., Hefner-Gravink, A., Baba, M., Scott,

- S.V., Ohsumi, Y., Dunn, W.A. Jr and Klionsky, D.J. (2001) Cvt9/Gsa9 functions in sequestering selective cytosolic cargo destined for the vacuole. *J. Cell Biol.* 153:381-396.
- Kirisako, T., Baba, M., Ishihara, N., Miyazawa, K., Ohsumi, M., Yoshimori, T., Noda, T. and Ohsumi, Y. (1999) Formation process of autophagosome is traced with Apg8/Aut7p in yeast. *J. Cell Biol.* 147:435-446.
- Kirisako, T., Ichimura, Y., Okada, H., Kabeya, Y., Mizushima, N., Yoshimori, T., Ohsumi, M., Takao, T., Noda, T. and Ohsumi, Y. (2000) The reversible modification regulates the membrane-binding state of Apg8/Aut7 essential for autophagy and the cytoplasm to vacuole targeting pathway. *J. Cell Biol.* 151:263-276.
- Kispal, G., Cseko, J., Alkonyi, I. and Sandor, A. (1991) Isolation and characterization of carnitine acetyltransferase from *S. cerevisiae*. *Biochim. Biophys. Acta* 1085:217-222.
- Kispal, G., Sumegi, B., Dietmeier, K., Bock, I., Gajdos, G., Tomcsanyi, T. and Sandor, A. (1993) Cloning and sequencing of a cDNA encoding *Saccharomyces cerevisiae* carnitine acetyltransferase. Use of the cDNA in gene disruption studies. *J. Biol. Chem.* 268:1824-1829.
- Kitamoto, K., Yoshizawa, K., Ohsumi, Y. and Anraku, Y. (1988) Dynamic aspects of vacuolar and cytosolic amino acid pools of *Saccharomyces cerevisiae*. *J. Bacteriol.* 170:2683-2686.
- Klionsky, D.J., Cueva, R. and Yaver, D.S. (1992) Aminopeptidase I of *Saccharomyces cerevisiae* is localized to the vacuole independent of the secretory pathway. *J. Cell Biol.* 119:287-299.
- Klionsky, D.J. and Ohsumi, Y. (1999) Vacuolar import of proteins and organelles from the cytoplasm. *Annu. Rev. Cell Dev. Biol.* 15:1-32.
- Klionsky, D.J., Cregg, J.M., Dunn, W.A., Emr, S.D., Sakai, Y., Sandoval, I.V., Sibirny, A., Subramani, S., Thumm, M., Veenhuis, M. and Ohsumi, Y. (2003) A unified nomenclature for yeast autophagy-related genes. *Dev. Cell* 5:539-545.
- Kuma, A., Mizushima, N., Ishihara, N. and Ohsumi, Y. (2002) Formation of the approximately 350-kDa Apg12-Apg5-Apg16 multimeric complex, mediated by Apg16 oligomerization, is essential for autophagy in yeast. *J. Biol. Chem.*

277:18619-18625.

- Kurita, O. and Nishida, Y. (1999) Involvement of mitochondrial aldehyde dehydrogenase *ALD5* in maintenance of the mitochondrial electron transport chain in *Saccharomyces cerevisiae*. *FEMS Microbiol. Lett.* 181:281-287.
- Laemmli, U.K. (1970) Cleavage of structural proteins during the assembly of the head of bacteriophage T4. *Nature* 227:680-685.
- Levine, B. and Klionsky, D.J. (2004) Development by self-digestion; molecular mechanisms and biological functions of autophagy. *Dev. Cell* 6:463-477.
- Meaden, P.G., Dickinson, F.M., Mifsud, A., Tessier, W., Westwater, J., Bussey, H. and Midgley, M. (1997) The *ALD6* gene of *Saccharomyces cerevisiae* encodes a cytosolic, Mg²⁺-activated acetaldehyde dehydrogenase. *Yeast* 13:1319-1327.
- Melendez, A., Tallozy, Z., Seaman, M., Eskelinen, E.L., Hall, D.H. and Levine, B. (2003) Autophagy genes are essential for dauer development and life-span extension in *C. elegans*. *Science* 301:1387-1391.
- Mizushima, N., Noda, T., Yoshimori, T., Tanaka, Y., Ishii, T., George, M.D., Klionsky, D.J., Ohsumi, M. and Ohsumi, Y. (1998) A protein conjugation system essential for autophagy. *Nature* 395:395-398.
- Mizushima, N., Noda, T. and Ohsumi, Y. (1999) Apg16p is required for the function of the Apg12p-Apg5p conjugate in the yeast autophagy pathway. *EMBO J.* 18:3888-3896.
- Mortimore, G.E. and Poso, A.R. (1987) Intracellular protein catabolism and its control during nutrient deprivation and supply. *Annu. Rev. Nutr.* 7:539-564.
- Muller, O., Sattler, T., Flotenmeyer, M., Schwarz, H., Plattner, H. and Mayer, A. (2000) Autophagic tubes: vacuolar invaginations involved in lateral membrane sorting and inverse vesicle budding. *J. Cell Biol.* 151:519-528.
- Murray, R.K., Granner, D.K., Mayes, P.A. and Rodwell, V.M. (2003) Harper's Illustrated Biochemistry, 26th Ed. McGraw-Hill Co., Columbus, OH.
- Nakamura, N., Matsuura, A., Wada, Y. and Ohsumi, Y. (1997) Acidification of vacuoles is required for autophagic degradation in the yeast, *Saccharomyces cerevisiae*. *J. Biochem. (Tokyo)* 121:338-344.

- Noda, T., Matsuura, A., Wada, Y. and Ohsumi, Y. (1995) Novel system for monitoring autophagy in the yeast *Saccharomyces cerevisiae*. *Biochem. Biophys. Res. Commun.* 210:126-132.
- Noda, T. and Ohsumi, Y. (1998) Tor, a phosphatidylinositol kinase homologue, controls autophagy in yeast. *J. Biol. Chem.* 273:3963-3966.
- Noda, T., Suzuki, K. and Ohsumi, Y. (2002) Yeast autophagosomes: *de novo* formation of a membrane structure. *Trends. Cell Biol.* 12:231-235.
- Nogae, I. and Johnston, M. (1990) Isolation and characterization of the *ZWF1* gene of *Saccharomyces cerevisiae*, encoding glucose-6-phosphate dehydrogenase. *Gene* 96:161-169
- O'Farrell, P.H. (1975) High resolution two-dimensional electrophoresis of proteins. *J. Biol. Chem.* 250:4007-4021.
- Ohsumi, Y., Kitamoto, K. and Anraku, Y. (1988) Changes induced in the permeability barrier of the yeast plasma membrane by cupric ion. *J. Bacteriol.* 170:2676-2682.
- Ohsumi, Y. (2001) Molecular dissection of autophagy: two ubiquitin-like systems. *Nat. Rev. Mol. Cell Biol.* 2:211-216.
- Okazaki, H., Ono, B., Ohsumi, Y. and Ohsumi, M. (2004) *apg15-1*, a UGA mutant allele in the *Saccharomyces cerevisiae* *APG16* gene, and its suppression by a cytoplasmic Factor. *Biosci. Biotechnol. Biochem.* 68:1541-1548.
- Otto, G.P., Wu, M.Y., Kazgan, N., Anderson, O.R. and Kessin, R.H. (2003) Macroautophagy is required for multicellular development of the social amoeba *Dictyostelium discoideum*. *J. Biol. Chem.* 278:17636-17645.
- Otto, G.P., Wu, M.Y., Kazgan, N., Anderson, O.R. and Kessin, R.H. (2004) *Dictyostelium* macroautophagy mutants vary in the severity of their developmental defects. *J. Biol. Chem.* 279:15621-15629.
- Palkova, Z., Devaux, F., Ilicova, M., Minarikova, L., Le Crom, S. and Jacq, C. (2002) Ammonia pulses and metabolic oscillations guide yeast colony development. *Mol. Biol. Cell* 13:3901-3914.
- Richter-Ruoff, B., Heinemeyer, W. and Wolf, D.H. (1992) The proteasome/multicatalytic-multifunctional proteinase. *In vivo* function in the

- ubiquitin-dependent N-end rule pathway of protein degradation in eukaryotes. *FEBS Lett.* 302:192-196.
- Roberts, P., Moshitch-Moshkovitz, S., Kvam, E., O'Toole, E., Winey, M. and Goldfarb, D.S. (2003) Piecemeal microautophagy of nucleus in *Saccharomyces cerevisiae*. *Mol. Biol. Cell* 14:129-141
- Robinson, J.S., Klionsky, D.J., Banta, L.M. and Emr, S.D. (1988) Protein sorting in *Saccharomyces cerevisiae*: isolation of mutants defective in the delivery and processing of multiple vacuolar hydrolases. *Mol. Cell Biol.* 8:4936-4948.
- Saint-Prix, F., Bonquist, L. and Dequin, S. (2004) Functional analysis of the *ALD* gene family of *Saccharomyces cerevisiae* during anaerobic growth on glucose: the NADP⁺-dependent Ald6p and Ald5p isoforms play a major role in acetate formation. *Microbiology* 150:2209-2220.
- Sakai, Y., Koller, A., Rangell, L.K., Keller, G.A. and Subramani, S. (1998) Peroxisome degradation by microautophagy in *Pichia pastoris*: identification of specific steps and morphological intermediates. *J. Cell Biol.* 141:625-636.
- Sambrook, J., Fritsch, E.F. and Maniatis, T. (1989) *Molecular Cloning: A Laboratory Manual*, 2nd Ed., Cold Spring Harbor Laboratory Press, Cold Spring Harbor, NY.
- Schimke, R.T. and Doyle, D. (1970) Control of enzyme levels in animal tissues. *Annu. Rev. Biochem.* 39:929-976.
- Scott, S.V., Hefner-Gravink, A., Morano, K.A., Noda, T., Ohsumi, Y. and Klionsky, D.J. (1996) Cytoplasm-to-vacuole targeting and autophagy employ the same machinery to deliver proteins to the yeast vacuole. *Proc. Natl. Acad. Sci. U. S. A.* 93:12304-12308.
- Scott, S.V., Guan, J., Hutchins, M.U., Kim, J. and Klionsky, D.J. (2001) Cvt19 is a receptor for the cytoplasm-to-vacuole targeting pathway. *Mol. Cell* 7:1131-1141.
- Seglen, P.O. and Bohley, P. (1992) Autophagy and other vacuolar protein degradation mechanisms. *Experientia* 48:158-172.
- Segui-Real, B., Martinez, M. and Sandoval, I.V. (1995) Yeast aminopeptidase I is post-translationally sorted from the cytosol to the vacuole by a mechanism mediated by its bipartite N-terminal extension. *EMBO J.* 14:5476-5484.

- Seufert, W. and Jentsch, S. (1992) *In vivo* function of the proteasome in the ubiquitin pathway. *EMBO J.* 11:3077-3080.
- Shintani, T., Mizushima, N., Ogawa, Y., Matsuura, A., Noda, T. and Ohsumi, Y. (1999) Apg10p, a novel protein-conjugating enzyme essential for autophagy in yeast. *EMBO J.* 18:5234-5241.
- Shintani, T., Huang, W.P., Stromhaug, P.E. and Klionsky, D.J. (2002) Mechanism of cargo selection in the cytoplasm to vacuole targeting pathway. *Dev. Cell* 3:825-837.
- Sikorski, R.S. and Hieter, P. (1989) A system of shuttle vectors and yeast host strains designed for efficient manipulation of DNA in *Saccharomyces cerevisiae*. *Genetics* 122:19-27.
- Slekar, K.H., Kosman, D.J. and Culotta, V.C. (1996) The yeast copper/zinc superoxide dismutase and the pentose phosphate pathway play overlapping roles in oxidative stress protection. *J. Biol. Chem.* 271:28831-28836.
- Suzuki, K., Kirisako, T., Kamada, Y., Mizushima, N., Noda, T. and Ohsumi, Y. (2001) The pre-autophagosomal structure organized by concerted functions of *APG* genes is essential for autophagosome formation. *EMBO J.* 20:5971-5981.
- Suzuki, K., Kamada, Y. and Ohsumi, Y. (2002) Studies of cargo delivery to the vacuole mediated by autophagosomes in *Saccharomyces cerevisiae*. *Dev. Cell* 3:815-824.
- Takehige, K., Baba, M., Tsuboi, S., Noda, T. and Ohsumi, Y. (1992) Autophagy in yeast demonstrated with proteinase-deficient mutants and conditions for its induction. *J. Cell Biol.* 119:301-311.
- Tanaka, K., Ii, K., Ichihara, A., Waxman, L. and Goldberg, A.L. (1986) A high molecular weight protease in the cytosol of rat liver. I. Purification, enzymological properties, and tissue distribution. *J. Biol. Chem.* 261:15197-15203.
- Tanaka, K., Yoshimura, T., Kumatori, A., Ichihara, A., Ikai, A., Nishigai, M., Kameyama, K. and Takagi, T. (1988) Proteasomes (multi-protease complexes) as 20 S ring-shaped particles in a variety of eukaryotic cells. *J. Biol. Chem.* 263:16209-16217.
- Tanida, I., Mizushima, N., Kiyooka, M., Ohsumi, M., Ueno, T., Ohsumi, Y. and Kominami, E. (1999) Apg7p/Cvt2p: A novel protein-activating enzyme essential for

- autophagy. *Mol. Biol. Cell* 10:1367-1379.
- Tessier, W.D., Meaden, P.G., Dickinson, F.M. and Midgley, M. (1998) Identification and disruption of the gene encoding the K⁺-activated acetaldehyde dehydrogenase of *Saccharomyces cerevisiae*. *FEMS Microbiol. Lett.* 164:29-34.
- Thomas, D., Cherest, H. and Surdin-Kerjan, Y. (1991) Identification of the structural gene for glucose-6-phosphate dehydrogenase in yeast. Inactivation leads to a nutritional requirement for organic sulfur. *EMBO J.* 10:547-553
- Thomas, D. and Surdin-Kerjan, Y. (1997) Metabolism of sulfur amino acids in *Saccharomyces cerevisiae*. *Microbiol. Mol. Biol. Rev.* 61:503-532.
- Trabalzini, L., Paffetti, A., Scaloni, A., Talamo, F., Ferro, E., Coratza, G., Bovalini, L., Lusini, P., Martelli, P. and Santucci, A. (2003) Proteomic response to physiological fermentation stresses in a wild-type wine strain of *Saccharomyces cerevisiae*. *Biochem. J.* 370:35-46.
- Tsukada, M. and Ohsumi, Y. (1993) Isolation and characterization of autophagy-defective mutants of *Saccharomyces cerevisiae*. *FEBS Lett.* 333:169-174.
- Thumm, M., Egner, R., Koch, B., Schlumpberger, M., Straub, M., Veenhuis, M. and Wolf, D.H. (1994) Isolation of autophagocytosis mutants of *Saccharomyces cerevisiae*. *FEBS Lett.* 349:275-280.
- Tuttle, D.L. and Dunn, W.A. Jr (1995) Divergent modes of autophagy in the methylotrophic yeast *Pichia pastoris*. *J. Cell Sci.* 108:25-35.
- van den Berg, M.A. and Steensma, H.Y. (1995) ACS2, a *Saccharomyces cerevisiae* gene encoding acetyl-coenzyme A synthetase, essential for growth on glucose. *Eur. J. Biochem.* 231:704-713.
- van den Berg, M.A., de Jong-Gubbels, P., Kortland, C.J., van Dijken, J.P., Pronk, J.T. and Steensma, H.Y. (1996) The two acetyl-coenzyme A synthetases of *Saccharomyces cerevisiae* differ with respect to kinetic properties and transcriptional regulation. *J. Biol. Chem.* 271:28953-28959.
- White, W.H., Skatrud, P.L., Xue, Z. and Toyn, J.H. (2003) Specialization of function among aldehyde dehydrogenases: the *ALD2* and *ALD3* genes are required for beta-alanine biosynthesis in *Saccharomyces cerevisiae*. *Genetics* 163:69-77.

- Yoshihisa, T. and Anraku, Y. (1990) A novel pathway of import of alpha-mannosidase, a marker enzyme of vacuolar membrane, in *Saccharomyces cerevisiae*. *J. Biol. Chem.* 265:22418-22425.
- Yuan, W., Stromhaug, P.E. and Dunn, W.A. Jr (1999) Glucose-induced autophagy of peroxisomes in *Pichia pastoris* requires a unique E1-like protein. *Mol. Biol. Cell* 10:1353-1366.